Online ISSN: 2249-4596
Print ISSN: 0975-5861
DOI: 10.17406/GJRE

Global Journal

of Researches in Engineering: A

Mechanical & Mechanics Engineering

Hydroelectric Dam Penstocks

Enhancing Composite Performance

Highlights

Friction Coefficient Evolution

Theoretical vs. Numerical Methods

Discovering Thoughts, Inventing Future

VOLUME 24 ISSUE 2 VERSION 1.0

Global Journal of Researches in Engineering: A
Mechanical and Mechanics Engineering

Global Journal of Researches in Engineering: A
Mechanical and Mechanics Engineering

Volume 24 Issue 2 (Ver. 1.0)

Open Association of Research Society

Incorporation No.: 0423089
License No.: 42125/022010/1186
Registration No.: 430374
Import-Export Code: 1109007027
Employer Identification Number (EIN):
USA Tax ID: 98-0673427

Global Journals Inc.

*(A Delaware USA Incorporation with "Good Standing"; **Reg. Number: 0423089**)*

Sponsors: Open Association of Research Society
Open Scientific Standards

Publisher's Headquarters office

Global Journals® Headquarters
945th Concord Streets,
Framingham Massachusetts Pin: 01701,
United States of America
USA Toll Free: +001-888-839-7392
USA Toll Free Fax: +001-888-839-7392

Offset Typesetting

Global Journals Incorporated
2nd, Lansdowne, Lansdowne Rd., Croydon-Surrey,
Pin: CR9 2ER, United Kingdom

Packaging & Continental Dispatching

Global Journals Pvt Ltd
E-3130 Sudama Nagar, Near Gopur Square,
Indore, M.P., Pin:452009, India

Find a correspondence nodal officer near you

To find nodal officer of your country, please email us at *local@globaljournals.org*

eContacts

Press Inquiries: *press@globaljournals.org*
Investor Inquiries: *investors@globaljournals.org*
Technical Support: *technology@globaljournals.org*
Media & Releases: *media@globaljournals.org*

Pricing (Excluding Air Parcel Charges):

Yearly Subscription (Personal & Institutional)
250 USD (B/W) & 350 USD (Color)

Editorial Board

Global Journal of Research in Engineering

Dr. Gordana Colovic

B.Sc Textile Technology, M.Sc. Technical Science Ph.D. in Industrial Management. The College of Textile? Design, Technology and Management, Belgrade, Serbia

Dr. Giacomo Risitano

Ph.D., Industrial Engineering at University of Perugia (Italy) "Automotive Design" at Engineering Department of Messina University (Messina) Italy

Dr. Maurizio Palesi

Ph.D. in Computer Engineering, University of Catania, Faculty of Engineering and Architecture Italy

Dr. Salvatore Brischetto

Ph.D. in Aerospace Engineering, Polytechnic University of Turin and in Mechanics, Paris West University Nanterre La D?fense Department of Mechanical and Aerospace Engineering, Polytechnic University of Turin, Italy

Dr. Wesam S. Alaloul

B.Sc., M.Sc., Ph.D. in Civil and Environmental Engineering, University Technology Petronas, Malaysia

Dr. Ananda Kumar Palaniappan

B.Sc., MBA, MED, Ph.D. in Civil and Environmental Engineering, Ph.D. University of Malaya, Malaysia, University of Malaya, Malaysia

Dr. Hugo Silva

Associate Professor, University of Minho, Department of Civil Engineering, Ph.D., Civil Engineering, University of Minho Portugal

Dr. Fausto Gallucci

Associate Professor, Chemical Process Intensification (SPI), Faculty of Chemical Engineering and Chemistry Assistant Editor, International J. Hydrogen Energy, Netherlands

Dr. Philip T Moore

Ph.D., Graduate Master Supervisor School of Information Science and engineering Lanzhou University China

Dr. Cesar M. A. Vasques

Ph.D., Mechanical Engineering, Department of Mechanical Engineering, School of Engineering, Polytechnic of Porto Porto, Portugal

Dr. Jun Wang

Ph.D. in Architecture, University of Hong Kong, China Urban Studies City University of Hong Kong, China

Dr. Stefano Invernizzi

Ph.D. in Structural Engineering Technical University of Turin, Department of Structural, Geotechnical and Building Engineering, Italy

Dr. Togay Ozbakkaloglu

B.Sc. in Civil Engineering, Ph.D. in Structural Engineering, University of Ottawa, Canada Senior Lecturer University of Adelaide, Australia

Dr. Zhen Yuan

B.E., Ph.D. in Mechanical Engineering University of Sciences and Technology of China, China Professor, Faculty of Health Sciences, University of Macau, China

Dr. Jui-Sheng Chou

Ph.D. University of Texas at Austin, U.S.A. Department of Civil and Construction Engineering National Taiwan University of Science and Technology (Taiwan Tech)

Dr. Houfa Shen

Ph.D. Manufacturing Engineering, Mechanical Engineering, Structural Engineering, Department of Mechanical Engineering, Tsinghua University, China

Prof. (LU), (UoS) Dr. Miklas Scholz

Cand Ing, BEng (equiv), PgC, MSc, Ph.D., CWEM, CEnv, CSci, CEng, FHEA, FIEMA, FCIWEM, FICE, Fellow of IWA, VINNOVA Fellow, Marie Curie Senior, Fellow, Chair in Civil Engineering (UoS) Wetland Systems, Sustainable Drainage, and Water Quality

Dr. Yudong Zhang

B.S., M.S., Ph.D. Signal and Information Processing, Southeast University Professor School of Information Science and Technology at Nanjing Normal University, China

Dr. Minghua He

Department of Civil Engineering Tsinghua University Beijing, 100084, China

Dr. Philip G. Moscoso

Technology and Operations Management IESE Business School, University of Navarra Ph.D. in Industrial Engineering and Management, ETH Zurich M.Sc. in Chemical Engineering, ETH Zurich, Spain

Dr. Stefano Mariani

Associate Professor, Structural Mechanics, Department of Civil and Environmental Engineering, Ph.D., in Structural Engineering Polytechnic University of Milan Italy

Dr. Ciprian Lapusan

Ph. D in Mechanical Engineering Technical University of Cluj-Napoca Cluj-Napoca (Romania)

Dr. Francesco Tornabene

Ph.D. in Structural Mechanics, University of Bologna Professor Department of Civil, Chemical, Environmental and Materials Engineering University of Bologna, Italy

Dr. Kitipong Jaojaruek

B. Eng, M. Eng, D. Eng (Energy Technology, Asian Institute of Technology). Kasetsart University Kamphaeng Saen (KPS) Campus Energy Research Laboratory of Mechanical Engineering

Dr. Burcin Becerik-Gerber

University of Southern Californi Ph.D. in Civil Engineering Ddes, from Harvard University M.S. from University of California, Berkeley M.S. from Istanbul, Technical University

Hiroshi Sekimoto

Professor Emeritus Tokyo Institute of Technology Japan Ph.D., University of California Berkeley

Dr. Shaoping Xiao

BS, MS Ph.D. Mechanical Engineering, Northwestern University The University of Iowa, Department of Mechanical and Industrial Engineering Center for Computer-Aided Design

Dr. A. Stegou-Sagia

Ph.D., Mechanical Engineering, Environmental Engineering School of Mechanical Engineering, National Technical University of Athens, Greece

Diego Gonzalez-Aguilera

Ph.D. Dep. Cartographic and Land Engineering, University of Salamanca, Avilla, Spain

Dr. Maria Daniela

Ph.D in Aerospace Science and Technologies Second University of Naples, Research Fellow University of Naples Federico II, Italy

Dr. Omid Gohardani

Ph.D. Senior Aerospace/Mechanical/ Aeronautical, Engineering professional M.Sc. Mechanical Engineering, M.Sc. Aeronautical Engineering B.Sc. Vehicle Engineering Orange County, California, US

Dr. Paolo Veronesi

Ph.D., Materials Engineering, Institute of Electronics, Italy President of the master Degree in Materials Engineering Dept. of Engineering, Italy

Contents of the Issue

Global Journal of Researches in Engineering: A Mechanical and Mechanics Engineering
Volume 24 Issue 2 Version 1.0 Year 2024
Type: Double Blind Peer Reviewed International Research Journal
Publisher: Global Journals
Online ISSN: 2249-4596 & Print ISSN: 0975-5861

Enhancing Composite Performance: Hydrothermally Treated Wood Reinforcement in Recycled Polypropylene

By Andressa dos Santos, Raphael Leonardo Bulla, Laís Weber Aguiar, Murilo Pereira Moises, Eduardo Radovanovic & Silvia Luciana Favaro

Universidade Estadual de Maringá

Abstract- The low thermal stability of cellulose presents unique technological challenges to the formulation of wood and plastic composites that are compatible and processable. For this, hydrothermal modification is a well-established technology for improving dimensional stability and durability of wood's components, in addition to providing better interaction with the polymer. This study produced polymer composites in which hydrothermally treated wood waste fibers (WT) reinforce a recycled polypropylene (RPP) matrix. Wood waste fibers were selected by grain size and distribution, treated hydrothermally, and characterized by SEM, ATR-FTIR, and water sorption. Composites were produced varying the reaction time of treatment hydrothermal (from 30 to 180 minutes), granulometric size (from 425 to 1400 μm) and percentage of WT (from 10 to 20%), following a 2^3 full-factorial experimental design, by extrusion with internal recirculation and the mechanical test specimens were modulated by injection. Tensile, flexion, IZOD impact and water sorption tests were statistically analyzed. Reaction time was the most statistically significant factor.

Keywords: *fibers, mechanical properties, polymer, plastic composite, statistics.*

GJRE-A Classification: *LCC: TA418.9.C6, TS255*

Strictly as per the compliance and regulations of:

Enhancing Composite Performance: Hydrothermally Treated Wood Reinforcement in Recycled Polypropylene

Andressa dos Santos [α], Raphael Leonardo Bulla [σ], Laís Weber Aguiar [ρ], Murilo Pereira Moises [ω], Eduardo Radovanovic [¥] & Silvia Luciana Favaro [§]

Abstract- The low thermal stability of cellulose presents unique technological challenges to the formulation of wood and plastic composites that are compatible and processable. For this, hydrothermal modification is a well-established technology for improving dimensional stability and durability of wood's components, in addition to providing better interaction with the polymer. This study produced polymer composites in which hydrothermally treated wood waste fibers (WT) reinforce a recycled polypropylene (RPP) matrix. Wood waste fibers were selected by grain size and distribution, treated hydrothermally, and characterized by SEM, ATR-FTIR, and water sorption. Composites were produced varying the reaction time of treatment hydrothermal (from 30 to 180 minutes), granulometric size (from 425 to 1400 μm) and percentage of WT (from 10 to 20%), following a 2^3 full-factorial experimental design, by extrusion with internal recirculation and the mechanical test specimens were modulated by injection. Tensile, flexion, IZOD impact and water sorption tests were statistically analyzed. Reaction time was the most statistically significant factor. Composites of wood waste fibers treated for 30 min and containing 20% of WT presented better mechanical properties than expected. However, the preservation of the lamellar fibers during the reaction time allowed for better adherence to the polymer, and the insertion of a greater quantity of fibers in the material provided greater rigidity in the composite. In general, the results obtained gives properties of stability and resistance to damage of composites containing hydrothermally treated wood fibers.

Keywords: fibers, mechanical properties, polymer, plastic composite, statistics.

I. Introduction

Environmental preservation is a crucial area in academia and industry, as both sectors can benefit from processes that recycle and reuse waste. [1,2]. Proper management of waste disposal and reuse protects the environment and allows sustainable product development [3]. In accordance with Abiplast, the global average consumption of plastics has reached 35 Kg/inhabitant in the last two years [4]. The increase in plastic consumption creates a significant challenge for proper waste disposal.

Most plastics are non-biodegradable polymers. Because of their low cost and versatility, plastics are consumed increasingly in urban areas. Plastic materials used in food packaging have specific thermophysical characteristics and are classified as thermoplastics or thermosetting polymers [5,6].

Thermoplastic materials are usually to form composites; each polymer has unique advantages and disadvantages. Polypropylene (PP) is a versatile semi-crystalline thermoplastic for general use. Its principal characteristics are high resistance to flexural ruptures, high resistance to chemicals and solvents, good electrical properties, good thermal stability, a low specific weight (0,905 g/cm^3), and low cost [5,7]. Thermoplastic polymers are fused via heating and solidified by cooling in a reversibly process. They are soft and pliable due to weak van der Waals forces, allowing reversibility [8].

Polymeric materials are prized as matrices that conform at low temperatures and pressure; however, they possess lower mechanical resistance than metallic and ceramic materials [9]. In the face of the global environmental scenario, the appeal for alternative reinforcement fibers has been growing. Natural fibers have revealed several economic and sustainable development advantages, mainly due to their characteristics, which include excellent mechanical properties, low cost, low density, low abrasiveness, ease of processing, abundance and biodegradability[10]. Fibers obtained from *Agave sisalana* (Sisal)[11], *Sansevieria cylindrica* (Saint George's Spear)[12], *Agave tequilana* (Blue Agave)[13], rice husk [14], sugarcane bagasse [15] and wood fiber[16] have shown promising results as reinforcement in composites, motivating the search for new species that show high potential as reinforcement.

Wooden residues, especially powder and bran, are primarily transported to rural areas, where they are used as ground cover or animal bedding. However, the storage and transportation of these materials is dangerous, as they are highly flammable and explosive [17]. Wood comprises cellulose, hemicellulose, lignin,

Author α σ ρ §: Departamento de Engenharia Mecânica, Universidade Estadual de Maringá, Maringá, Paraná, Brazil.
e-mail: dossantos.andressa@hotmail.com
Author ω: Departamento de Química, Universidade Tecnológica Federal do Paraná, Apucarana, Paraná, Brazil.
Author ¥: Laboratório de Química de Materiais e Sensores, Departamento de Química, Universidade Estadual de Maringá, Maringá, Paraná, Brazil.

and extractives in various proportions. The cellulose and hemicellulose components contain hydroxyl groups, making wood a hygroscopic material, which can expand the cellular wall and cause dimensional swelling [18]. Efforts have been made to improve the dimensional stability of wood and, consequently, that of the final products. However, is that the compounding of polymer matrix with the wood fiber often leads to weak mechanical properties of the composites, which are tensile, impact strengths and elongation at break. The poor mechanical properties of composites can be attributed to the low compatibility between the polar hydrophilic wood fiber and the non-polar hydrophobic polypropylene, with weak interfacial adhesion and the low dispersion of wood fiber in the polypropylene matrix due to strong interactions between of the fiber, resulting from hydrogen bonding [16].

In industry, thermal treatment is used most often to modify the characteristics of wood in order to improve dimensional stability [15]. This technique involves exposing wood to different factors, such as temperature, time, pressure, and work conditions, enhance the quality of wood for specific applications. Thermal treatment changes wood's physical, chemical, and mechanical properties due to the degradation of its principal chemical components [20].

CARVALHO (2015) studied the hydrothermal treatment of wood panels and observed the degradation of some chemical constituents, specifically mannans, xylans, and arabinanas, which caused acidification and loss of mass; this resulted in a consequent decrease in swelling, but did not negatively influence the quality of the panel [18]. Hydrothermal treatment stands out among the various treatments for fiber surfaces since it does not modify the chemical composition of the fibers. Hydrothermal treatment employs different reactions (extraction, hydrolysis, carbonization, liquefaction) at various temperatures, between 100–374°C [21]. Hydrothermal treatments do not require acid; consequently, reactors are not required to be highly resistant to corrosion, reducing the cost of this process[22].

Herein, we describe the incorporation of hydrothermally treated wood fiber into wood and plastic composites. The treated wood fibers replace polymer matrices in recycled polypropylene to improve the composites' mechanical properties for their use in residential and commercial construction.

II. Experimental

a) Materials

Solid wood waste shavings (WW) extracted from *Pinus* and *Eucalyptus* woods, provided by *Madereira Altônia* located in Maringá, Paraná, Brazil, were collected, dried in an oven at 60°C for 24 hours, and triturated in a TROPP electric crusher (model TRF 750) with motor speed of 60Hz/3600rpm, equipped with 20 hammers and 2 knives. For the matrix phase, recycled polypropylene (RPP) was supplied by *Plaspet Reciclagem Maringa LTDA ME* from Maringá, Paraná, Brazil.

b) Characterization of Recycled Polypropylene

Recycled polypropylene sample, compression molding to 350mm diameter and 190mm thickness, was characterized by X-ray diffraction (XRD) using a Shimadzu XRD-7000 X-ray diffractometer equipped with a Cu Kα radiation source (λ = 1.5406 Å) over the 2θ range 5–60° at a scan rate of 1°/min. Differential Scanning Calorimetry (DSC) was recorded on a DSC Q20 thermal analyzer from TA Instruments under a nitrogen flow atmosphere at 50 mL/min, with a heating rate of 10°C/min, over the range 40–220°C, used approximately 10 mg of the rPP slivers.

c) Hydrothermal Treatment and Characterization of Wood Waste

Wood waste was hydrothermally treated (WT) at 180°C in a Teflon-coated stainless steel autoclave (100 mL) using 3g of WW and 80 mL of deionized water. After the reaction time (30, 60, 120, 180, and 240 minutes) elapsed, the sample was dried at 100°C for 24h.

Wood waste was analyzed before and after hydrothermal treatment by Scanning Electron Microscopy (SEM) using an FEI QUANTA 250 with 5000x magnification. Attenuated Total Reflectance - Fourier Transform Infrared Spectroscopy (ATR-FTIR) was performed on a Bruker Vertex 70v FTIR spectrometer fitted with a Platinum ATR single reflection diamond ATR module. Spectra were collected from 4000 to 600 cm-1, with 4 cm-1 resolution and 32 scans. Free hydroxyl groups (Free-OH) and lignin degradation were determined for the peak ratios *I*3340/1029 and *I*1734/1029, respectively [23]. Water Sorption (WS) was performed at 75.3 ± 0.2% relative humidity with sodium chloride, following the ASTM-E-104 standard, for 78h at 25°C. Tangential swelling (SW) measurements were obtained with an electronic digital caliper to within 300 mm; the tangential thickness of the WS test specimens was measured before and after treatment. The statistical influences of Free-OH, lignin degradation, WA, and TS in wood wastes before and after hydrothermal treatment were analyzed using one-way analysis of variance (ANOVA), followed by Tukey's test at a significance level 5%.

d) Composite RPP/WT Experiments

Treated wood waste was mixed with a recycled polypropylene matrix according to the compositions in 23 full-factorial experimental designs with a central point (Table 1); reaction time, granulometric size distribution, and WT percentage were varied. All tests were performed in duplicate, and the response variance of each assay was used to estimate the overall variance of

individual responses. The statistical data used in response to the mechanical properties were obtained from IZOD traction and impact tests using the Design-Expert® software.

Table 1: Factors and levels used in 23 full-factorial experimental designs with a central point

Factor	Name	Units	Type	Level (-1)	Level (0)	Level (+1)
A	Reaction time	minutes	Numeric	30	105	180
B	Granulometric	µm	Numeric	425–610	710-850	850–1400
C	WT percentage	%	Numeric	10	15	20

e) Preparation of Composites

The samples were processed in a Thermo Scientific HAAKE MiniLab II Rheomex CTM 5 twin-screw extruder at 190°C at 60 rpm for 5 min with internal recirculation. Mechanical test specimens were processed in an injection machine (Thermo Scientific HAAKE MiniJet II) with a cannon temperature of 210°C, mold temperature of 40°C, injection pressure of 450 bar, injection time of 15s, repression pressure of 300 bar, repression time of 30s.

f) Characterization of Composites

Tensile strength tests were conducted following ASTM D638 using an EMIC DL10000 machine at 20mm/min crosshead speed, using specimens (dogbone shape) with dimensions 16.15 mm x 3.25 mm x 3.25 mm. Flexural strength was measured according to ASTM D790 - 00 on a universal Lloyd machine (Instruments LR 10K plus model) using a crosshead speed of 20 mm/min. Specimens were prepared with dimensions of 84.00 mm x 12.66 mm x 3.25 mm. Izod impact strength measurements were conducted according to ASTM D256 - 02A using CEAST equipment (Resil Impactor Junior) with rectangular samples measuring 84.00 mm x 12.65 mm x 3.25 mm that were fractured by a test pendulum with a load (impact action) of 2.75 J. Water absorption was measured following ASTM D570; before testing, the specimens (20.00 mm diameter and 5.00 mm thickness) were dried at 60°C for 24h, then immersed in distilled water for three weeks at 23 ± 2°C. All properties were tested using five samples for each group.

III. Results and Discussion

a) Characterization of Recycled Polypropylene

The X-ray diffraction patterns obtained for RPP are shown in Figure 1a. Peaks observed at 2θ = 14.1, 16.8, 18.5, and 21.4° correspond to the (110), (040), (130), and (131) planes of isotactic polypropylene, respectively [24–26]. A peak confirms the presence of syndiotactic polypropylene at 25.4°[24]. High-density polyethylene (HDPE) exhibits lower intensity peaks at 23.7, 29.4, and 36.1°, which correspond to the (200), (210), and (020) reflection planes in the typical orthorhombic unit cell structure [27,28]. Compatibility of the recycled polymers increases the amorphous halo, indicating good dispersion of the components throughout the amorphous phase and decreasing the crystallinity [25]. Polypropylene and high-density polyethylene are considered semi-crystalline thermoplastics, as they have crystalline (ordered) and amorphous (disordered) domains. The recycled polymers tend to become fragile materials, reducing their deformation at rupture and impact resistance [29].

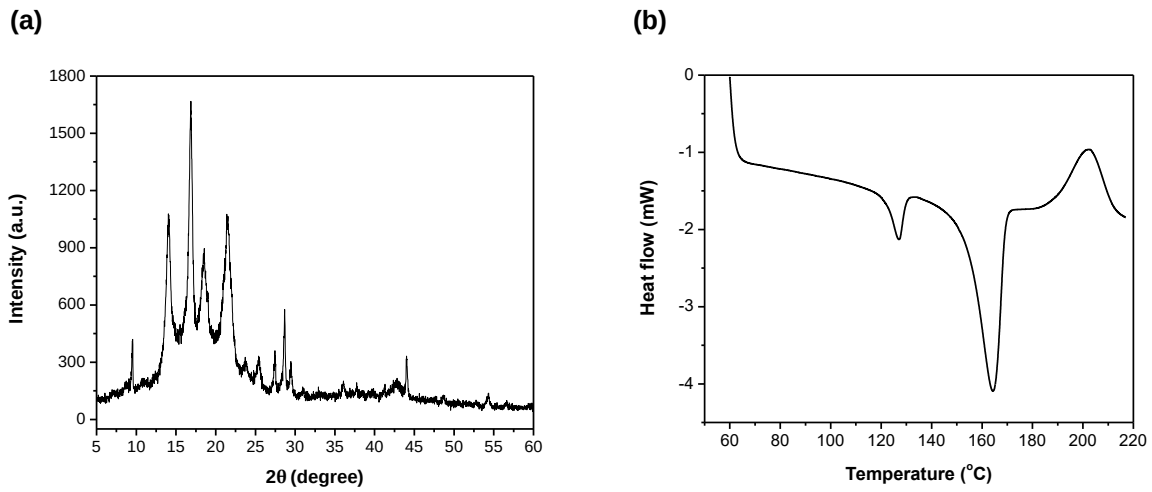

Figure 1: (a) X-ray diffractogram (b) DSC curve of the RPP

The DSC curve of RPP, shown in Figure 1b, exhibits two melting temperature (Tm) peaks at approximately 127°C and 164°C, corresponding to high-density polyethylene and polypropylene, respectively; and one exothermic transition at approximately 202°C, related to recycling additive compounds [24,28,30,31]. Generally, post-consumer polypropylene contains contaminants; in this case, the sample contains polyethylene [2]. Contamination is a byproduct of density-based separation used at recycling facilities since polypropylene and polyethylene have very similar densities [24]. The two endothermic transitions on the thermograph indicate that PP and HDPE co-exist and imply decreased compatibility between the polymers [31]. The exothermic event suggests the presence of a recycling additive, a compatibilizer agent, which serves as a polymer surfactant with low surface tension that promotes interfacial adhesion between different phases in a polyblend [32]. Polymers when melted, peak endothermic, in the manufacture of composites directly affect crystallinity, as a consequence of their mechanical, thermal and optical properties[33]. This first-order thermal event is necessary for the fusion and incorporation of reinforcement, such as fibers. The exothermic peak is the thermal event in which recrystallization or curing of the polymer occurs, promoting the formation of a crystalline nucleus in the sample[33].

b) Characterization of Wood Waste

Scanning electron micrographs of the untreated and hydrothermally treated wood waste fibers are presented in Figure 2. The control fiber demonstrates a well-defined wood structure, with continuous fibers exhibiting a large, ordered surface along its length. During hydrothermal treatment, the surface area increases due to gaps formed in the lignocellulose structure on the surface of the fibers. This results in a vitreous and brittle appearance with depolymerization and solubilization from lignin and hemicellulose [31,32,34]. Throughout the reaction, sample deformation becomes visible with the formation of small holes in the surface [32]. The ray cells along the tangential direction of the wood retain their shape, but small cracks appear in the middle of the lamella [35]. Large cavities or cracks are observed along the fibers transverse section [34]. The formation of intercellular spaces can be attributed to the disruption of ray cells with thin cell walls by gases released as extractives degrade during the drying phase; this process is hampered by the lignins present in Eucalyptus wood [34].

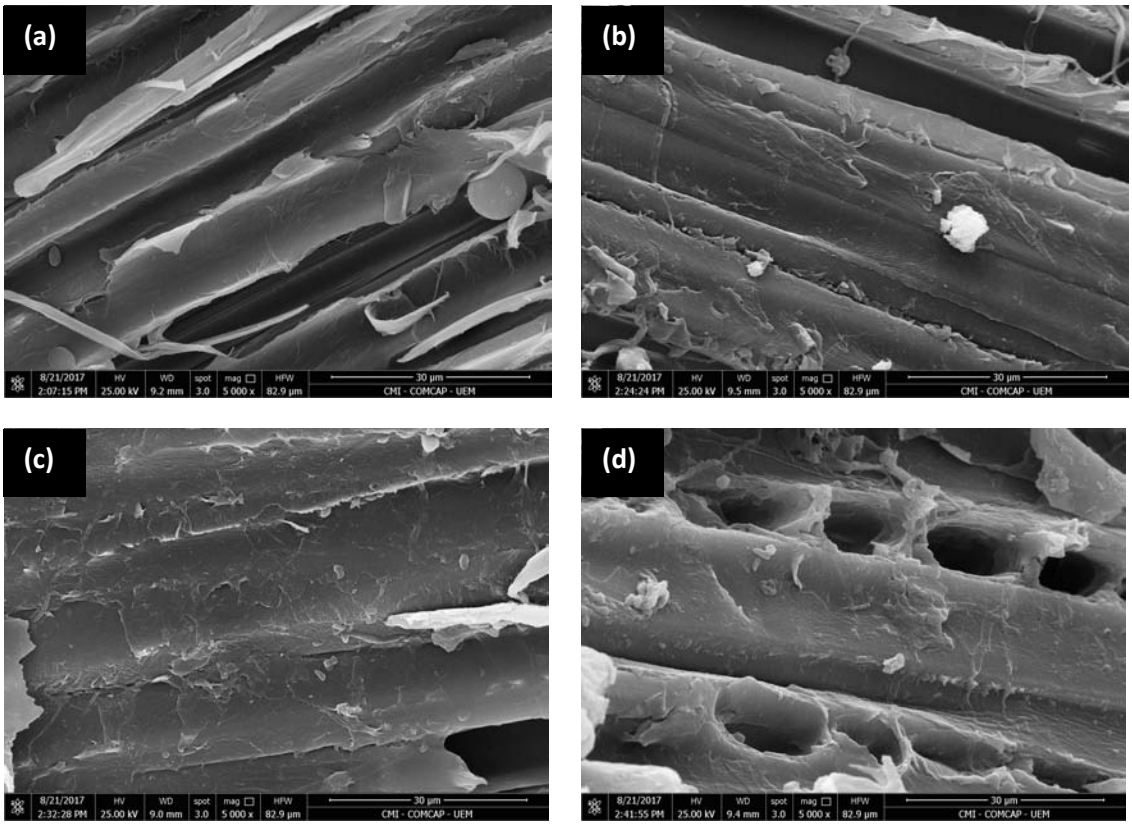

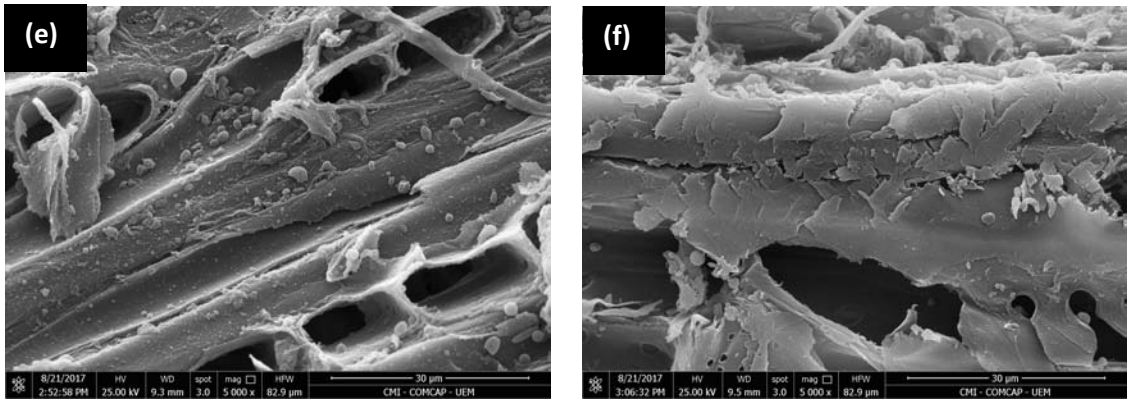

Figure 2: SEM images of wood waste non-treated, (a) control, and treated, (b) WT30, (c) WT60, (d) WT120, (e) WT180, and (f) WT240

Infrared spectra of the untreated and hydrothermally treated wood fibers display characteristic absorption signals for lignin and cellulose structures, as shown in Figure 3. The major absorption bands are associated with the vibrational stretch of the OH bond at 3336 cm^{-1} [34,35]. Lignin is confirmed by the absorption signal at 1734 cm^{-1}, corresponding to C=O ketone vibrational stretches [35,36]. The reference absorption band at 1031 cm^{-1} corresponds to C-O cellulose binding, a highly stable structure to thermal and chemical treatments [23].

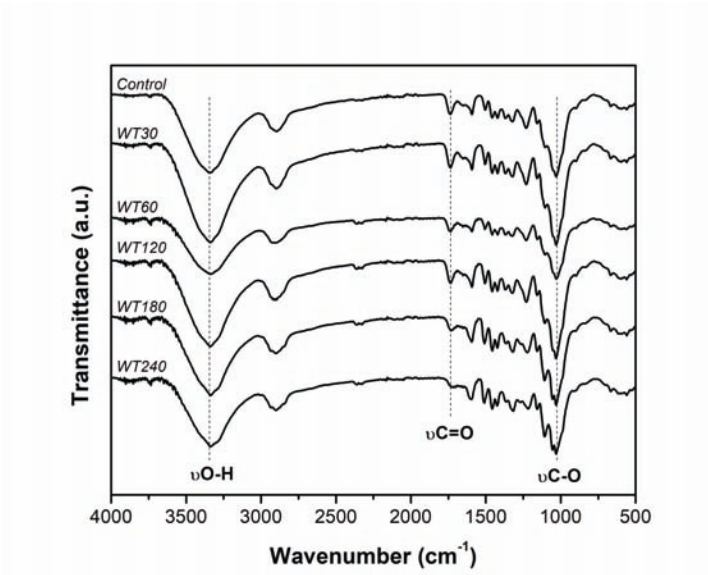

Figure 3: ATR-FTIR spectra of wood waste non-treated (Control) and treated (WT) at different times

ATR-FTIR analysis was used to study the relationship between stable absorption bands and bands modified by hydrothermal treatment. The assignments of the absorption bands observed in the infrared spectra of the main functional groups are presented in detail in Table 2. After hydrothermal treatment, the I3338/1031 ratio tends to decreases, confirming the loss of free hydroxyl groups (-OH free) on the WT surface. In general, wood fibers subjected to longer reaction times (over 120 min) exhibited a reduction in hydrophilic character. The decrease in I1734/1031 also corresponds to a decrease in the lignin ketone groups. This decrease may result from the decomposition of lignin at prolonged reaction times (over 180 min) since lignin is known to have more excellent thermal stability for hydrothermal processes than cellulose [37]. The results demonstrate increased hydrophobic character and lignin degradation with increasing reaction time. These fiber modifications facilitate a more comprehensive study of the affinity between wood fibers and recycled polymer.

Table 2: Chemical and physical properties of wood waste

Sample	Peak ratio ($I_{3336/1021}$)	Peak ratio ($I_{1734/1031}$)	Water sorption* (%)	Tangential sweeling* (%)
Control	0.956	0.242	10.617 ± 0.098[a]	74.6 ± 4.6[a]
WT30	0.976	0.240	10.188 ± 0.067[b]	56.6 ± 2.5[b]
WT60	0.925	0.225	9.685 ± 0.128[c]	42.2 ± 3.8[c]
WT120	0.877	0.236	8.993 ± 0.138[d]	37.4 ± 1.8[c]
WT180	0.891	0.158	7.407 ± 0.072[e]	18.8 ± 3.9[d]
WT240	0.906	0.121	6.700 ± 0.034[f]	7.0 ± 2.2[e]

**Similar letters on the column are not significantly different (p> 0.05)*

Water absorption and tangential swelling of wood fibers (shown in Table 2) reached equilibrium after 22h. Decreased water absorption percentage was observed with increasing treatment time; this corroborates spectral data indicating a decrease in the number of free hydroxyl groups on the surface of the wood fibers. The same trend was also observed with tangential swelling: decreased water absorption resulted in reduced sample swelling. This results from increased hydrophobicity of the wood fibers due to partial degradation of the cellulose and lignin molecules after hydrothermal treatment [19].

c) Statistical Analysis of Composite RPP/WT

Responses for the strain (Y1), yield strength (Y2), Young's Modulus (Y3), impact strength (Y4), flexural strength (Y5), and water absorption (Y6) are shown in Table 3. A 2^3 full-factorial design with four central points and one replicate, generating 20 total runs, was executed, and the factors for these responses were analyzed using statistical analysis Design Expert® software.

Table 3: Factors levels and responses for complete factorial design with four central points

	Factor			Response					
Run	A	B	C	Strain (MPa)	Yield Strength (Mpa)	Young's Modulus (Mpa)	Impact Strength (J/m)	Flexural Strength (MPa)	Water Absorption (%)
1	(+1)	(-1)	(+1)	24.315	23.625	936.154	45.736	38.216	0.920
2	(-1)	(-1)	(+1)	24.627	24.059	932.944	32.306	37.882	0.957
3	(-1)	(+1)	(-1)	22.727	21.275	652.237	35.746	33.072	0.465
4	(+1)	(-1)	(-1)	23.552	22.468	681.088	34.056	33.887	0.487
5	(-1)	(-1)	(-1)	24.339	22.830	711.690	46.101	35.680	0.475
6	(-1)	(+1)	(+1)	23.537	23.817	919.156	31.859	36.506	0.834
7	(0)	(0)	(0)	24.022	22.635	795.726	44.128	36.539	0.475
8	(+1)	(+1)	(+1)	22.344	22.111	727.958	30.028	34.596	0.758
9	(-1)	(-1)	(+1)	24.645	24.266	917.110	35.330	36.991	1.216
10	(-1)	(+1)	(+1)	23.645	23.004	922.100	30.404	36.796	0.731
11	(+1)	(+1)	(-1)	22.313	20.771	605.654	30.918	32.837	0.440
12	(0)	(0)	(0)	23.796	23.238	700.702	40.374	38.991	0.783
13	(+1)	(-1)	(-1)	23.641	22.559	690.824	34.861	33.567	0.451
14	(+1)	(-1)	(+1)	24.751	23.658	938.145	42.309	39.190	1.020
15	(0)	(0)	(0)	24.056	22.720	697.690	40.794	37.533	0.690
16	(-1)	(+1)	(-1)	22.740	21.294	652.076	33.120	35.649	0.389
17	(+1)	(+1)	(+1)	22.288	21.426	703.482	30.131	36.685	0.661
18	(0)	(0)	(0)	23.401	22.297	717.314	43.544	36.708	0.831
19	(-1)	(-1)	(-1)	23.530	22.816	717.884	45.998	36.228	0.554
20	(+1)	(+1)	(-1)	22.100	20.538	609.110	30.477	33.159	0.408

Table 4 shows the six estimated responses for the properties studied. The *p*-value of the model was below 0.05, indicating a probability of less than 5% of the null hypothesis. ANOVA verifies this low p-value for all responses, shown in Supplementary Materials (Appendix A), for which the models obtained have a *p*-value less than 0.05. R-squared values close to 1.0 indicate that the model accurately predicts a fitting curve and adjusted R^2.

Table 4: Estimated parameters

Factor	Y1	Y2	Y3	Y4	Y5	Y6
Intercept	23.44	22.53	769.85	35.59	35.68	0.67
A	-0.28[a]	-0.39[a]	-33.30[a]	-0.77	-0.42	-0.030
B	-0.73[a]	-0.75[a]	-45.88[a]	-4.00[a]	-0.77[a]	-0.087[a]
C	0.33[a]	0.71[a]	104.78[a]	-0.82	1.42[a]	0.21[a]
AB	-0.17[a]	-0.18[a]	-29.12[a]	-0.42	-0.18	0.011
AC	-0.064	-0.15	-14.90[a]	3.06[a]	0.48	-0.018
BC	-0.084	0.097	-10.58	-0.16	-0.19	-0.054
ABC	-0.12	-0.100	-25.14[a]	-2.39[a]	-0.39	0.000125
R-Squared	0.9445	0.9510	0.9739	0.9521	0.8329	0.8763
Adj R-Squared	0.9091	0.9198	0.9573	0.9216	0.7265	0.7976
Pred R-Squared	0.8299	0.8508	0.9504	0.8825	0.5387	0.6631
***p*-Value**	<0.0001	<0.0001	<0.0001	<0.0001	0.0015	0.0003

[a]*statistically significant value (model p> 0.05). Y1: Strain, Y2: Yield Strength, Y3: Young's Modulus, Y4: Impact Strength, Y5: Flexural Strength, Y6: Water Sorption.*

i. *Strain*

From the strain data (Y1 response), all main factors (A, B, C, and the AB interaction) were statistically significant, as predicted by the estimation. Figure 4a shows the contour plot for strain, where the optimal conditions for the composite concerning condition Y1 can be determined. The interaction between the amount of wood fiber and reaction time (20% treated wood fiber for 30 min) produced the best results for strain since fibers treated for shorter times to preserve their structure, as seen in the SEM results. The fibers possess sufficient roughness for better interaction without gaps between the interface reinforcement and polymer [38,39].

(a)

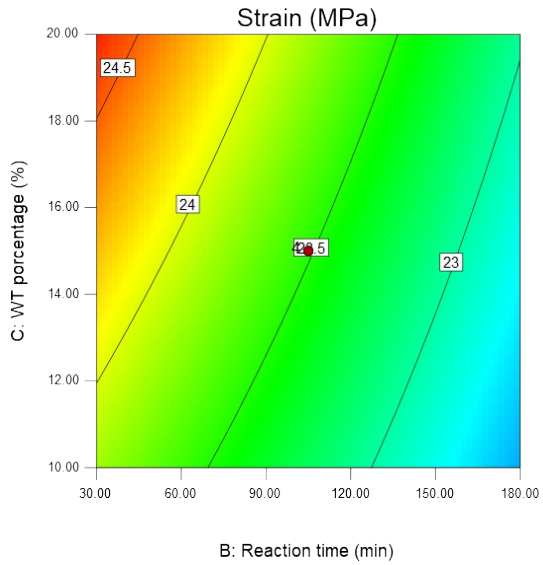

(b)

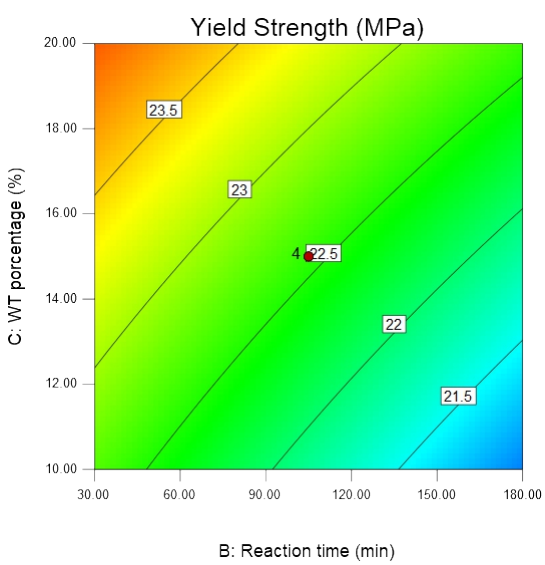

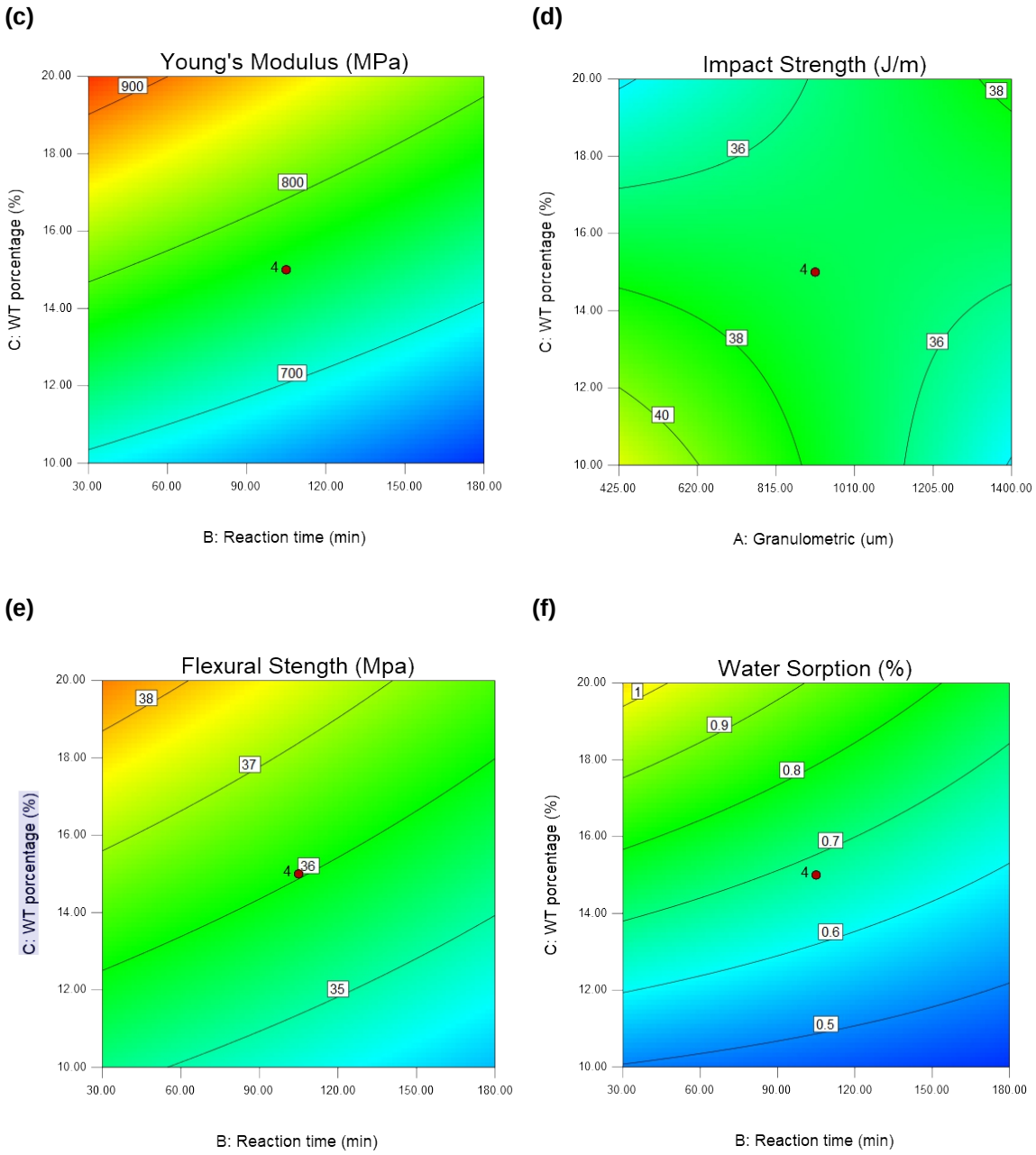

Figure 4: Surface contour response plot for (a) Strain, (b) Yield Strength, (c) Young's Modulus, (d) Impact Strength, (e) Flexural Strength and (f) Water Sorption

ii. *Yield Strength*

Considering the values obtained for the yield strength, the statistically significant interactions were the main factors A, B, C, and AB interaction, based on estimated data. The contour plot in Figure 4b demonstrates the best conditions for the composite for condition Y2. The interaction between wood fiber percentage and reaction time exhibited the best results, with 20% of wood waste treated for 30 min. Preserving the fiber lamellae in WT/30 produced good adhesion to RPP, increasing the yield strength of plastic deformation [39,40].

iii. *Young's Modulus*

The estimated parameters for Young's Modulus test indicate that all factors and interactions were statistically significant except for BC. Y3 values increase with WT percentage since adding fibers with greater stiffness causes increased stiffness in the composite, as shown in Figure 4c [41]. Young's Modulus values for the composite depend on the fibers' properties; a material's rigidity is determined when subjected to an external tensile stress [14,42]. Reaction time (B) also produced a significant effect, as low values of Y3 were observed for composites containing fibers treated for 180 min; that is, more significant elastic deformation occurred for these

fibers [42]. Increased crystallinity is expected in fibers with higher reaction times; thus, hydrothermally treated fibers tend to form less amorphous structures, reducing the elastic characteristics of the material [19]. Hydrothermal treatment can also cause the appearance of carbon microspheres incompatible with the polymer, thus reducing its Young's Modulus values [43].

iv. *Impact Strength*

Impact strength measurements highlight that the main factor B and the AC and ABC interactions were statistically significant, according to estimated data. The surface contour plot of impact strength is shown in Figure 4d; this value can be used to determine the best conditions for the formulation of the composite. The interaction between WT percentage and granulometric size indicated that the best formulations for impact resistance include 10% treated wood fiber with a 425 μm particle size and 20% treated wood fiber with a particle size of 1400 μm. The first formulation is favorable because wood fibers with low granulometry behave as hardening centers, blocking the propagation of cracks under impact [44]. In contrast, in the second formulation, the larger fibers bridge the cracks and increase crack propagation resistance by improving impact resistance [42].

v. *Flexural Strength*

Estimated values from the flexural strength test indicate that only factors B and C were statistically significant. Figure 4e shows the surface contour plot, where the optimal conditions for the composite concerning Y5 can be observed. Interaction between wood fiber quantity and reaction time provided the best results for tensile strength, with 20% wood fiber treated for 30 min. In this work, we have shown that fibers treated for shorter times preserve their structures, as observed with SEM, presenting sufficient roughness for improved interaction without gaps between the interface reinforcement and polymer [38,39].

vi. *Water Sorption*

Factors B and C were statistically significant from the water sorption estimated data. Figure 4f shows the surface contour plot where the optimal conditions for the composite to condition Y6 can be observed. The interaction between WT percentage and reaction time indicated higher water adsorption for the composite with 20% wood fiber treated for 30 min; composites with a more significant amount of fibers tend to absorb a greater amount of water [14]. In addition, fibers treated for less time preserve their structure, as observed in SEM; thus, these fibers can absorb more water than those treated for longer times [39].

IV. Conclusion

Hydrothermal treatment of wood waste fibers results in intercellular spaces and degradation along the fibers that increase with reaction time to produce rough and highly porous WTs. Hydrophobicity of surface fibers and lignin degradation increase with reaction times exceeding 180 min. The mechanical properties of the RPP/WT composites indicate that reaction time (main factor B) was the most statistically significant. Fibers treated hydrothermally for 30 min obtained good adhesion with RPP since fiber lamellae were preserved and the polymer retained compatible porosity. WT percentage (main factor C) was statistically significant in all factors tested; the material's rigidity increased with the amount of fiber in the material.

One of the biggest advantages of the composites is the flexibility in preparation in relation to the composition rPP/WT, offering the possibility of producing materials with different final mechanical properties. The proposed recycling method has great chances of success, due to the low cost of the equipment used and the innovative and ecological factor, as well as the association of cooperatives to supply the recyclable material.

From these results, the polymer composite of recycled polypropylene and hydrothermally treated wood waste fibers possesses favorable mechanical properties, making it a promising construction material that benefits the economy and the environment. The composites can be used to produce a variety of materials, including domestic use such as buckets and bowls, as well as products for civil construction, for manufacturing pipes and floorings. So those materials to be developed, more research must be carried out to evaluate the degradation of materials over long periods of environmental exposure.

Acknowledgments

The authors thank the State University of Maringa (UEM), COMCAP-UEM, CAPES, and Brazil's National Council of Scientific and Technological Development (CNPq) for the scholarship concession (152453/2022-9) and financial support. We want to thank Editage (www.editage.com) for English language editing.

References Références Referencias

1. Azambuja, R. da R., de Castro, V. G., Trianoski, R., & Iwakiri, S. (2018). Recycling wood waste from construction and demolition to produce particle boards. *Maderas: Ciencia y Tecnologia*, *20*(4), 681–690. https://doi.org/10.4067/S0718-221X2018005041401
2. Caraschi, J. C., & Leão, A. L. (2008). Avaliação das propriedades mecânicas dos plásticos reciclados provenientes de resíduos sólidos urbanos. *Acta Scientiarum. Technology*, *24*, 1599–1602. https://

doi.org/http://dx.doi.org/10.4025/actascitechnol.v24i0.2462

3. de la Casa, J. A., Bueno, J. S., & Castro, E. (2021). Recycling of residues from the olive cultivation and olive oil production process for manufacturing of ceramic materials. A comprehensive review. *Journal of Cleaner Production*, *296*, 126436. https://doi.org/10.1016/j.jclepro.2021.126436
4. ABIPLAST. (2015). Perfil 2015 - Indústria Brasileira de Transformação de Material Plástico. *Associação Brasileira Da Indústria de Plástico.*, 21–41.
5. Tajeddin, B., & Arabkhedri, M. (2020). Polymers and food packaging. In *Polymer Science and Innovative Applications* (pp. 525–543). Elsevier. https://doi.org/10.1016/B978-0-12-816808-0.00016-0
6. Li, R., Wang, N., Bai, Z., Chen, S., Guo, J., & Chen, X. (2021). Microstructure design of polypropylene/expandable graphite flame retardant composites toughened by the polyolefin elastomer for enhancing its mechanical properties. *RSC Advances*, *11*(11), 6022–6034. https://doi.org/10.1039/d0ra09978c
7. Mano, E. B. (1991). *Polímeros como Materiais de Engenharia* (E. E. Blucher (ed.); 1a Edição, p. 218). Blucher, Editora Edgard.
8. Balani, K., Verma, V., Agarwal, A., & Narayan, R. (2015). Physical, Thermal, and Mechanical Properties of Polymers. *Biosurfaces*, 329–344. https://doi.org/10.1002/9781118950623.app1
9. Zhou, H., Li, W., Hao, X., Zong, G., Yi, X., Xu, J., Ou, R., & Wang, Q. (2022). Recycling end-of-life WPC products into ultra-high-filled, high-performance wood fiber/polyethylene composites: a sustainable strategy for clean and cyclic processing in the WPC industry. *Journal of Materials Research and Technology*, *18*, 1–14. https://doi.org/10.1016/j.jmrt.2022.02.091
10. Majela, H., Vitor, S., Duarte, A., Rodrigo, P., Bittencourt, S., Radovanovic, E., & Luciana, S. (2021). *Characterization of natural cellulosic fibers from Yucca aloifolia L. leaf as potential reinforcement of polymer composites*. *0123456789*, 5477–5492. https://doi.org/10.1007/s10570-021-03866-y
11. da Luz, J., Losekann, M. A., dos Santos, A., Halison de Oliveira, J., Girotto, E. M., Moises, M. P., Radovanovic, E., & Fávaro, S. L. (2019). Hydrothermal treatment of sisal fiber for composite preparation. *Journal of Composite Materials*, *53*(17), 2337–2347. https://doi.org/10.1177/0021998319826384
12. Sreenivasan, V. S., Rajini, N., Alavudeen, A., & Arumugaprabu, V. (2015). Composites: Part B Dynamic mechanical and thermo-gravimetric analysis of Sansevieria cylindrica/polyester composite: Effect of fiber length, fiber loading and chemical treatment. *COMPOSITES PART B*, *69*, 76–86. https://doi.org/10.1016/j.compositesb.2014.09.025
13. Langhorst, A. E., Burkholder, J., Long, J., Thomas, R., & Kiziltas, A. (2025). *com Blue-Agave Fiber-Reinforced Polypropylene Composites for Automotive Applications*. *13*(2018), 820–835.
14. Väisänen, T., Haapala, A., Lappalainen, R., & Tomppo, L. (2016). Utilization of agricultural and forest industry waste and residues in natural fiber-polymer composites: A review. *Waste Management*, *54*, 62–73. https://doi.org/10.1016/j.wasman.2016.04.037
15. El-Fattah, A. A., EL Demerdash, A. G. M., Alim Sadik, W. A., & Bedir, A. (2015). The effect of sugarcane bagasse fiber on the properties of recycled high density polyethylene. *Journal of Composite Materials*, *49*(26), 3251–3262. https://doi.org/10.1177/0021998314561484
16. Kazayawoko, M., Balatinecz, J. J., & Matuana, L. M. (1999). Surface modification and adhesion mechanisms in woodfiber-polypropylene composites. *Journal of Materials Science*, *34*(24), 6189–6199. https://doi.org/10.1023/A:1004790409158
17. Wang, H., Zhang, X., Guo, S., & Liu, T. (2021). A review of coextruded wood–plastic composites. *Polymer Composites*, *42*(9), 4174–4186. https://doi.org/10.1002/pc.26189
18. Carvalho, A. G., Zanuncio, A. J. V., Vital, B. R., Carneiro, A. de C. O., da Silva, C. M. S., & Tonoli, G. H. D. (2018). Hydrothermal treatment of strand particles of pine for the improvement of OSB panels. *European Journal of Wood and Wood Products*, *76*(1), 155–162. https://doi.org/10.1007/s00107-017-1234-3
19. Pelaez-Samaniego, M. R., Yadama, V., Lowell, E., & Espinoza-Herrera, R. (2013). A review of wood thermal pretreatments to improve wood composite properties. *Wood Science and Technology*, *47*(6), 1285–1319. https://doi.org/10.1007/s00226-013-0574-3
20. Hill, C., Altgen, M., & Rautkari, L. (2021). Thermal modification of wood—a review: chemical changes and hygroscopicity. *Journal of Materials Science*, *56*(11), 6581–6614. https://doi.org/10.1007/s10853-020-05722-z
21. Yokoyama, S., & Matsumura, Y. (2008). The Asian Biomass Handbook - A Guide for Biomass Production and Utilization. In J. The University of Tokyo and Hiroshima University (Ed.), *The Japan Institute of Energy*.
22. Ruiz, H. A., Ruzene, D. S., Silva, D. P., Quintas, M. A. C., Vicente, A. A., & Teixeira, J. A. (2011). Evaluation of a hydrothermal process for pretreatment of wheat straw-effect of particle size and process conditions. *Journal of Chemical*

Technology and Biotechnology, *86*(1), 88–94. https://doi.org/10.1002/jctb.2518

23. Missio, A. L., Mattos, B. D., De Cademartori, P. H. G., Pertuzzatti, A., Conte, B., & Gatto, D. A. (2015). Thermochemical and physical properties of two fast-growing eucalypt woods subjected to two-step freeze-heat treatments. *Thermochimica Acta*, *615*, 15–22. https://doi.org/10.1016/j.tca.2015.07.005
24. Mantovani, G. A., Oliveira, J. H. De, Santos, A. dos, Rinaldi, A. W., Moisés, M. P., Radovanovic, E., & Fávaro, S. L. (2017). Mechanical recycling of tags and labels residues using sugarcane bagasse ash. *Polímeros*, *27*(1), 8–15. https://doi.org/10.1590/0104-1428.2278
25. Campoy, I., Arribas, J. M., Zaporta, M. A. M., Marco, C., Gómez, M. A., & Fatou, J. G. (1995). Crystallization kinetics of polypropylene-polyamide compatibilized blends. *European Polymer Journal*, *31*(5), 475–480. https://doi.org/10.1016/0014-3057(94)00185-5
26. Laoutid, F., Estrada, E., Michell, R. M., Bonnaud, L., Müller, A. J., & Dubois, P. (2013). The influence of nanosilica on the nucleation, crystallization and tensile properties of PP–PC and PP–PA blends. *Polymer*, *54*(15), 3982–3993. https://doi.org/10.1016/j.polymer.2013.05.031
27. Chouit, F., Guellati, O., Boukhezar, S., Harat, A., Guerioune, M., & Badi, N. (2014). Synthesis and characterization of HDPE/N-MWNT nanocomposite films. *Nanoscale Research Letters*, *9*(1), 288. https://doi.org/10.1186/1556-276X-9-288
28. Lin, J. H., Pan, Y. J., Liu, C. F., Huang, C. L., Hsieh, C. T., Chen, C. K., Lin, Z. I., & Lou, C. W. (2015). Preparation and compatibility evaluation of polypropylene/high density polyethylene polyblends. *Materials*, *8*(12), 8850–8859. https://doi.org/10.3390/ma8125496
29. Fernandes, B. L., & Domingues, A. J. (2007). Caracterização mecânica de polipropileno reciclado para a indústria automotiva. *Polímeros*, *17*(2), 85–87. https://doi.org/10.1590/S0104-14282007000200005
30. Luda, M. P., Brunella, V., & Guaratto, D. (2013). Characterisation of Used PP-Based Car Bumpers and Their Recycling Properties. *ISRN Materials Science*, *2013*(March), 1–12. https://doi.org/10.1155/2013/531093
31. Mengeloglu, F., & Karakus, K. (2008). Thermal Degradation, Mechanical Properties and Morphology of Wheat Straw Flour Filled Recycled Thermoplastic Composites. *Sensors*, *8*(12), 500–519. https://doi.org/10.3390/s8010500
32. Datta, R. K., Polk, M. B., & Kumar, S. (1995). Reactive Compatibilization of Polypropylene and Nylon. *Polymer-Plastics Technology and Engineering*, *34*(4), 551–560. https://doi.org/10.1080/03602559508012204
33. Da Costa, H. M., Ramos, V. D., De Andrade, M. C., & Da Silva Richter Quintana Nunes, P. (2016). Análise térmica e propriedades mecânicas de resíduos de polietileno de alta densidade (PEAD). *Polimeros*, *26*, 75–81. https://doi.org/10.1590/0104-1428.2104
34. Kondo, T. (1997). The assignment of IR absorption bands due to free hydroxyl groups in cellulose. *Cellulose*, *4*(4), 281–292. https://doi.org/10.1023/A:1018448109214
35. Oudiani, A. El, Msahli, S., & Sakli, F. (2017). In-depth study of agave fiber structure using Fourier transform infrared spectroscopy. *Carbohydrate Polymers*, *164*, 242–248. https://doi.org/10.1016/j.carbpol.2017.01.091
36. Popescu, C. M., Popescu, M. C., Singurel, G., Vasile, C., Argyropoulos, D. S., & Willfor, S. (2007). Spectral characterization of eucalyptus wood. *Applied Spectroscopy*, *61*(11), 1168–1177. https://doi.org/10.1366/000370207782597076
37. Li, H., Wang, S., Yuan, X., Xi, Y., Huang, Z., Tan, M., & Li, C. (2018). The effects of temperature and color value on hydrochars' properties in hydrothermal carbonization. *Bioresource Technology*, *249*, 574–581. https://doi.org/10.1016/j.biortech.2017.10.046
38. Laverde, V., Marin, A., Benjumea, J. M., & Rincón Ortiz, M. (2022). Use of vegetable fibers as reinforcements in cement-matrix composite materials: A review. *Construction and Building Materials*, *340*(May), 127729. https://doi.org/10.1016/j.conbuildmat.2022.127729
39. Fang, J., Zhan, L., Ok, Y. S., & Gao, B. (2018). Minireview of potential applications of hydrochar derived from hydrothermal carbonization of biomass. *Journal of Industrial and Engineering Chemistry*, *57*, 15–21. https://doi.org/10.1016/j.jiec.2017.08.026
40. Georgopoulos, S. T., Tarantili, P. A., Avgerinos, E., Andreopoulos, A. G., & Koukios, E. G. (2005). Thermoplastic polymers reinforced with fibrous agricultural residues. *Polymer Degradation and Stability*, *90*(2 SPEC. ISS.), 303–312. https://doi.org/10.1016/j.polymdegradstab.2005.02.020
41. Saheb, D. N., & Jog, J. P. (1999). Natural fiber polymer composites: A review. *Advances in Polymer Technology*, *18*(4), 351–363. https://doi.org/10.1002/(SICI)1098-2329(199924)18:4<351::AID-ADV6>3.0.CO;2-X
42. Sanadi, A. R., Caulfield, D. F., & Jacobson, R. E. (1997). Agro-Fiber Thermoplastic Composites. In C. Press (Ed.), *Paper and composites from agro-based resources* (pp. 377–401). Lewis Publishers.
43. Gao, Y., Wang, X.-H., Yang, H.-P., & Chen, H.-P. (2012). Characterization of products from

hydrothermal treatments of cellulose. *Energy*, *42*(1), 457–465. https://doi.org/10.1016/j.energy.2012.03.023

44. Taflick, T., Maich, É. G., Ferreira, L. D., Bica, C. I. D., Rodrigues, S. R. S., & Nachtigall, S. M. B. (2015). Acacia bark residues as filler in polypropylene composites. *Polímeros*, *25*(3), 289–295. https://doi.org/10.1590/0104-1428.1840

Global Journal of Researches in Engineering: A Mechanical and Mechanics Engineering
Volume 24 Issue 2 Version 1.0 Year 2024
Type: Double Blind Peer Reviewed International Research Journal
Publisher: Global Journals
Online ISSN: 2249-4596 & Print ISSN: 0975-5861

Comparative Analysis of Friction Coefficient Evolution in Hydroelectric Dam Penstocks: Theoretical vs. Numerical Methods

By Tchawe Tchawe Moukam, Nkontchou Ngongang François, Tientcheu Nsiewe Max-well, Djiako Thomas, Djeumako Bonaventure, Tcheukam-Toko Dénis & Kenmeugne Bienvenu
University of Ngaoundere-Cameroon

Summary- The objective of this study was to investigate the evolution of the friction coefficient throughout a full penstock using two different approaches. Two approaches were considered in order to assess their effectiveness in predicting head loss. A theoretical approach that based on direct determination using the commonly used Colebrook-While formula. A graphical approach that based on numerical modeling of the structure under study using Gambit 2.2 software. For the theoretical approach, the results show that whatever the other parameters set out in the Colebrook-White formula (Reynolds number, diameter and absolute roughness), only absolute roughness has a visible impact on the result obtained. For the numerical approach, the results obtained show that the friction coefficient is neither identical on the same wall, nor identical in the same portion. Nor is it identical in the same section of the pipe, as shown by the theoretical approach. This shows that head loss in a section of pipe can change over time.

Keywords: *friction coefficient, penstock, hydroelectric dam, theoretical approach, numerical approach.*

GJRE-A Classification: *LCC: TC540-599*

Strictly as per the compliance and regulations of:

Comparative Analysis of Friction Coefficient Evolution in Hydroelectric Dam Penstocks: Theoretical vs. Numerical Methods

Tchawe Tchawe Moukam [α], Nkontchou Ngongang François [σ], Tientcheu Nsiewe Max-well [ρ], Djiako Thomas [ω], Djeumako Bonaventure [¥], Tcheukam-Toko Dénis [§] & Kenmeugne Bienvenu [χ]

Summary- **The objective of this study was to investigate the evolution of the friction coefficient throughout a full penstock using two different approaches. Two approaches were considered in order to assess their effectiveness in predicting head loss. A theoretical approach that based on direct determination using the commonly used Colebrook-While formula. A graphical approach that based on numerical modeling of the structure under study using Gambit 2.2 software. For the theoretical approach, the results show that whatever the other parameters set out in the Colebrook-White formula (Reynolds number, diameter and absolute roughness), only absolute roughness has a visible impact on the result obtained. For the numerical approach, the results obtained show that the friction coefficient is neither identical on the same wall, nor identical in the same portion. Nor is it identical in the same section of the pipe, as shown by the theoretical approach. This shows that head loss in a section of pipe can change over time.**

Keywords: friction coefficient, penstock, hydroelectric dam, theoretical approach, numerical approach.

I. Introduction

Investing in a hydropower plant is very expensive, but it has an operating life of more than 30 years, with very low operating and maintenance costs compared to other power plants. In addition, in recent years, the experience gained in forecasting risks and production have facilitated the financing of hydropower projects, including private investments. The field of hydropower also boasts state-of-the-art technology. These days, turbines have attained efficiencies of over 97% and are extremely reliable. These data hence ensure that we have installations that function properly and also reduces the risk of downtime.

The function of penstocks is to transfer water from the reservoirs to the installations (turbines in a hydroelectric plant) that convert hydraulic energy into electrical energy [1]. They are made up of sections with singularities where the local hydrodynamic pressures take on high values, as they follow the shape of the relief: slopes, obstacles, crossing of troughs, etc. The hydraulic plant therefore supports a pressure that is of the order of the head, but the effects of head loss reduce this value [1].

For a conduit flow, forces normal to walls are not involved; only tangential and therefore viscous forces contribute to the drag and power input [2]. The pressure drop thus depends on the type of flow, determined by the Reynolds number, and on the internal roughness of the pipe. It should be noted that the absolute roughness represents the average thickness of the surface roughness of the pipe material [3]. The gradient of the linear head loss, also called friction slope, depends on the friction coefficient, the flow volume and the geometrical characteristics of the structure [4], [5].

The friction coefficient is a function of the Reynolds number characterizing the flow, and the relative roughness of the pipe under consideration [6]. Since the roughness in a penstock is closely related to the coefficient of friction, an accurate estimate of roughness is crucial to plant performance.

According to ENEO [7], the Songloulou hydroelectric plant is the largest (384 MW) and the Lagdo plant one of the most recent (72 MW) of the Cameroonian plants. The first is the largest dam on the South Interconnected Network (RIS), and the second the only hydroelectric power station on the North Interconnected Network (RIN). The objective of this work is to approach the reality of the field with regard to the environment of these dams, based on their structures. We will therefore characterize the friction in the penstock of each. This study is one of the preliminary analyses of the flow in the penstock of a Cameroonian hydroelectric dam. No previous study on the friction parameters in the penstocks of the two dams studied is available.

Therefore, this study will examine the hydraulic characteristics influenced by the penstock walls on the flow within the penstock and at its outlet. The study focuses on the evolution of the friction coefficient in the

Author α σ ¥: Department of Mechanical Engineering, ENSAI, University of Ngaoundere-Cameroon. e-mails: christophetchawe@yahoo.fr, christophetchawe88@gmail.com, moukam.tchawe@univ-ndere.cm
Author ρ: Department of Fundamental Sciences, EGCIM, University of Ngaoundere-Cameroon.
Author ω: Department of Mechanical Engineering and Energy, ISTA, University Institute of the Gulf of Guinea-Cameroon.
Author §: Department of Mechanical Engineering, COT, University of Buea-Cameroon.
Author χ: Department of Mechanical Engineering, ENSPY, University of Yaounde 1-Cameroon.

whole structure, obtained analytically by the conventional method and by a graphical approach. Our analysis will enable us to identify the most interesting method for approximating the exact value of the coefficient of friction. It may also give rise to a new approach to monitoring these delicate structures.

II. Materials

The materials on which our study is based are the Songloulou and Lagdo dams. Figures 1 and 2 below show the mesh of the structures in question (the Songloulou and the Lagdo dams study area respectively).

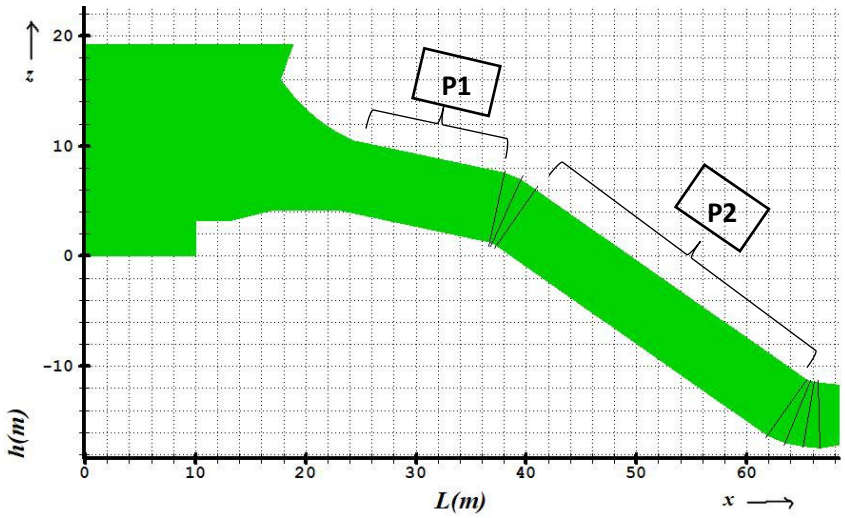

Figure 1: Songloulou Dam mesh

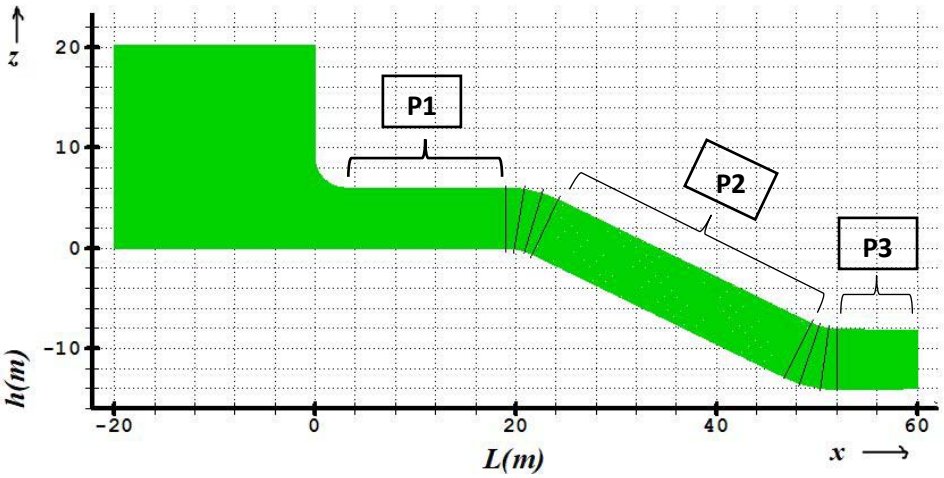

Figure 2: Lagdo Dam meshing

We modeled our power plants in Gambit 2.2. For Figure 1, the mesh type used is regular with 675845 quadrilateral meshes, 1108245 faces and 661186 nodes. For figure 2, the type of mesh used is regular with 197455 quadrilateral faces. On these figures, we have highlighted the portions in which we will present the results obtained (i.e. portions 1, 2 and 3 in the case of Lagdo). Thus for the case of Songloulou, we have P1 for the first portion of the pipe and P2 for the second portion. The same is true for the case of Lagdo where we have three portions, including P1, P2 and P3. Note that these portions represent the straight portions from which the results will be presented.

III. Methods

a) Theoretical Approach

To determine the friction coefficient f of a turbulent flow, the empirical equation developed by Colebrook-White remains the reference equation. This equation is well known among hydraulic engineers, and continues to be the subject of research. The calculations and plots in this work are obtained from the following equation (equation 1) [8].

$$\frac{1}{\sqrt{f}} = -2log_{10}\left[\frac{\varepsilon/D}{3.7} + \frac{2.51}{Re\sqrt{f}}\right] \quad (1)$$

Where ε/D is the relative roughness (derived from the absolute roughness ε and the diameter D), Re

the Reynolds number and f the desired coefficient of friction. For the pressure drop, equation 2 below is used from the friction coefficient obtained previously [4], [5].

$$J = \frac{8f}{g\pi^2}\frac{Q^2}{D^5} \quad (2)$$

In the case of the conduite, another definition of the drag coefficient λ is used, called the friction coefficient [2]:

$$\lambda = \frac{d}{1/2\rho U_0^2}\frac{\Delta P}{l} \quad (3)$$

b) Numerical Approach

The Fluent software is used for this approach, as it has a large number of turbulence models to cope with many physical problems. The geometry of the structure as well as the type of boundary conditions of the physical domain of the parameters that characterize the fluid-structure interaction were modelled in Gambit version 2.2. Knowing that the fluid is incompressible, the motion is described using differential equations with derivatives in the following form [9]:

$$\frac{\partial u}{\partial x} + \frac{\partial v}{\partial y} + \frac{\partial w}{\partial z} = 0 \quad (4)$$

For the u component parallel to the wall, the stationary Navier-Stokes equation simplifies considerably in the very near wall.

$$u\frac{\partial u}{\partial x} + v\frac{\partial u}{\partial y} = -\frac{1}{\rho}\frac{\partial p}{\partial x} + v\frac{\partial^2 u}{\partial x^2} + v\frac{\partial^2 u}{\partial y^2} \quad (5)$$

The convective terms tend to zero (adhesion condition) and the term $\frac{\partial^2 u}{\partial x^2}$ is negligible in front of the term $\frac{\partial^2 u}{\partial y^2}$ (weakly non-parallel flow condition). In short, all that remains is:

$$\frac{1}{\rho}\frac{\partial p}{\partial x} = v\frac{\partial^2 u}{\partial y^2} \quad (6)$$

It can be seen that the pressure gradient in the boundary layer imposes the curvature $\frac{\partial^2 u}{\partial y^2}$ of the velocity profile *u(y)*.

The energy equation is represented by the relation below [10]:

$$\frac{\partial T}{\partial t} + u\frac{\partial T}{\partial x} + v\frac{\partial T}{\partial y} + w\frac{\partial T}{\partial z} = a\left(\frac{\partial^2 T}{\partial x^2} + \frac{\partial^2 T}{\partial y^2} + \frac{\partial^2 T}{\partial z^2}\right) \quad (7)$$

The decomposition of the viscous stress tensor is written:

$$\underline{\tau} = \underline{\overline{\tau}} + \underline{\tau'} \quad (8)$$

with the viscous stress tensor given by:

$$\begin{cases} \overline{\tau_{ij}} = \mu\left(\frac{\partial \overline{u_i}}{\partial x_j} + \frac{\partial \overline{u_j}}{\partial x_i}\right) - \frac{2}{3}\mu\frac{\partial \overline{u_k}}{\partial x_k}\delta_{ij} \\ \tau'_{ij} = \mu\left(\frac{\partial u'_i}{\partial x_j} + \frac{\partial u'_j}{\partial x_i}\right) - \frac{2}{3}\mu\frac{\partial u'_k}{\partial x_k}\delta_{ij} \end{cases} \quad (9)$$

The equations of the turbulent kinetic energy and its dissipation rate give us:

$$\begin{cases} \rho\overline{u_j}\frac{\partial \varepsilon}{\partial x_j} = \frac{\mu_i}{\sigma_k}\frac{\partial^2 k}{\partial x^2{}_j} + \rho p_k - \rho\varepsilon \\ \rho\overline{u_j}\frac{\partial \varepsilon}{\partial x_j} = \frac{\mu_i}{\sigma_\varepsilon}\frac{\partial^2 \varepsilon}{\partial x^2{}_j} + \rho\frac{\varepsilon}{k}(c_{\varepsilon 1}p_k) - c_{\varepsilon 2}\varepsilon \end{cases} \quad (10)$$

The turbulence model is ***k-ε*** and the resolution method is RANS. The flow and site (location) parameters of each structure were considered in obtaining the different results. The Colebrook-White formula was integrated into the fluent solver via a calculation code.

IV. Results and Discussion

a) Theoretical Approach

The theoretical approach is based on the Colebrook-white's formula [8] for a steel pipe in an evolving state, i.e. from new (**ε** = 0.03mm) to worn (**ε** = 1mm). We note that these values are those defined by hydraulic engineers and available in literature to characterize the evolution of roughness in steel pipes, as is the case in our dams.

i. *Case of the Songloulou Dam*

Starting from five velocities corresponding to the variation of velocity in the water intake for the periods of low water and flood, we calculated the friction coefficient ***f*** for four values of the absolute roughness **ε**. Table 1 below shows the results obtained.

Table 1: Evolution of the friction coefficient in our pipe as a function of **ε**

Velocity (V)	Ab. Roughness (ε)	Relative roughness (ε/D)	Friction Coef. (*f*)
4,045; 4,1.	0.05	0,00781	0,03495
	0.09	0,01406	0,04270
	0.3	0,04688	0,06946
	0.8	0,12500	0,11550
4,3; 4,5; 4,73.	0.05	0,00781	0,03495
	0.09	0,01406	0,04270
	0.3	0,04688	0,06946
	0.8	0,12500	0,11549

We find that the friction coefficient remains almost identical in the pipe with increasing Reynolds number for a given **ε**. Similarly, the only element influencing the friction coefficient ***f*** in this formula is ε. In the same logic, we have looked for the influence of these parameters on another structure, in order to compare the results obtained.

ii. *Case of the Lagdo Dam*

The approach is identical to that used for the Songloulou dam, with the speed ranges corresponding to the variation of speed in the water intake for the periods of low water and flood for this structure. Table 2 below presents the results obtained.

Table 2: Evolution of the friction coefficient in our pipe according to **ε**

Velocity (V)	Ab. Roughness (ε)	Relative roughness (ε/D)	Friction Coef. (*f*)
3,1; 3,3	0.05	0,00833	0,03571
	0.09	0,01500	0,04371
	0.3	0,05000	0,07156
	0.8	0,13333	0,12003
3,5; 3,7; 3,87	0.05	0,00833	0.03570
	0.09	0,01500	0,04371
	0.3	0,05000	0,07156
	0.8	0,13333	0,12003

The observation is the same as that made from Table 1. The friction coefficient remains practically the same in the pipe with the increase of the Reynolds number for a given ε. We can therefore conclude that for these results that whatever the other parameters in the Colebrook-White's formula, only the absolute roughness has an impact on the result obtained. However, in view of the two tables above, the coefficient of friction is also influenced by the flow rate (with higher values in the Lagdo dam penstock, which has a lower flow rate). We also note that the head loss corresponding to this approach according to formula 2 can only be static in a considered portion.

b) Numerical Approach

This is the friction coefficient obtained graphically on each point constituting the portions of the penstock. The idea is to identify the evolution of the turbulent friction in each portion of the penstock according to the parameters of its environment. To do this, we seek by the same approach the maximum thickness of the asperities influencing the structure of the flow (what we will call real absolute roughness). Note that the fluid considered here is clear water with a density of 1000kg/m^3.

i. *Case of the Songloulou Dam*

a. *Research of the real value of ε*

In order to find out the real thickness of the roughness influencing the friction coefficient in the pipe, we proceeded by the creation of graphic study zones. These study areas leave the walls towards the axis of the penstock at a small pitch (1mm to 5mm). Figure 3 below illustrates the evolution of turbulent friction in the penstock for three defined absolute roughness steps (starting **ε**=15mm towards the wall), with an initial velocity of 4.045 m/s. Note that the same test was carried out on the upper wall.

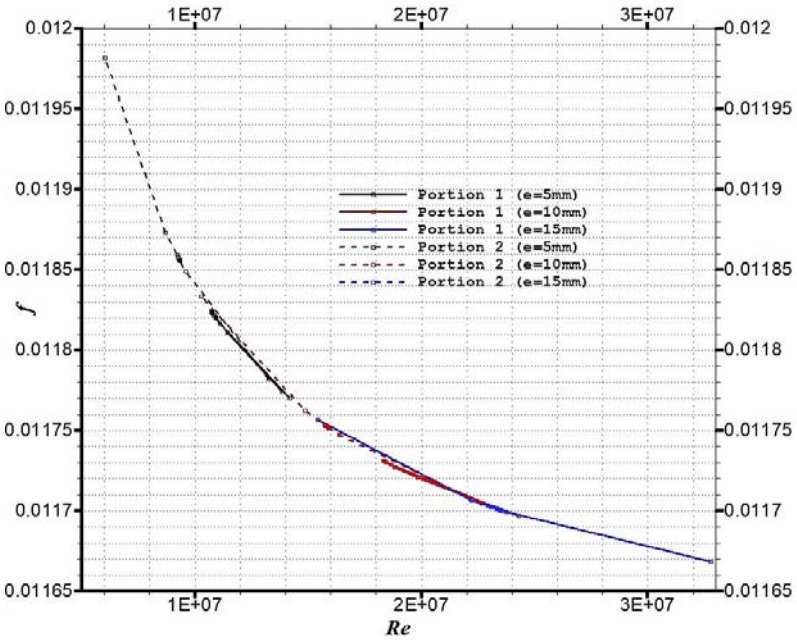

Figure 3: Evolution of turbulent friction in the pipe for e = ε_{max} different

The idea here is to see at what thickness e we have maximum friction. This thickness will then be considered as our maximum relative roughness (ε_{max}). We can see from this figure that the maximum value of *f* is observed for e=5mm (ε_{max}=5mm). This is justified by the fact that as we approach the axis of our pipe (e > 5mm), turbulent friction begins to drop considerably. It is in this logic that in the continuation of our work on this dam, we will carry out the evaluation of turbulent friction on a thickness of 5mm. It should also be noted that these plots are made only in the different portions.

b. *Determination of the evolution of the friction coefficient f in the penstock*

Figure 4 below shows the evolution of the friction coefficient *f* as a function of the actual parameters of the structure. Thus, for a good appreciation of the values, the result will be presented for each section separately.

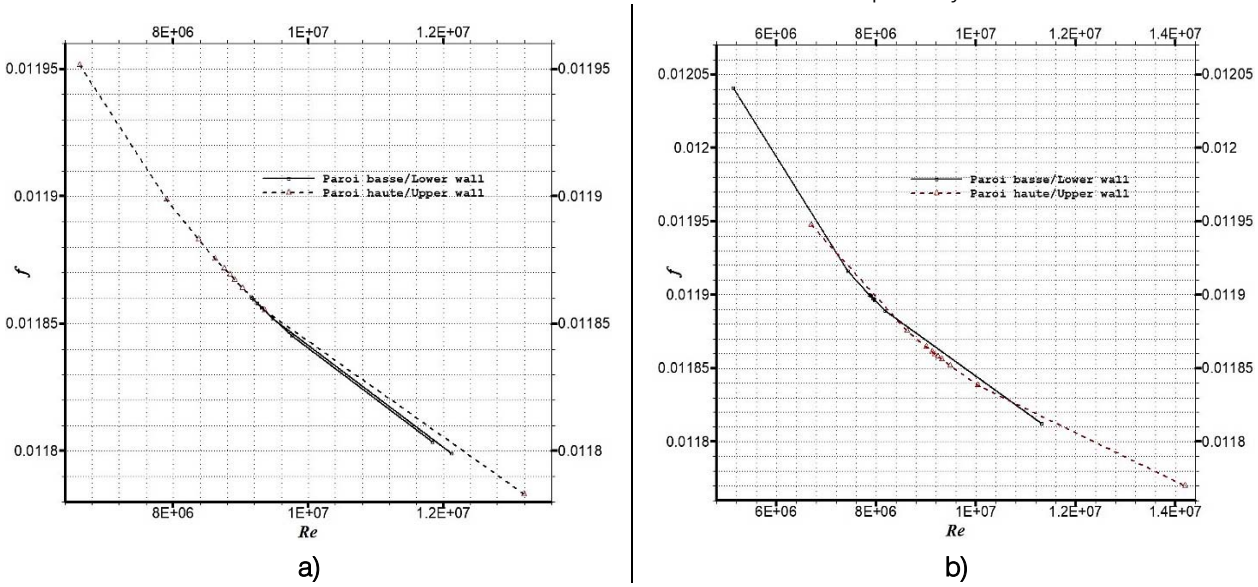

Figure 4: Evolution of the friction coefficient in section 1 (a) and section 2 (b) for Re=26.9x10^6

We can see that the turbulent friction varies from one wall to the other. Also, it is not identical in the two portions. It is dominant on the upper wall in the first portion of the penstock of our dam (Figure 4.a). On the other hand, in the second portion of our penstock (Figure 4.b), it is dominant on the lower wall with a higher value than the one observed in Figure 4.a. We will verify this hypothesis by applying this approach to another structure.

ii. *Case of the Lagdo Dam*

a. *Finding the real value of ε*

We proceed in the same way as in the case of the previous structure. Figure 5 below shows the turbulent friction in the pipe for $\boldsymbol{\varepsilon} \leq 15$mm on the low wall, with an initial speed of 3.1 m/s.

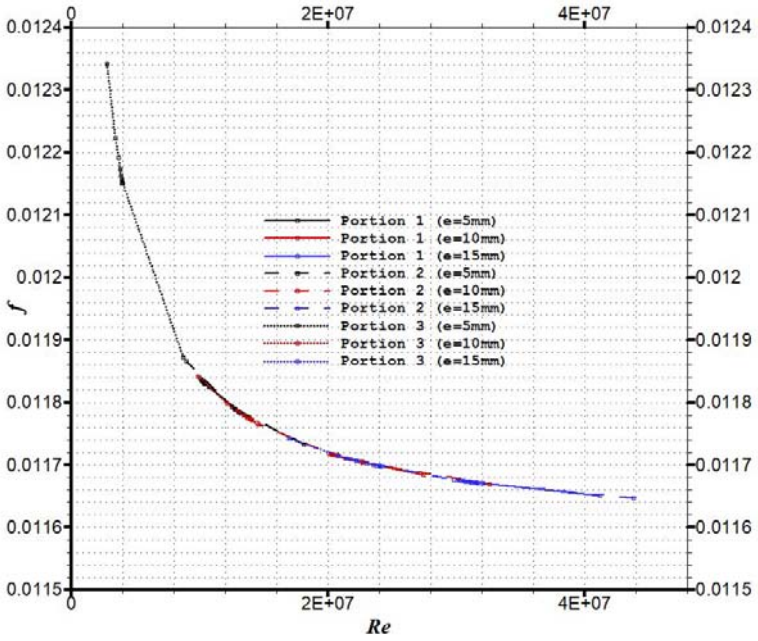

Figure 5: Evolution of the turbulent friction in the pipe for e = ε_{max} different

As in the previous case, the maximum value of f is still found when $\boldsymbol{\varepsilon}$=5mm as shown in Figure 5 above. This is the case for the lower and upper walls.

b. *Determination of the evolution of the friction coefficient f in the penstock*

Figure 6 below shows the evolution of the friction coefficient *f* as a function of the actual parameters of the structure. The result is presented separately for each of the three sections for a good appreciation of the values.

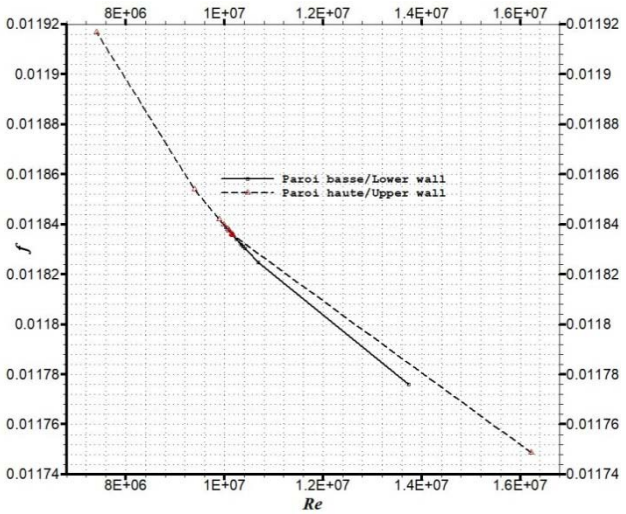

a)

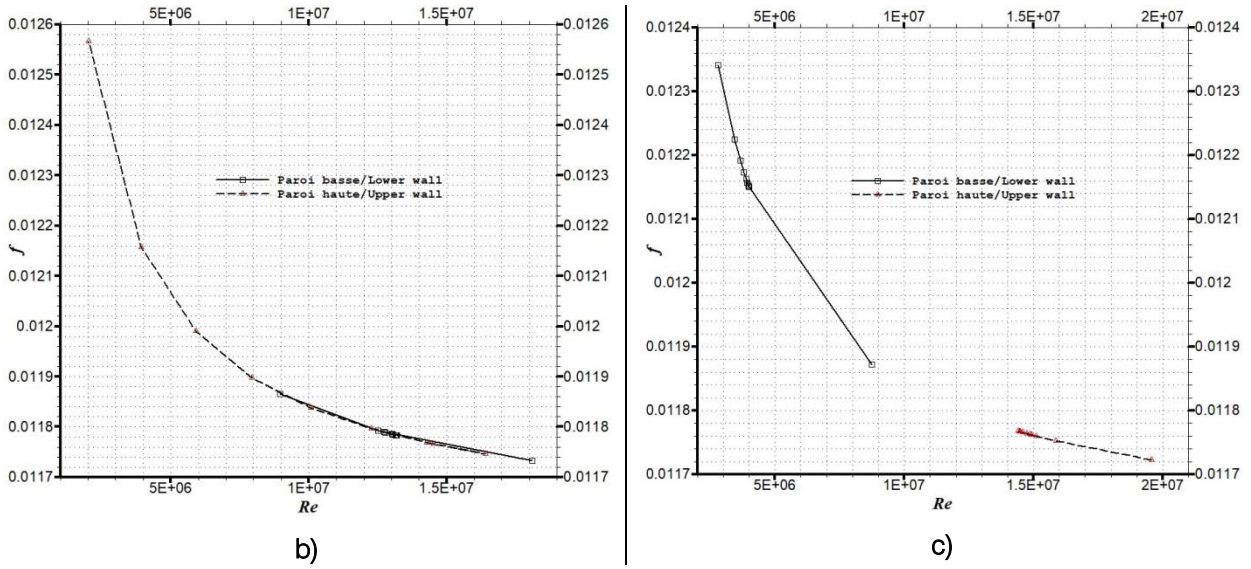

Figure 6: Evolution of turbulent friction in section 1 (a), section 2 (b) and section 3 (c) for different Re

We observe once again that the friction coefficient is not identical on the walls of the same section of pipe. It will be even less for each portion of our penstock. Apart from the third section of the pipe where turbulent friction is dominant on the lower wall (Figure 6.c), we rather have maximum turbulent friction on the upper wall for the other two sections (Figures 6.a and 6.b).

As a general remark, we observe that the friction coefficient is neither identical on the same wall nor identical in the same portion, as presented by the theoretical approach. More importantly, it is not identical on the same section of the pipe. As another remark, the impact of the Reynolds number is visible on the evolution of the friction and was not felt on the results of the theoretical approach for our case. As a final remark, the head loss resulting from the numerical approach cannot be static in any portion of the pipe. This is not the case in the theoretical approach, given the shape of the curves obtained. Some researchers have already pointed out this shortcoming in the theoretical approach (for example Levin [11]).

c) Validation of the Numerical Model

To validate our model, the studies of Moss and Baker [12] and Abdalla et *al*. [13] were used. Figure 7 below shows the results obtained under similar study conditions. It shows the velocity profile over a reversal peak.

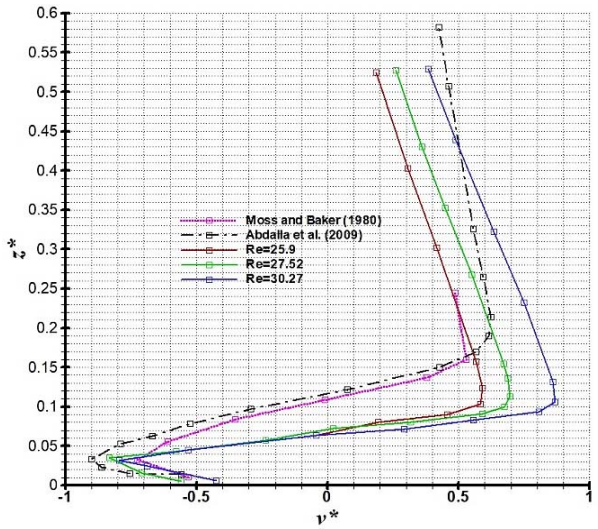

Figure 7: Flow structure on the sill for

In this figure, our study is presented by the Reynold's numbers *Re*. In addition to the determination on the reversal peak, we have applied it to our case which is the Songloulou dam. The cause of the backdrop of our profiles is the transition from a free surface flow to a loaded flow, which doesn't exists in the

study of Abdalla et al [13]. In the same logic, Abdalla et al [13] in their study evaluate the impact of the threshold (peak) on the energy dissipation at this level. They observe the pointed shape which explains the recirculation phenomenon. This is also evident in our case as shown in Figure 8 below.

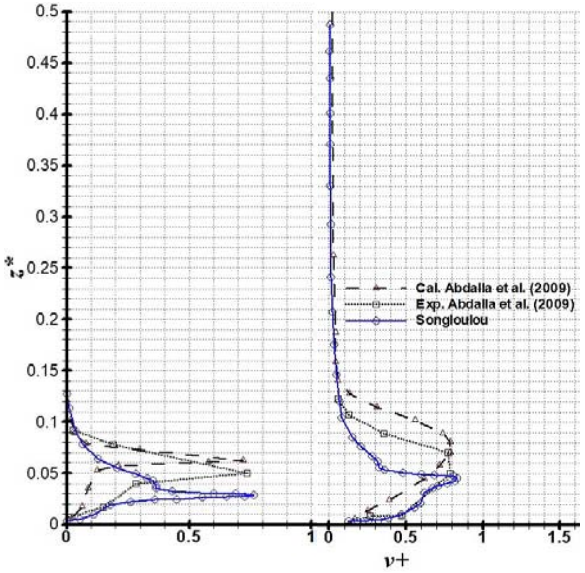

Figure 8: Turbulent intensity structure on the sill at x=11m (left) and x=13m (right)

V. Conclusion

The aim of this study was to investigate the impact of penstock walls on flow characteristics within the penstock and at its outlet. More precisely, it was to determine the evolution of the friction coefficient in the whole penstock. To carry out this work, two approaches were used. A theoretical approach, based on the direct determination by a commonly used formula (Colebrook-White's formula in this case), and another approach, the graphical, based on the numerical modelling of the structure under study.

In the theoretical approach, five velocities corresponding to the variation of velocity in the water intake for periods of low and high water were used. The coefficient of friction *f* was calculated for four values of absolute roughness ε. The results of this approach for our structures show that whatever the other parameters in the Colebrook-White formula (Reynolds number, diameter and absolute roughness), only absolute roughness has a visible impact on the result obtained. This can't be true, as clogging reduces the diameter and consequently modifies the flow rate.

In the numerical approach, we looked for the maximum thickness of the asperities influencing the structure of the flow; what we called real absolute roughness. We have thus observed that the maximum value of *f* is found for e=5mm on the low and high walls. The results obtained from this approach show that the coefficient of friction is neither identical on the same wall, nor identical in the same portion. More importantly, it is not identical on the same section of the conduit, contrary to the theoretical approach which is a fixed result in a portion of pipe. In the same way, the impact of the Reynolds number is visible on the evolution of the friction coefficient in the numerical approach. This is not felt in the results of the theoretical approach for our cases. These remarks demonstrate the limitations of the theoretical approach to evaluating and determining head loss in hydraulic structures. The numerical approach would appear to be more useful for planning the maintenance of such structures, and also for optimizing their performance.

We note, however, that apart from the geometric parameters of each structure studied, the usual data available in literature were used (absolute roughness, diameter and density of clear water). It is therefore recommended to take into account the characteristics of the sediments present in each site for the research to be upgraded.

Référence Bibliographique

1. Frédéric E., (2014), Les conduites forcées: principes, aménagements, sécurités, Rapport des travaux, 19p.
2. Olivier C., (2013), Introduction à la turbulence, cours de l'ENSTA-ParisTech 2A. École d'ingénieur. Introduction à la turbulence, ENSTA-ParisTech, France, pp.83. <cel-01228137>.
3. Guidett F., Caleffi M., Doninelli M., Doninelli M., Ardizzoia C., Carlier J. & Meskel R., (2005), Les pertes de charge dans les installations: Le dimensionnement des mitigeurs, Hydraulique, Caleffi France ISSN 1769-0609, 37P.
4. Weisbach J., (1845), Lehrbuch der Ingenieur- und Maschinen-Mechanik, Braunschweig.
5. Darcy H., (1857), Recherches Experimentales Relatives au Mouvement de L'Eau dans les Tuyaux, 2 volumes, Mallet-Bachelier, Paris. 268 pages and atlas. ("Experimental Research Relating to the Movement of Water in Pipes").
6. Colebrook C.F., (1939), "Turbulent flow in pipes with particular reference to the transition region between the smooth and rough pipe laws", J Inst Civil Engineers, London, Vol. 11, pp. 133-156.
7. Energy of Cameroon (ENEO) S.A.
8. Colebrook C.F. & White C.M., (1937), "Experiments with Fluid Friction in Roughened Pipes", Proc. Roy. Soc., Series A, 161, 367.
9. Tchawe T., Djiako T., Kenmeugne B., Tcheukam-Toko D., (2018), "Numerical Study of the Flow Upstream of a Water Intake Hydroelectric Dam in Stationary Regime". American Journal of Energy Research, 2018, Vol. 6, No. 2, 35-41.

10. Tcheukam-Toko D., Kongue L., Koueni-Toko C., Mouangue R. & Bélorgey M., (2012), Numerical Simulation and Experimental Validation of Boundary Layer Generated by a Turbulent Flow on a hydraulically Smooth Bed, Res. J. of Applied Sci., Vol. 7(2). pp.108-112.
11. Levin L., (1966), Difficultés du calcul des pertes de charge linéaires dans les conduites forcées, *La Houille Blanche,* N° 1-1966.
12. Moss W.D. & Baker S., (1980), Re-circulating Flows Associated with Two-dimensional Steps, Aeronautics Quarterly, 151–172.
13. Abdalla I. E., Yang Z. & Cook M., (2009), Computational analysis and flow structure of a transitional separated-reattached flow over a surface mounted obstacle and a forward-facing step, International Journal of Computational Fluid Dynamics, Vol. 23, No. 1, 25–57.

This page is intentionally left blank

Global Journal of Researches in Engineering: A Mechanical and Mechanics Engineering
Volume 24 Issue 2 Version 1.0 Year 2024
Type: Double Blind Peer Reviewed International Research Journal
Publisher: Global Journals
Online ISSN: 2249-4596 & Print ISSN: 0975-5861

Thermal Vibration of Thick FGM Circular Cylindrical Shells by using Fully Homogeneous Equation and TSDT

By C. C. Hong
Hsiuping University of Science and Technology

Abstract- The third-order shear deformation theory (TSDT) effects on functionally graded material (FGM) thick circular cylindrical shells with entirely homogeneous equation under thermal vibration were investigated by using the generalized differential quadrature (GDQ) method. The nonlinear coefficient term of displacement field of TSDT was used in the equations of motion for thermal vibration of FGM thick circular cylindrical shells. Parametric effects of environment temperature and FGM power law index on the thermal stress and centre deflection of FGM thick circular cylindrical shells were investigated.

Keywords: shear deformation theory, sinusoidal, stress, displacement, environment temperature, shear correction coefficient.

GJRE-A Classification: LCC: TA654, TA660.C9

Strictly as per the compliance and regulations of:

Thermal Vibration of Thick FGM Circular Cylindrical Shells by using Fully Homogeneous Equation and TSDT

C. C. Hong

Abstract- **The third-order shear deformation theory (TSDT) effects on functionally graded material (FGM) thick circular cylindrical shells with entirely homogeneous equation under thermal vibration were investigated by using the generalized differential quadrature (GDQ) method. The nonlinear coefficient term of displacement field of TSDT was used in the equations of motion for thermal vibration of FGM thick circular cylindrical shells. Parametric effects of environment temperature and FGM power law index on the thermal stress and centre deflection of FGM thick circular cylindrical shells were investigated.**

Keywords: shear deformation theory, sinusoidal, stress, displacement, environment temperature, shear correction coefficient.

I. Introduction

Some studies of shear deformation effects in functionally graded material (FGM) shells were presented. In 2018, Cong et al. [1] used Reddy's third-order shear deformation theory (TSDT) for the nonlinear displacements to study the time response of displacements of double curves shallow shells. The effecting numerical solutions for honeycomb materials in geometrical parameters, material properties and damping loads were presented. In 2017, Sobhaniaragh et al. [2] used the TSDT for the displacements to study the buckling loads of FGM carbon nano-tube (CNT)-reinforced shells in an environment (room temperature 300K) without thermal strains, parametric effects on material properties and critical buckling loads were presented by using the generalized differential quadrature (GDQ) method. In 2017, Dung and Vuong [3] used an analytical method with TSDT to study the buckling of FGM shells in elastic foundation under thermal environment and external pressure. In 2016, Dai et al. [4] presented a 2000-2015 review focused on coupled mechanics, e.g. thermo-mechanical responses with the first-order shear deformation theory (FSDT) models, HSDT models in widely used TSDT to study the bending, buckling, free and forced vibrations of FGM cylindrical shells by using various theoretical, analytical and numerical methods. In 2016, Fantuzzi et al. [5] used the numerical GDQ methods to study the free vibration of FGM spherical and cylindrical shells, frequency solutions in FGM exponent number and thickness ratio were included. There were some numerical studies in the thick shells. In 2016, Kar and Panda [6] used the code of finite element method (FEM) and the TSDT displacements to get the numerical static bending results of deflections and stresses for the heated FGM spherical shells under thermal load and thermal environment. In 2015, Kurtaran [7] used the methods of GDQ and FSDT to get the numerical transient results of moderately thick laminated composite spherical and cylindrical shells. In 2012, Viola et al. [8] presented static analyses of FGM cylindrical shells under mechanical loading by using the GDQ method and a 2D unconstrained third-order shear deformation theory (UTSDT). The numerical solutions for stresses without thermal effect are obtained. In 2010, Sepiani et al. [9] used the FSDT formulation to get the numerical free vibration and buckling results for the FGM cylindrical shells without considering the thermal effect.

Many GDQ computational experiences in the composited FGM shells and plates were presented by including and considering the effects of thermal temperature of environment and heating loads. In 2017, Hong [10] presented the numerical thermal vibration results of FGM thick plates by considering the FSDT model and the varied shear correction factor effects. In 2017, Hong [11] presented the numerical thermal vibration and flutter results of a supersonic air flowed over FGM thick circular cylindrical shells by considering the FSDT model and the varied shear correction factor effects. In 2017, Hong [12] presented the numerical displacement and stresses results of FGM thin laminated magnetostrictive shells by considering with velocity feedback and suitable control gain values under thermal vibration. In 2016, Hong [13] presented the thermal vibration of Terfenol-D FGM circular cylindrical shells by considering the FSDT model and the constant modified shear correction factor effects. The computational GDQ solutions for the parametric effects of thickness of mounted Terfenol-D layer, control gain values, temperature of environment and power law index were investigated. In 2016, Hong [14] presented the transient response of Terfenol-D FGM circular cylindrical shells without considering the shear deformation effects. The computational GDQ solutions for the normal

Author: Department of Mechanical Engineering, Hsiuping University of Science and Technology, Taichung, Taiwan, ROC.
e-mail: cchong@mail.hust.edu.tw

direction displacement and thermal stress were obtained. In 2016, Hong [15] presented the investigation of rapid heating-induced vibration of Terfenol-D FGM circular cylindrical shells. The computational GDQ solutions for both the amplitudes of displacement and stress are increasing with rapid heating value. In 2015, Hong [16] presented the rapid heating-induced vibration of Terfenol-D FGM cylindrical shells with FSDT transverse shear effects. The computational GDQ solutions for thermal stresses and centre deflections in the parametric effects of magnetostrictive layer thickness, control gain values, temperature of environment, power law index of FGM shells and applied heat flux were obtained. In 2014, Hong [17] presented the thermal vibration and transient response of Terfenol-D FGM plates by considering the FSDT model and the varied modified shear correction factor effects. The computational GDQ solutions for the effect of different mechanical boundary conditions were investigated. In 2014, Hong [18] presented the rapid heating-induced vibration of Terfenol-D FGM circular cylindrical shells without considering the effects of shear deformation. The computational GDQ solutions for the displacement of Terfenol-D FGM shells versus the thickness of Terfenol-D is stable for all power law index values. It was interesting to investigate the thermal stresses and centre displacement of GDQ computation in this nonlinear TSDT vibration approach and the varied effects of shear correction coefficient of FGM circular cylindrical shells with four edges in simply supported boundary conditions. Two parametric effects of environment temperature and FGM power law index on the thermal stress and centre displacement of FGM circular cylindrical shells including the effect of varied shear correction coefficient were also investigated.

II. Formulation Procedure

For a two-material FGM circular cylindrical shell is shown in *Fig. 1* with thickness h_1 of inner layer FGM material 1 and thickness h_2 of outer layer FGM material 2, L is the axial length of FGM shells, h^* is the total thickness of FGM shells. The material properties of power-law function of FGM shells are considered with Young's modulus E_{fgm} of FGM in standard variation form of power law index R_n. The others are assumed in the simple average form [19]. The properties of individual constituent material of FGMs are functions of environment temperature T. The time-dependent of nonlinear displacements u, v and w of thick FGM circular cylindrical shells are assumed in the nonlinear coefficient c_1 term of TSDT equations can be referred to the displacement equations [20], with the parameters u_0 and v_0 are tangential displacements in the in-surface coordinates x and θ axes direction, respectively, w is transverse displacement in the out of surface coordinates z axis direction of the middle-plane of shells, ϕ_x and ϕ_θ are the shear rotations, R is the middle-surface radius of FGM shell, t is time. Coefficient for $c_1 = \frac{4}{3(h^*)^2}$ is used in the TSDT expression. Thus $c_1 = 0$ is used and became the FSDT mode.

For the normal direction stresses (σ_x and σ_θ) and the shear stresses ($\sigma_{x\theta}$, $\sigma_{\theta z}$ and σ_{xz}) in the thick FGM circular cylindrical shells under temperature difference ΔT for the kth layer can be referred to the constitutive equations in terms of stresses, stiffness and strains [21-22], with the parameters α_x and α_θ are the coefficients of thermal expansion, $\alpha_{x\theta}$ is the coefficient of thermal shear, $\overline{Q}_{ij}$ is the stiffness of FGM shells. ε_x, ε_θ and $\varepsilon_{x\theta}$ are in-plane strains, not negligible $\varepsilon_{\theta z}$ and ε_{xz} are shear strains.

A temperature difference ΔT between the FGM shell and curing area is given in functions of cylindrical coordinates x, θ and t. The heat conduction equation in simple form for the FGM shell in the cylindrical coordinates is used [13]. The dynamic equations of motion with TSDT for an FGM shell can be referred to the partial derivatives of external forces, thermal loads, mechanical loads and inertia terms [23], with the parameters $I_i = \sum_{k=1}^{N^*} \int_k^{k+1} \rho^{(k)} z^i dz$, ($i$= 0, 1, 2,…, 6), in which N^* is total number of layers, $\rho^{(k)}$ is the density of kth ply. $J_i = I_i - c_1 I_{i+2}$, $(i = 1,4)$, $K_2 = I_2 - 2c_1 I_4 + c_1^2 I_6$.

The Von Karman type of strain-displacement relations with $\frac{\partial v_0}{\partial z} = \frac{-v_0}{R}$, $\frac{\partial u_0}{\partial z} = \frac{-u_0}{R}$ and $\frac{\partial w}{\partial z} = \frac{\partial \phi_x}{\partial z} = \frac{\partial \phi_\theta}{\partial z} = 0$ are used to simplify the strain equations. Thus the dynamic equilibrium differential equations in the cylindrical coordinates with TSDT of FGM shells in terms of partial derivatives of displacements and shear rotations subjected to partial derivatives of thermal loads, mechanical loads (p_1, p_2, q) and inertia terms can be derived in matrix forms. By assuming that mid-plane strain terms $\frac{1}{2}(\frac{\partial w}{\partial x})^2$, $\frac{\partial w}{\partial x}\frac{\partial w}{R\partial \theta}$ and $\frac{1}{2}(\frac{\partial w}{R\partial \theta})^2$ are in constant values, the relative parameters are listed as follows,

$$(A_{i^s j^s}, B_{i^s j^s}, D_{i^s j^s}, E_{i^s j^s}, F_{i^s j^s}, H_{i^s j^s}) = \int_{\frac{-h^*}{2}}^{\frac{h^*}{2}} \overline{Q}_{i^s j^s}(1, z, z^2, z^3, z^4, z^6)dz, \ (i^s, j^s = 1,2,6),$$

$$(A_{i^* j^*}, B_{i^* j^*}, D_{i^* j^*}, E_{i^* j^*}, F_{i^* j^*}, H_{i^* j^*}) = \int_{\frac{-h^*}{2}}^{\frac{h^*}{2}} k_\alpha \overline{Q}_{i^* j^*}(1, z, z^2, z^3, z^4, z^5)dz, \ (i^*, j^* = 4,5), \quad (1)$$

in which p_1 and p_2 are external in-plane distributed forces in x and θ direction respectively. q is external pressure load, k_α is the shear correction coefficient, computed and varied values of k_α are usually functions of total thickness of shells, FGM power law index and environment temperature [24]. The $\overline{Q}_{i^s j^s}$ and $\overline{Q}_{i^* j^*}$ for FGM thick circular cylindrical shells with z/R terms cannot be neglected are used in the simple forms in 2010 by Sepiani et al. [9] [24].

The time sinusoidal displacements and shear rotations are varied with $\sin(\omega_{mn} t)$ can be referred [13]. The time sinusoidal temperature difference ΔT of thermal vibration is assumed in the following simple equation varied with $\sin(\gamma t)$,

$$\Delta T = \frac{z}{h^*} \bar{T}_1 \sin(\pi x/L) \sin(\pi\theta/R) \sin(\gamma t), \quad (2)$$

where ω_{mn} is the natural frequency in mode shape subscript numbers m and n of the shells, γ is the frequency of applied heat flux, $\bar{T}_1$ is the amplitude of applied temperature.

The GDQ numerical method is presented and referred [17][25-27]. The boundary conditions in dynamic GDQ discrete equations approach are to be considered for four sides simply supported, not symmetric, orthotropic of laminated FGM thick circular cylindrical shells and assumed that $A_{16} = A_{26} = 0$, $B_{16} = B_{26} = 0$, $D_{16} = D_{26} = 0$, $E_{16} = E_{26} = 0$, $F_{16} = F_{26} = 0$, $H_{16} = H_{26} = 0$, $A_{45} = D_{45} = F_{45} = 0$ under sinusoidal temperature loading. For a typical grid point (i, j), the dynamic GDQ discrete equations can be rewritten into the matrix form as follows,

$$[A]\{W^*\} = \{B\}, \quad (3)$$

where $[A]$ is a dimension of N^{**} by N^{**} coefficient matrix ($N^{**} = (N-2)\times(M-2)\times 5$), $\{W^*\}$ is a N^{**} th-order unknown column vector and $\{B\}$ is a N^{**} th-order row external loads vector.

III. Numerical Results

The FGM material 1 is SUS304, the FGM material 2 is Si_3N_4 used for the numerical computations under four sides simply supported. The frequency γ of applied heat flux for the thermal loads is given in the heat conduction equation can be reduced and simplified [13]. It is needed to get the calculation values of ω_{mn} under $p_1 = p_2 = 0$ and $q = 0$ for the free vibration. It is reasonable to assumed that u_0, v_0, w, ϕ_x and ϕ_θ are expressed in the referred time sinusoidal form of free vibration and expressed in the referred entirely homogeneous matrix equation [29] with varied parameters $m\pi/L$ and $n\pi/R$. The determinant of the coefficient matrix in the entirely homogeneous equation vanishes for obtaining non-trivial solution of amplitudes, thus the ω_{mn} and γ can be found.

The non-dimensional frequency $\Omega = (\omega_{11} L^2/h^*)\sqrt{\rho_1/E_1}$ and $f^* = 4\pi\omega_{11} R\sqrt{I_2/A_{11}}$ for SUS304/Si_3N_4 thick circular cylindrical shells with entirely homogeneous equation and TSDT under free vibration are compared with published literature as shown in *Table 1,* in which ω_{11} is the fundamental first natural frequency $m = n = 1$, ρ_1 is the density of FGM material 1. The present value of Ω =1.906986 on c_1 =0.925925/mm^2, L/h^* =10, h^* =1.2mm, T=700K, R_n =1 is in close to the value of Ω =1.65127 with the material variation type A, three layers thickness ratio 1-8-1, the L directional radius of curvature is ∞, L/h^* =10, R_n =1 for the FGM sandwich shell presented by Chen et al. [28]. The present value of f^* =5.041756 at L/h^* =10, h^* =2mm, T=300K, R_n =0.5 is in close to the value of f^* =5.10 on n =9 with silicon nitride–nickel under classical shell theory (CST), no external pressure (Ke = 0) by Sepiani et al. [9].

The following coordinates x_i and θ_j for the grid points numbers N and M of FGM thick circular cylindrical shells are used to study the GDQ results,

$$x_i = 0.5[1 - \cos\left(\frac{i-1}{N-1}\pi\right)]L, \ i = 1,2,\ldots,N,$$

$$\theta_j = 0.5[1 - \cos\left(\frac{j-1}{M-1}\pi\right)]R, \ j = 1,2,\ldots,M. \quad (4)$$

The convergence of centre deflection $w(L/2, 2\pi/2)$ (mm) in the thermal vibration under c_1 =0.925925 and c_1 =0 for FGM thick circular cylindrical shells L/h^* = 10 with applied heat flux γ =0.2618004/s and L/h^* =5 with γ =0.2618019/s, respectively at t = 6s, $L/R = 1$, h^* =1.2mm, $h_1 = h_2$ =0.6mm, T=100K,

$\bar{T}_1$ =100K are presented in *Table 2.* Considering the varied effects of k_α and ω_{11} for three values of R_n, in the nonlinear case of c_1 =0.925925/mm^2: (a) for value of R_n =0.5, k_α =0.111874 and ω_{11} =0.0001156/s are obtained. (b) for value of R_n =1, k_α =0.149001 and ω_{11} =0.0001151/s are obtained. (c) for value of R_n =2, k_α =0.231364 and ω_{11} =0.000114/s are obtained. In the linear case of c_1 =0/mm^2: (d) for value of R_n =0.5, k_α =0.111874 and ω_{11} =0.001000/s are obtained. (e) for value of R_n =1, k_α =0.149001 and ω_{11} =0.001000/s are obtained. (f) for value of R_n =2, k_α =0.231364 and ω_{11} =0.001000/s are obtained. The error accuracy is 0.000011 for the $w(L/2,2\pi/2)$ in R_n =0.5 and L/h^* = 10. The $N\times M$ =13×13 grid points can be used in the following GDQ computations of time responses for deflection and stress.

The $w(L/2,2\pi/2)$ (mm) for the thermal vibration of FGM thick circular cylindrical shells are calculated with varied γ and ω_{11}. The γ values are decreasing from γ =15.707960/s at t =0.1s to γ =0.523601/s at t =3.0s used for L/h^* =5, from γ =15.707963/s at t =0.1s to γ =0.523599/s at t =3.0s used for L/h^* =10. *Fig. 2* shows the response values of $w(L/2,2\pi/2)$ (mm) versus time t under c_1 =0.925925/mm^2 and c_1 =0 for thick L/h^* =5 and 10, respectively, $L/R=1$, $R_n=1$, k_α =0.120708, T=600K, $\bar{T}_1$ =100K during t =0.1s-3.0s. The maximum absolute value of $w(L/2,2\pi/2)$ is 33.955818mm occurs at t =0.1s for thick L/h^* =5 with c_1 =0.925925/mm^2 and γ =15.707963/s. The maximum absolute value of $w(L/2,2\pi/2)$ is 267.064789mm occurs at t = 0.1s for thick L/h^* =10 with c_1 =0/mm^2 and γ =15.707963/s.

Usually the normal direction stress σ_x and shear stress $\sigma_{x\theta}$ are three-dimensional components and in functions of x, θ and z for the thermal vibration of nonlinear TSDT FGM circular cylindrical shells as shown in *Fig. 3.* Typically their values vary through the thickness direction of circular cylindrical shells. *Fig. 3a* shows the normal direction stress σ_x(GPa) versus z/h^* and *Fig. 3b* shows the shear stress $\sigma_{x\theta}$ (GPa) versus z/h^* on centre position $x=L/2$ and $\theta=2\pi/2$ of FGM circular cylindrical shells, respectively at t =3.0s for thick a/h^* =10 with c_1 =0.925925/mm^2 and R_n =1. The value 1.702E-03GPa of σ_x on z =-0.5 h^* is found in the greater value than the value 1.955E-04GPa of $\sigma_{x\theta}$ on z =0.5 h^*, thus the σ_x can be treated as the dominated stress. *Figs. 3c-3d* show the time responses of the σ_x(GPa) on centre position of inner surface z =-0.5 h^* for R_n =1, thick L/h^* =5 and 10 with c_1 =0.925925/mm^2, respectively. The maximum value of σ_x is 2.005E-03GPa occurs at t =0.1s in the periods t =0.1s-3s for thick L/h^* =5.

In *Fig. 4* shows the response values of $w(L/2,2\pi/2)$ (mm) versus T in 100K, 600K and 1000K with R_n values from 0.1 to 10 for thick L/h^* =5 and 10, respectively under c_1 =0.925925/mm^2, $\bar{T}_1$ =100K, γ and k_α at t =0.1s. *Fig. 4a* shows the curves of $w(L/2,2\pi/2)$ vs. T and R_n for the L/h^* =5 case, the maximum absolute value of $w(L/2,2\pi/2)$ is 49.057815mm occurs in T=1000K for R_n = 2. The $w(L/2,2\pi/2)$ absolute values are all decreasing versus T from T=600K to T=1000K, for R_n =5 only, it can withstand for higher T=1000K. *Fig. 4b* shows the curves of $w(L/2,2\pi/2)$ vs. T and R_n for the L/h^* =10 case, they are almost located in the same curves for all value of R_n. The maximum value of $w(L/2,2\pi/2)$ is 7.039238mm occurs in T=1000K for all value of R_n. The $w(L/2,2\pi/2)$ values are all increasing versus T for all value of R_n, the amplitude $w(L/2,2\pi/2)$ of the L/h^* =10 cannot withstand for higher T=1000K.

In *Fig. 5* shows the σ_x(GPa) on centre position of inner surface z =-0.5 h^* versus T and all different values R_n for the thermal vibration of thick L/h^* =5 and 10 cases. *Fig. 5a* shows the curves of σ_x vs. T and R_n for the L/h^* =5 case, the values of σ_x versus T are all increasing from T=100K to T=600K and then all decreasing from T=600K to T=1000K for all value of R_n. The maximum value of σ_x is 0.002018GPa occurs on T=600K for R_n =2. The stress σ_x of the L/h^* =5 can withstand for higher T=1000K. *Fig. 5b* shows the curves of σ_x vs. T and R_n for the L/h^* =10 case, they are all located in the same curves for all value of R_n, the values of σ_x versus T are all increasing from T=100K to T=600K and then all decreasing from T=600K to T=1000K for all value of R_n. The maximum value of σ_x is 0.001745GPa occurs on T=600K. The stress σ_x of the L/h^* =10 can withstand for higher T=1000K.

IV. Conclusions

The GDQ solutions could be calculated and investigated for the deflections and stresses in the thermal vibration of FGM thick circular cylindrical shells by considering the varied effects of shear correction coefficient and nonlinear coefficient c_1 term of TSDT. The novel contribution of the GDQ stress and deflection solutions work is to investigate the effects of over estimation and under estimation of nonlinear coefficient term of TSDT in the thermal vibration of FGM circular shells. The natural frequency and parameter results of frequency including the entirely element effect in the homogeneous equation are also investigated and used to calculate the corresponding results in dynamic

convergence, vibration response of deflections and stresses.

References Références Referencias

1. Cong, P.H., Khanh, N.D., Khoa, N.D., Duc, N.D., 2018. New approach to investigate nonlinear dynamic response of sandwich auxetic double curves shallow shells using TSDT. Composite Structures 185, 455–465.
2. Sobhaniaragh, B., Nejati, M., Mansur, W.J., 2017. Buckling modelling of ring and stringer stiffened cylindrical shells aggregated by graded CNTs. Composites Part B 124, 120–133.
3. Dung, D.V., Vuong, P.M., 2016. Analytical investigation on buckling and postbuckling of FGM toroidal shell segment surrounded by elastic foundation in thermal environment and under external pressure using TSDT. Acta Mechanica 228, 3511–3531.
4. Dai, H.L., Rao, Y.N., Dai, T., 2016. A review of recent researches on FGM cylindrical structures under coupled physical interactions 2000–2015. Composite Structures 152, 199–225.
5. Fantuzzi, N., Brischetto, S., Tornabene, F., Viola, E., 2016. 2D and 3D shell models for the free vibration investigation of functionally graded cylindrical and spherical panels. Composite Structures 154, 573–590.
6. Kar, V.R., Panda, S.K., 2016. Nonlinear thermomechanical deformation behaviour of P-FGM shallow spherical shell panel. Chinese Journal of Aeronautics 29, 173–183.
7. Kurtaran, H., 2015. Geometrically nonlinear transient analysis of moderately thick laminated composite shallow shells with generalized differential quadrature method. Composite Structures 125, 605–614.
8. Viola, E., Rossetti, L., Fantuzzi, N., 2012. Numerical investigation of functionally graded cylindrical shells and panels using the generalized unconstrained third order theory coupled with the stress recovery. Composite Structures 94, 3736–3758.
9. Sepiani, H.A., Rastgoo, A., Ebrahimi, F., Arani, A.G., 2010. Vibration and buckling analysis of two-layered functionally graded cylindrical shell considering the effects of transverse shear and rotary inertia. Materials and Design 31, 1063–1069.
10. Hong, C.C., 2017. Varied effects of shear correction on thermal vibration of functionally graded material plates. Journal of Mechanical Engineering and Biomechanics 2, 1–7.
11. Hong, C.C., 2017. Effects of varied shear correction on the thermal vibration of functionally-graded material shells in an unsteady supersonic flow. Aerospace 4, 1–15.
12. Hong, C.C., 2017. The GDQ method of thermal vibration laminated shell with actuating magnetostrictive layers. International Journal of Engineering and Technology Innovation 7, 188–200.
13. Hong, C.C., 2016. Thermal vibration of magnetostrictive functionally graded material shells with the transverse shear deformation effects. Applications and Applied Mathematics: An International Journal 11, 127–151.
14. Hong, C.C. 2016. Transient response of functionally graded material circular cylindrical shells with magnetostrictive layer. Journal of Mechanics 32, 473–478.
15. Hong, C.C., 2016. Rapid heating-induced vibration of composite magnetostrictive shells. Mechanics of Advanced Materials and Structures 23, 415–422.
16. Hong, C.C., 2015. Rapid heating induced vibration of magnetostrictive functionally graded material cylindrical shells with transverse shear effects. Universal Journal of Structural Analysis 3, 35–47.
17. Hong, C.C., 2014. Thermal vibration and transient response of magnetostrictive functionally graded material plates. European Journal of Mechanics - A/Solids 43, 78–88.
18. Hong, C.C., 2014. Rapid heating induced vibration of circular cylindrical shells with magnetostrictive functionally graded material. Archives of Civil and Mechanical Engineering 14, 710–720.
19. Chi, S.H., Chung, Y.L., 2006. Mechanical behavior of functionally graded material plates under transverse load, Part I: Analysis. International Journal of Solids and Structures 43, 3657–3674.
20. Lee, S.J., Reddy, J.N., Rostam-Abadi, F., 2004. Transient analysis of laminated composite plates with embedded smart-material layers. Finite Elements in Analysis and Design 40, 463–483.
21. Lee, S.J., Reddy, J.N., 2005. Non-linear response of laminated composite plates under thermomechanical loading. Int. J. of Non-lin. Mech. 40, 971–985.
22. Whitney, J.M., 1987. Structural analysis of laminated anisotropic plates. Lancaster: Pennsylvania, USA, Technomic Publishing Company, Inc.
23. Reddy, J.N., 2002. Energy principles and variational methods in applied mechanics. Wiley, New York.
24. Hong, C.C., 2014. Thermal vibration of magnetostrictive functionally graded material shells by considering the varied effects of shear correction coefficient. International Journal of Mechanical Sciences 85, 20–29.
25. Hong, C.C., 2007. Thermal vibration of magnetostrictive material in laminated plates by the GDQ method. The Open Mech. J. 1, 29–37.
26. Bert, C.W., Jang, S.K., Striz, A.G., 1989. Nonlinear bending analysis of orthotropic rectangular plates by the method of differential quadrature. Computational Mechanics 5, 217–226.

27. Shu, C., Du, H., 1997. Implementation of clamped and simply supported boundary conditions in the GDQ free vibration analyses of beams and plates. International Journal of Solids and Structures 34, 819–835.
28. Chen, H., Wang, A., Hao, Y., Zhang, W., 2017. Free vibration of FGM sandwich doubly-curved shallow shell based on a new shear deformation theory with stretching effects. Composite Structures 179, 50–60.
29. Hong, C.C., 2019. GDQ computation for thermal vibration of thick FGM plates by using fully homogeneous equation and TSDT. Thin-Walled Structures 135, 78–88.

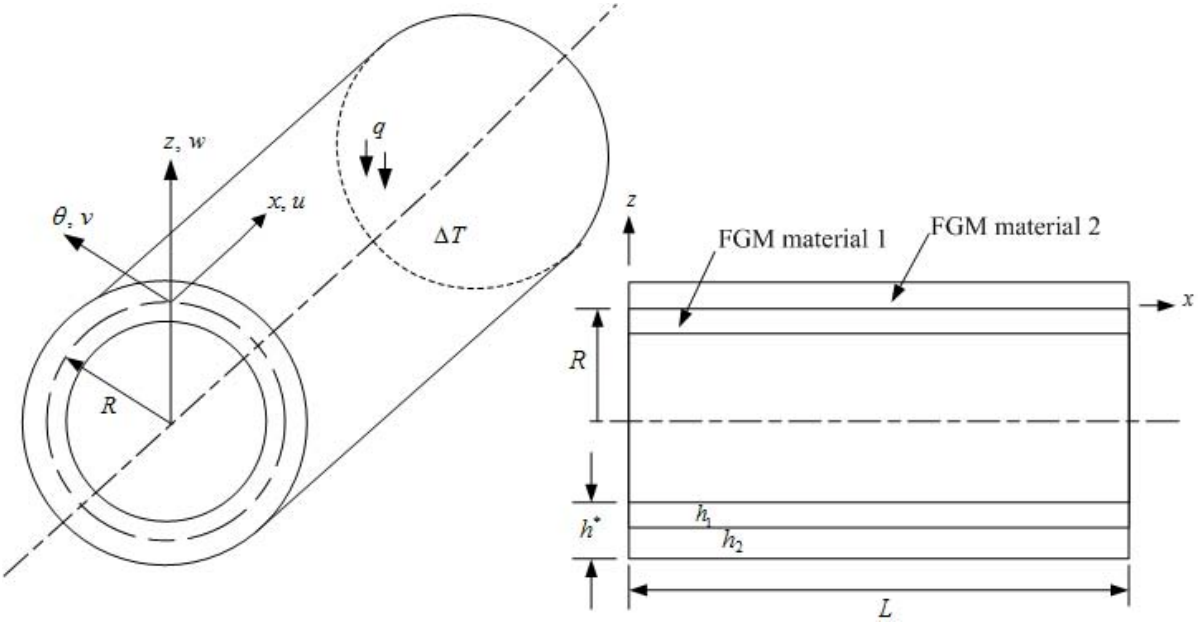

Fig. 1: Two-material FGM circular cylindrical shell

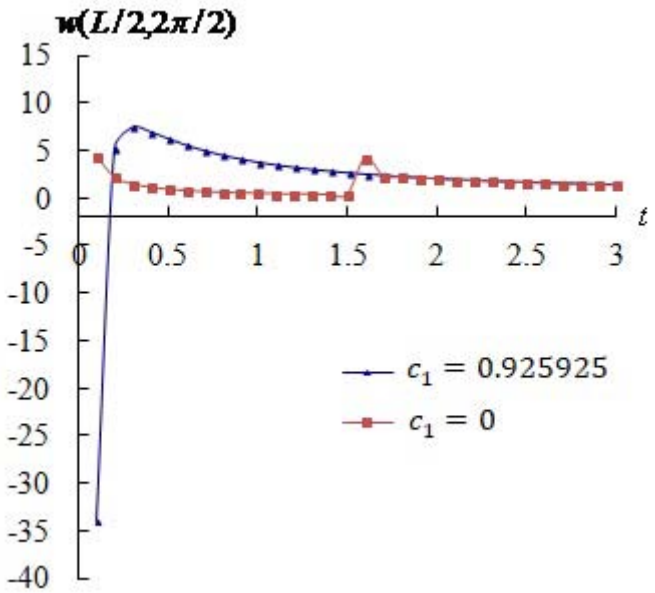

Fig. 2a: $w(L/2,2\pi/2)$ versus t for $L/h^* = 5$

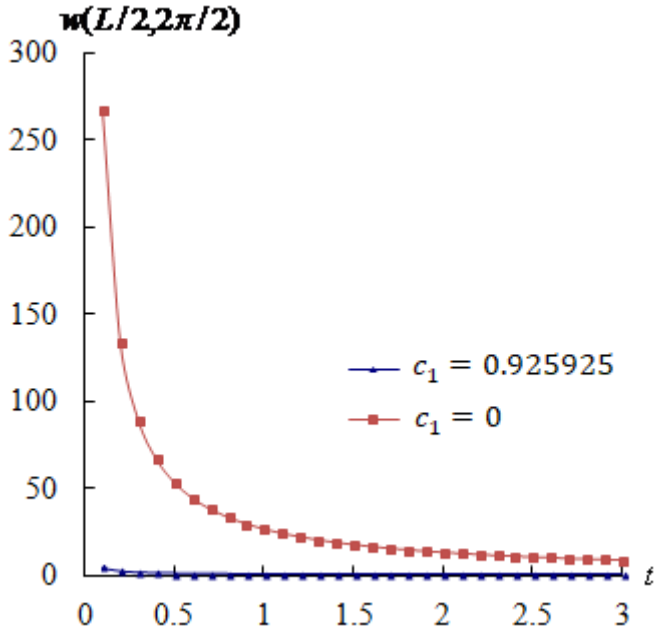

Fig. 2b: $w(L/2,2\pi/2)$ versus t for $L/h^* = 10$

Fig. 2: $w(L/2,2\pi/2)$ (mm) versus t (s) for $L/h^* = 5$ and 10

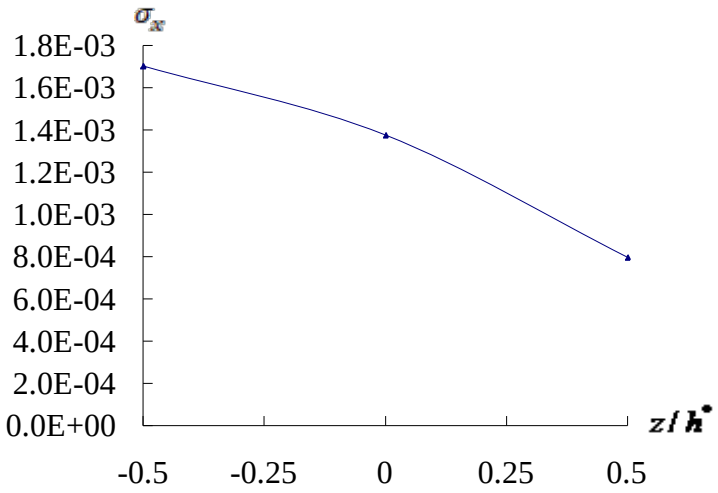

Fig. 3a: σ_x versus z/h^* for $L/h^* = 10$

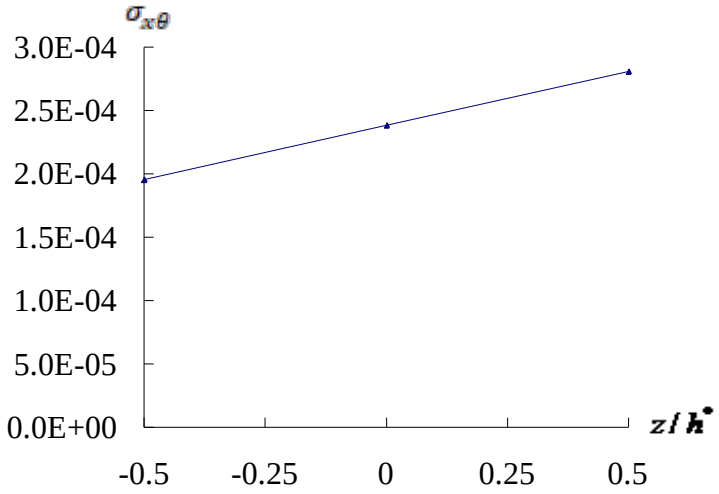

Fig. 3b: $\sigma_{x\theta}$ versus z/h^* for $L/h^*=10$

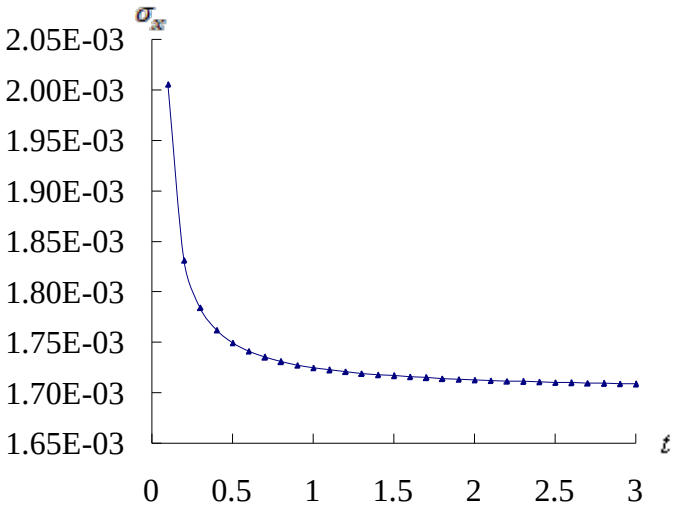

Fig. 3c: σ_x versus t for $L/h^*=5$

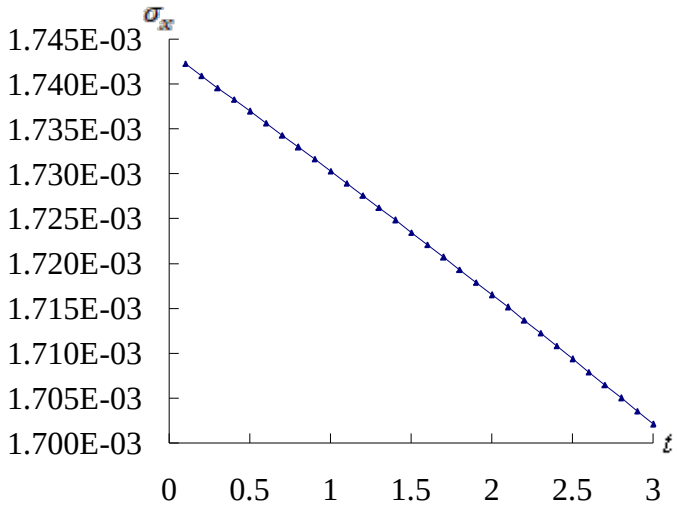

Fig. 3d: σ_x versus t for $L/h^*=10$

Fig. 3: Stresses (GPa) versus z/h^* and t (s) for $L/h^*=5$ and 10

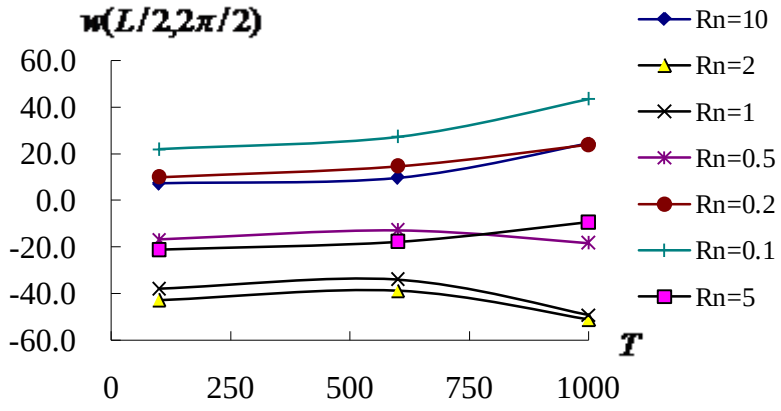

Fig. 4a: $w(L/2,2\pi/2)$ versus *T* for $L/h^*=5$ with R_n from 0.1 to 10

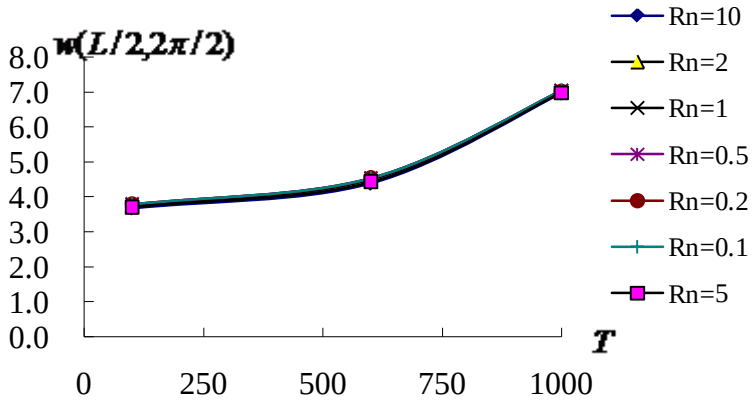

Fig. 4b: $w(L/2,2\pi/2)$ versus *T* for $L/h^*=10$ with R_n from 0.1 to 10

Fig. 4: $w(L/2,2\pi/2)$ (mm) versus *T* (K) for $L/h^*=5$ and 10

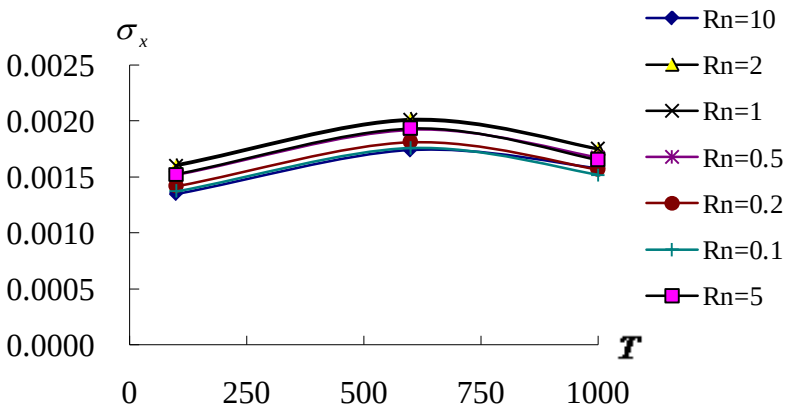

Fig. 5a: σ_x versus T for $L/h^*=5$

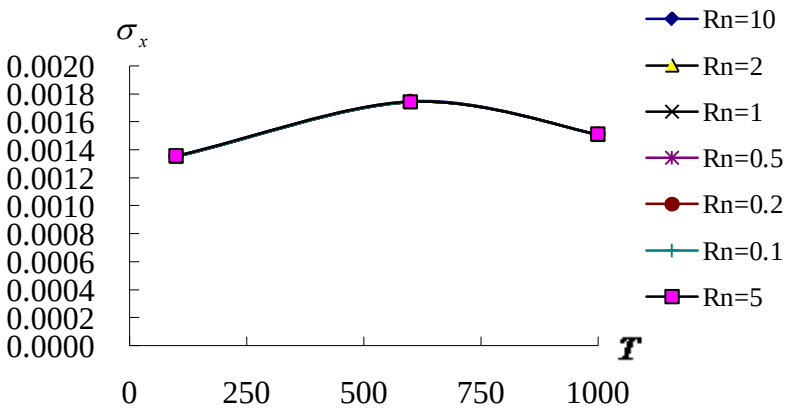

Fig. 5b: σ_x versus T for $L/h^* = 10$

Fig. 5: σ_x(GPa) versus T (K) for $L/h^* = 5$ and 10

Table 1: Compared values of Ω and f^* for $SUS304/Si_3N_4$

c_1 (1/mm²)	h^* (mm)	Ω		f^*	
		Present method, T=700K $R_n = 1$	Chen et al. 2017, type A, 1-8-1 $R_n = 1$ [28]	Present method, T=300K, $R_n = 0.5$	Sepiani et al. 2010, silicon nitride–nickel [9]
0.925925	1.2	1.906986	1.65127	0.517127	-
0.333333	2	11.14739	-	5.041756	5.10
0.000033	200	17704.31	-	800796.6	-
0.000014	300	3771.748	-	253980.0	-

Table 2: Dynamic convergence of the nonlinear TSDT FGM thick circular cylindrical shells

c_1 (1/mm²)	L/h^*	GDQ grids	$w(L/2, 2\pi/2)$ (mm) at $t = 6s$		
		$N \times M$	$R_n = 0.5$	$R_n = 1$	$R_n = 2$
0.925925	10	7×7	5.093878	5.113268	5.162740
		9×9	5.086901	5.107157	5.157094
		11×11	5.086960	5.107170	5.157115
		13×13	5.086899	5.107180	5.157098
	5	7×7	0.591193	0.595686	0.615068
		9×9	0.589491	0.594395	0.614112
		11×11	0.589487	0.594404	0.614114
		13×13	0.589495	0.594400	0.614107
0	10	7×7	23.807663	20.502832	21.591730
		9×9	3.210114	3.212350	3.193146
		11×11	3.216680	3.219491	3.210730
		13×13	3.213940	3.215927	3.197326
	5	7×7	0.524448	0.621863	0.832298
		9×9	0.505710	0.599383	0.798741
		11×11	0.505719	0.599400	0.798779
		13×13	0.505719	0.599401	0.798781

Global Journal of Researches in Engineering: A Mechanical and Mechanics Engineering
Volume 24 Issue 1 Version 1.0 Year 2024
Type: Double Blind Peer Reviewed International Research Journal
Publisher: Global Journals
Online ISSN: 2249-4596 & Print ISSN: 0975-5861

The Main Methodological Postulate of Pyrometry and the Need for its Revision

By Alexandr Frunze

Abstract- The analysis of the methodological principles on which pyrometry is based is carried out. Special attention is paid to the main methodological postulate and its consequences. The roots of its formation are considered. It is shown that the large methodological errors characteristic of pyrometry are a direct consequence of the system of priorities arising from this postulate. A new basic methodological postulate of pyrometry is formulated, it is shown that the development of the ideas contained in it will reduce the number of methodological errors by an order of magnitude or more, and the necessary and sufficient conditions for this reduction are formulated.

Keywords: *pyrometry, methodological principles, radiation laws, spectral emissivity, temperature dependence of emissivity, reference means for spectral emissivity.*

GJRE-A Classification: *LCC Code: TJ1-570*

Strictly as per the compliance and regulations of:

The Main Methodological Postulate of Pyrometry and the Need for its Revision

Alexandr Frunze

Abstract- **The analysis of the methodological principles on which pyrometry is based is carried out. Special attention is paid to the main methodological postulate and its consequences. The roots of its formation are considered. It is shown that the large methodological errors characteristic of pyrometry are a direct consequence of the system of priorities arising from this postulate. A new basic methodological postulate of pyrometry is formulated, it is shown that the development of the ideas contained in it will reduce the number of methodological errors by an order of magnitude or more, and the necessary and sufficient conditions for this reduction are formulated.**

Keywords: pyrometry, methodological principles, radiation laws, spectral emissivity, temperature dependence of emissivity, reference means for spectral emissivity.

I. Introduction

The rapid development of microelectronics and microprocessor technology in the last quarter of the 20th century made it possible to bring instrument engineering to a qualitatively higher level. In many industries, the instrumental errors of measuring instruments have decreased to fractions of a percent. Pyrometers are no exception here.

But at the same time, as is known, any of the pyrometry methods has inherent methodical errors[1], the magnitude of which can reach 10 ... 15%, i.e. an order of magnitude or more exceeding the instrumental ones. There are still no ways to *guarantee* their reduction to the level of 1-2%. And the most significant thing is that over the past half century, it has not been possible to reduce the magnitude of these methodological errors in relation to any material whose non-contact temperature measurement may be in demand. And the reason for this, of course, is not at all due to dishonesty or low qualifications of researchers.

II. On the Need to Analyze the Methodology of Pyrometry

The author of this work argues that the problems of pyrometry are methodological in nature. Their solution requires analysis and possible revision of the methodological principles of pyrometry. The work [1] is devoted to this analysis.

Author: e-mail: alex.fru@mail.ru

[1] The errors of the method

For applied science, methodology is understood as a system (complex, interconnected set) of postulates and principles of research activity, which a scientist relies on in the course of obtaining and developing knowledge within a given specific scientific discipline or several scientific disciplines ([2]).

Obviously, there are methodological postulates, principles and approaches common to all branches of technical sciences (the obligation of mathematical calculations or modeling, the correspondence of calculated data to experimental data, etc.), and there are also particular, specific ones that apply only to individual industries or to one specific industry. It is quite obvious that it is not methodological principles and postulates common to all branches of technical sciences that slow down the development of pyrometry, because even in related fields (for example, in contact methods of temperature control) there are no problems of large methodical errors. Therefore, the source of irreducible methodical errors should be sought in specific methodological postulates and principles of pyrometry.

However, the methodological postulates and principles specific to pyrometry have not yet been clearly formulated. The reason is that most specialists in this field have not yet realized that the problems of incessant huge methodical errors are methodical in nature. The desire to formulate methodological principles and postulates that determine the course of development of a particular industry arises only after realizing the futility of trying to solve the problem within the framework of existing knowledge. Half a century of stomping in place on the issue of reducing methodical errors from a 10...20 percent level to units or fractions of a percent just suggests that there is a need to revise the methodological postulates and principles of pyrometry.

III. Methodological Principles and Approaches in Pyrometry

The principles and approaches most characteristic of modern pyrometry are listed below ([1]):

1. Regular resumption of attempts to find the temperature of the measured object only by its radiation, based only on Planck's or Wien's laws, without taking into account its radiative properties.

2. Consideration of the emissivity [2] as a minor, secondary, and even interfering factor, both in theoretical constructions and in the practical implementation of pyrometry methods.
3. The use of only those reference means during verification[3] and calibration that perfectly implement the laws of radiation ("absolutely black bodies", BB).
4. The lack of reference means and measuring instruments of spectral emissivity.
5. The almost universal disregard of the dependence of the spectral emissivity characteristic of most objects on the temperature of the object and on the state of its surface (roughness, the presence of liquids, oil films, etc.).
6. Reduction (both in theoretical calculations and in practice) of the complex influence of emissivity to a one–dimensional effect described by a simple numerical coefficient, with complete disregard for the fact that emissivity is not a coefficient, but a function of at least two variables.
7. The use of various adjustment organs in almost all modern pyrometers, which make it possible to adjust the measurement results in any direction within a fairly wide range.
8. The lack of developed algorithms for determining the actual temperature of an object by its pseudo-temperature (brightness, partial radiation, radiation or spectral ratio), taking into account the temperature dependence of the emissivity characteristic of most objects.

As for paragraphs 3, 4 and 7, they are obvious. The statement of paragraph 2 also becomes obvious when analyzing almost all books published over the past 50 years, the authors of which try to cover pyrometry as a whole, rather than highlight certain selected issues. In these books, the laws of Planck, Wien, Stefan-Boltzmann, Rayleigh-Jeans, Kirchhoff, Lambert are usually described in detail first, and only after that the concept of emissivity is introduced, characterizing the difference between the radiation of real objects and the radiation of the BB.

According to claim 1, measurements in polarized light can be noted [3], the use of multiband spectral-ratio pyrometers with narrow spectral bands [4], the use of spectrometers [5], etc.

As a confirmation of what was said in paragraphs 5, 6 and 8, the following can be cited.

In the known relations present in almost all books on pyrometry, linking the actual temperature of an object T_d with its brightness or radiation temperature, the emissivity appears in the form of constants ε_λ, ε_s:

$$\frac{1}{T_d} = \frac{1}{T_b} + \frac{\lambda}{c_2}\ln \varepsilon_\lambda \qquad (1)$$

where T_d is the actual temperature, K; T_b is the brightness temperature measured by the pyrometer, K; $c_2 = 1.4380 \cdot 10^{-2}$ m·K; λ is the operating wavelength of the monochromatic brightness pyrometer, m; ε_λ is the radiation coefficient of the object at the wavelength λ.

$$T_д = T_r / \sqrt[4]{\varepsilon_s} \qquad (2)$$

where T_d is the actual temperature, K; T_r is the radiation temperature measured by the pyrometer, K; ε_s is the integral radiation coefficient.

However, if we take into account that ε_λ and ε_s are not constants, but functions of wavelength λ and temperature T_d, and instead of *constants* substitute *functions* $\varepsilon(\lambda,T_d)$ in (1) and $\varepsilon_s(T_d)$ in (2), then simple calculation relations (1) and (2) turn into equations unsolvable in analytical form. There are no algorithms for solving these equations in general.

IV. The Main Methodological Postulate of Pyrometry

The analysis of the above methodological principles and approaches characteristic of modern pyrometry allows us to identify something common to all of them without exception. This is the *implicitly postulated priority of radiation laws in this industry over all other laws and patterns* used to determine the temperature of heated bodies by their radiation. It is she who is today the main methodological postulate specific to pyrometry, which hinders its development.

This methodological postulate has a historical origin, since the laws of radiation were formulated back in the XIX century, and there is still no theory that would link the radiative characteristics of a substance with its physico-chemical constants, and at the same time would not diverge from experimental data *in the entire spectral range.*

Of particular importance is the fact that this priority is postulated implicitly, by stealth. None of the researchers claims that finding the *exact* temperature of an object by its radiation without knowing its radiative properties is possible. But in practice, all modern research in pyrometry is aimed precisely at finding the temperature of heated objects without knowing their radiative characteristics. After all, if this succeeds, it will be possible to forget about the dreary measurements of the emissivity, depending on both the state of the object's surface and its temperature. From this point of view, the game is worth the candle, since there are still no devices for measuring emissivity, and experimental installations that allow this to be done are large, expensive, low-mobility, measurements on them require

[2] Further, everywhere by the emissivity of an object we will understand its spectral $\varepsilon(\lambda)$ or temperature-spectral $\varepsilon(\lambda,T)$ emissivity

[3] In Russia, verification is the confirmation by one of the accredited state metrological centers of the declared metrological characteristics of the device being verified

high qualifications and a lot of time. Therefore, the prospect of learning how to measure temperature by radiation without knowing the radiative properties looks very tempting.

The most likely solution to this problem seems to be using spectrometers, so today most research is conducted in this area [5]. However, the possibility of such a solution *for any predetermined material* is not yet obvious.

If we return to the pyrometers, then the following should be noted. The above-mentioned emissivity characterizes the difference between the radiation of a real object and the radiation of an BB. If the differences are small, then the measurement error with a pyrometer calibrated according to the BB is also small. But for many objects that have to be measured with pyrometers, the differences in their radiation spectrum are quite large from the spectrum of the radiation of the BB.

An BB-calibrated pyrometer, by definition, cannot correctly measure the temperature of an object that does not emit as an BB. The error that occurs during such measurements is the main methodical error, it is determined not by the quality of calibration, but by the problem of the measurement method (i.e., the need to measure an object that emits differently from the sample from which the pyrometer was calibrated). How can such an error be reduced or eliminated altogether?
In today's practice, pyrometers are equipped with regulators, with the help of which a certain coefficient can be entered into them, usually taking a value from 0.1 to 0.99...1. This coefficient is usually called the "blackness coefficient", "degree of blackness" or "radiation coefficient". Using this coefficient, the operator can change the measurement result. It is assumed that he knows the "correct" value of this coefficient, and by setting it, he will correct the pyrometer readings and eliminate the mentioned methodical error.

To understand the negative consequences of this approach, you need to ask yourself – where do these coefficients come from? In the best case, measurements once made under these conditions are usually quite rough, with a small number of samples, without fully taking into account all factors affecting the result, without estimating the error. But more often – from literary sources compiled according to the same measurement results, performed by unknown people, unknown when, and with the same disadvantages.

The main thing here is that with this approach, *the correction value is not calculated, but determined experimentally by selecting the radiation coefficient for the value at which the pyrometer will show the correct result (or one that is considered correct for one reason or another)*[4]. Let's add to this that manufacturers do not provide information about what the algorithm for correcting the measurement results of the radiation coefficient entered into this pyrometer is. The latter completely excludes the possibility of correctly accounting for the effect on the pyrometer measurement result of the difference between the radiation spectrum of the measuring object and the frequency response spectrum, the dependence of this difference on the temperature of the object itself, and on the spectral range of the pyrometer, and on the width of the range, and on the state of the surface of the object, and a number of other parameters. As a result, fitting to the expected result remains the only way to correct. In production practice, this leads to the fact that the technologist does not know which of the radiation coefficients to choose from the abundance available in various sources. As a result, the selection is made "by eye" so that the measurement result corresponds to the expected one. This is where users have measurement errors with pyrometers up to 10-20%.

That is, the user is trying to eliminate the methodical error, but the method used today to exclude it does *not guarantee* its reduction. With a successful combination of circumstances, it can decrease to the level of 1-2%, and if unsuccessful, it can remain at the same level of 10-20%. And at the same time, the instrumental errors of modern pyrometers often do not exceed 0.2... 0.5%. That is, the improvement of pyrometers in terms of further reducing the instrumental error at this stage is meaningless, because it does not lead to an increase in measurement accuracy. *Improving the accuracy of measurements in pyrometry has run into a barrier of methodical errors.* How to overcome it?

[4] This is a problem that many still do not realize. Correction by experimentally selected coefficients causes very serious complaints from the point of view of metrology. This can be explained using such a simple example. Let's assume that we measure small voltage values in a printed circuit assembly with a DC microvoltmeter. As is known, when the copper probe of the device comes into contact with the Kovar pin of the chip, a fairly significant contact potential difference occurs, about 30 mV at room temperature. It is quite obvious that if, instead of subtracting this potential difference from the measurement result (adjusted, moreover, taking into account the temperature of the output of the chip), we smoothly "tweak" the gain of the microvoltmeter to the value that, according to someone once made estimates, gives the correct value of the measured value, then not only about the unity of measurements in radio engineering, but also their accuracy can be forgotten. *It is unacceptable to exclude errors by the method of "fitting an experimentally selected coefficient to the correct result",* without relying on the measurement of the influencing quantity and on knowledge of its dependencies on certain environmental parameters.

V. The Need to Isolate the Planck Component from the Total Radiation of the Object

To overcome this barrier, it is necessary to realize what happens when measuring when we neglect the influence of the radiative properties of the measured object. Let's turn to Fig. 1. Here are the Spectral Radiance (SR) of transformer steel when heated to 1127°C in a nitrogen-hydrogen atmosphere (1) and high-alumina firebrick heated in air to the same temperature (2). The results are obtained based on the data given in [4]. Here, for comparison, the SR of the source of ideal Planck radiation – BB (3) at the same 1127°C is given. Obviously, the isolation of the Planck component[5] 3 from dependencies 1 and 2 is an operation completely unobvious, none of the radiation temperature measuring devices is designed to solve this problem.

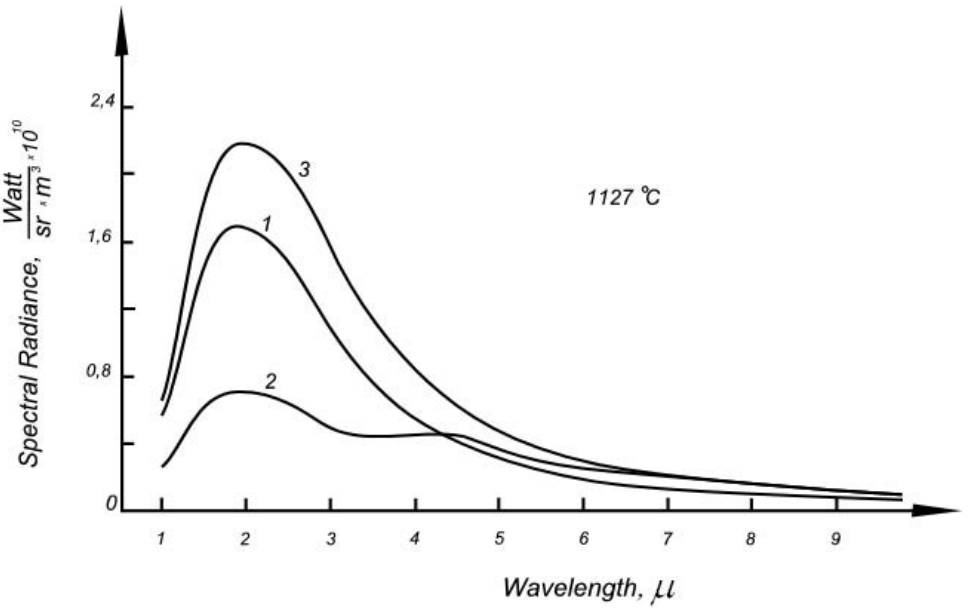

Figure 1: Spectral Radiance (SR) of transformer steel when heated to 1127°C in a nitrogen-hydrogen atmosphere (1), high-alumina firebrick heated in air to the same temperature (2) and BB at 1127°C (3)

The need to isolate the Planck component from the complete SR of an object arose at the dawn of the development of practical pyrometry. This turned out to be necessary because pyrometers are universally calibrated by BB, and after such calibration they can correctly measure the temperature of only those objects that emit as BB – "black" and "gray". When measuring other objects, it is that part of their radiation that distinguishes it from the radiation of the BB, and introduces an additional error, which we call methodical. Therefore, in order to exclude it, one way or another, its banking component must be isolated from the entire radiation of the object. Or somehow exclude the influence of non-Plank component.

VI. Spectral Emissivity and its Role in Eliminating Methodical Errors

The spectral emissivity can be defined as the result of the functional division of the SR of a real object into the SR of an BB (hereinafter, functional division is understood to be the division of the ordinate of the function-divisible by the ordinate of the divisor function for the same abscissa for the set of all possible abscissae).

Figure 2 shows the dependences on the wavelength of the spectral emissivity of transformer steel (1) and high alumina firebrick (2), corresponding to a temperature of 1127°C [4]. As noted, we call these *functions* spectral emissivity in order to distinguish them from the *coefficients*[6] *introduced into energy pyrometers* and still called by inertia by many users of pyrometers and authors of articles on pyrometry "emissivity". Let's add that the spectral emissivity is also a function of the temperature of the object.

[5] Here and further, under the Planck component (Planck curve), we will understand the CR BB.

[6] In this paper, the author calls this coefficient the "radiation coefficient", not emissivity.

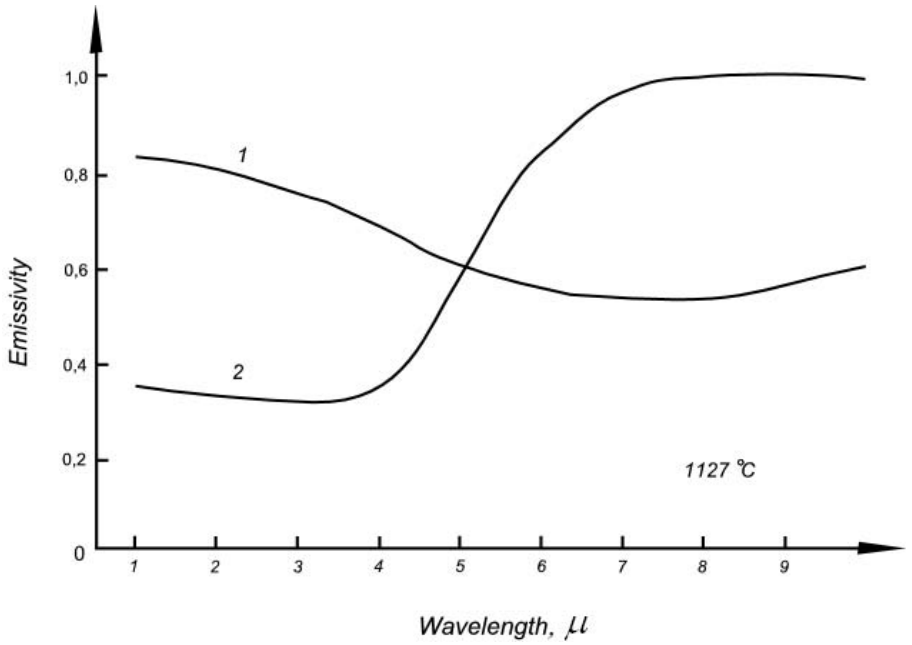

Figure 2: Spectral emissivity of transformer steel when heated to 1127°C in a nitrogen-hydrogen atmosphere (1), and high-alumina firebrick heated in air to the same temperature (2)

Thus, the spectral emissivity is a function that contains the difference between the SR of a real object and the SR of an BB having an equal temperature with the object. Its non-accounting (or incorrect accounting) does not make it possible to correctly convert the SR of the measured object into a Planck curve of equal temperature with the object, according to which this temperature can be measured without any systematic errors using an BB-calibrated pyrometer.

One of the ways of such a separation of the Planck component from the total radiation spectrum is the functional division of the SR of a real object into its real spectral emissivity. However, this is possible only if we have at our disposal almost complete spectral dependences of the SR and emissivity, i.e. lying in the wavelength range where the values of the Planck curves for these objects exceed 0.5-1% of their maxima. This is typical for spectral pyrometry, which is at the initial stage of its development. But pyrometers are not spectrometers, and such a functional division is impossible for them. Nevertheless, knowledge of the spectral emissivity is also necessary for classical energy pyrometers[7] and pyrometers of spectral ratio (at least in the range of spectral sensitivity of these measuring instruments). However, it should be used in the allocation of the Planck component in a slightly different way. Here is one of the options for such a selection.

First, the full view of the object's SR is calculated for all measured temperatures (for example, with a given step within the entire measurement range). To do this, for each of the temperatures, its spectral emissivity is functionally multiplied by its Planck function. Next, using the obtained SR, a set of pseudo–temperatures (brightness, or radiation, or spectral ratio - depending on which type of devices the correction is performed) is calculated. This calculation can be performed using calibration[8] functions. Then a table is formed in which the actual temperature is assigned to each of the obtained pseudo–temperatures - the one whose Planck curve was used to calculate this pseudo-temperature. And at the last stage, the actual temperature of the measured object is determined based on the result of the pyrometer measurement using the above-mentioned recalculation table ([6]). When using the real spectral emissivity in this algorithm, methodical errors are excluded, and the error is determined only by the instrumental errors of the pyrometer used.

In fact, in this case, we modify the scale determining function (inverse of the calibration function) of the pyrometer so that it takes into account the difference between the SR of the measured object and the SR of the BB. Which is essentially equivalent to separating the Planck component from the total flux of its radiation.

Once again, I would like to draw readers attention to an important statement – if we want to measure temperature with a pyrometer without

[7] Energy pyrometers are understood to be all pyrometers having only one radiation receiver, which determine the temperature by the magnitude of the signal from the receiver, i.e. by the magnitude of the energy flow that came to it

[8] The calibration function is, in this case, the dependence of the voltage at the output of the receiver signal amplifier (for an energy pyrometer) or the spectral ratio (for a pyrometer of the spectral ratio) on the temperature of the BB

methodical errors, we must somehow isolate the aforementioned Planck component from all the radiation that came to the pyrometer. Its measurement with an BB-calibrated pyrometer will give the desired result. Or, one way or another, exclude the influence of a non-Planck component, which will lead to the same measurement result.

And how do we allocate the Planck component today? Few people have thought about this – the extraction operation, which is the result of a complex mathematical calculation, has been replaced by correction using coefficients [9] introduced into pyrometers, most often determined experimentally. The task of isolating the Planck component in today's pyrometry has been simplified to the limit – the radiation flux that came to the energy pyrometer is actually simply divided by the radiation coefficient introduced into it. A complex functional transformation is ultimately reduced to division by a constant taken from tables, which very often have a very distant relation to the measured object. Hence the methodical errors, which are absolutely independent of the pyrometer's own instrumental error.

Naturally, classical pyrometers are not spectrometers, they do not measure the SR with some kind of normalizing coefficient, but its integral value in the form of a signal at the output of their radiation receiver. Therefore, the functional division mentioned above is not a task for them. If we are talking about energy pyrometers, then correction by the radiation coefficient is all they can do. But then the procedure for isolating the Planck component should somehow "migrate" at least to the calculation of the radiation coefficient. Such a calculation of the radiation coefficient, taking into account the spectral emissivity $\varepsilon(\lambda,T)$, is described below (see (4)). However, it has certain limitations, which will be described later. Therefore, the task of comprehensively eliminating the influence of temperature-spectral emissivity on the pyrometer measurement result is still relevant. Taking into account all the above, it will be formulated and specified in the last subsection of this article.

It is safe to say that devices for remote temperature measurement will continue to be calibrated according to BB in the future. Consequently, the task of isolating the Planck component from the full SR, according to which these devices will measure temperature, will also remain. And its solution is impossible without knowledge of the spectral emissivity. And the more precisely it is determined (as well as the more accurately the calibration of the measuring instrument used is carried out), the more accurately the temperature of the measured object will be determined. In a different way, using some averaged coefficients introduced into pyrometers, it will not be possible to get rid of methodical errors.

VII. About the New Basic Methodological Postulate of Pyrometry

All of this means the need to rethink the basic methodological postulate mentioned above, which is specific to pyrometry, which consists in the fact that to determine the temperature of an object by its radiation, it is enough to know and use only the laws of radiation, ignoring accumulated or still missing knowledge about the radiative properties of specific objects. It should be replaced by a postulate proclaiming that *the exclusion of methodical errors in non-contact measurement of its temperature is impossible without knowledge of the real* (not generalized or averaged!) *the spectral emissivity of a particular measured object, and its correct accounting.* Attempts to deceive nature and continue to ignore the need to accumulate knowledge about the radiative properties of objects will leave unchanged methodical errors that have hindered the development of pyrometry for more than half a century.

However, this is not all. Since until now there has not been a theory that adequately connects the spectral emissivity with the physico-chemical constants of the object's material, it will be necessary to obtain the necessary information about the spectral emissivity experimentally. At the same time, it should be noted that at the moment there are no specialized measuring instruments for spectral emissivity on the market. Nevertheless, in the works of the author ([7, 8] the technical possibility of creating such measuring instruments is demonstrated, two such devices are described, one of which is protected by a patent of the Russian Federation.

The author also argues the need to have a verification scheme for such devices, as well as a currently missing standard of emissivity, which will stand at the top of this verification scheme ([9, 10]).

VIII. About what else is Needed

However, knowledge of the spectral emissivity is only a necessary condition for reducing or completely eliminating large methodical errors inherent in pyrometry methods. It is not sufficient for this reduction, since algorithms and methods for minimizing/eliminating these errors with full consideration of temperature-spectral emissivity are either insufficiently developed or

[9] For very narrow-band pyrometers and for full-radiation pyrometers, correction in accordance with (1) and (2) is quite acceptable, but with certain reservations: firstly, it is still necessary to know the temperature-spectral emissivity of the object, and secondly, the radiation coefficients depend on temperature, sometimes strongly, and for the choice of their exact values require knowledge of the very temperature of the object for which they are needed to measure. The latter greatly limits the correction according to (1) and (2) for accurate measurements.

absent. Therefore, it is necessary to solve the following scientific problems.

1. As is known, when measuring of "non-gray" objects with spectral-ratio pyrometers, they have a methodical error, the mechanism of which is discussed in detail in [11]. The ratio (3) is known, which allows (knowing the spectral emissivity) to compensate for this methodical error:

$$\frac{1}{T_d}-\frac{1}{T_{sp.rel}}=\ln\frac{\varepsilon_{\lambda_1}}{\varepsilon_{\lambda_2}}\frac{1}{c_2}\frac{1}{\frac{1}{\lambda_1}-\frac{1}{\lambda_2}} \quad (3)$$

where T_d is the actual temperature, K; $T_{sp.rel}$ is the temperature of the spectral ratio measured by the pyrometer, K; $c_2 = 1.4380 \cdot 10^{-2}$ m· K; λ_1 and λ_2 are the operating wavelengths of the narrowband pyrometer of the spectral ratio, m; ε_{λ_1} and ε_{λ_2} are the emission coefficients at wavelengths λ_1 and λ_2.

However, this ratio is valid only for pyrometers with narrow (no more than 10…20nm) spectral bands. At the same time, the vast majority of spectral-ratio pyrometers produced today are broadband, the width of the spectral bands of their sensitivity is tens or even hundreds of nanometers. As a result, ratio (3) is essentially inapplicable for the absolute majority of pyrometers used in practice, and has more theoretical than practical value. Therefore, a universal method is needed to correct the methodical error that occurs when measuring the temperature of "non-gray" objects with any pyrometers of spectral ratio. This method is developed and described in [6, 12]. They present an algorithm for machine calculation of the temperature of the spectral ratio of "non-gray" objects using a calibration function, and an experimental study of the method is carried out. However, the proposed method (as well as in the ratio (3)) does not take into account the temperature dependence of the spectral emissivity. Therefore, the method needs to be improved, taking into account this dependence.

Thus, the problem can be formulated as follows: the above-mentioned universal method for correcting pyrometers of the spectral ratio must be improved in such a way as to take into account the temperature dependence of the spectral emissivity. After that, it, together with information about the spectral emissivity, will become necessary and sufficient conditions for minimizing/eliminating methodical errors in the method of pyrometry of the spectral ratio.

The solution of this problem is described by the author in [13].

2. In contrast to the spectral ratio pyrometry method, the emissivity correction is fundamentally necessary in the energy pyrometry method. To do this, before measuring, a correction factor is introduced into the energy pyrometer, which in this work is called the radiation coefficient. The radiation coefficients introduced into pyrometers are almost universally determined experimentally, by adjusting this coefficient to the value at which the result of temperature measurement using a pyrometer is close to the result of measurement by contact methods. Once selected in this way, the radiation coefficient is then usually transferred to all pyrometers that have to measure such an object. The measurement errors caused by such a transfer are described in [14]. And, moreover, with this approach, it is impossible to correctly take into account not only the spectral range of the pyrometer used, but also the temperature dependence of the emissivity. And this in turn leads to the appearance of additional methodical errors described in [15].

In [16], a ratio is given that allows the recognition of the spectral emissivity and spectral sensitivity characteristics of a photodiode pyrometer to correctly determine the radiation coefficient:

$$\varepsilon_{\lambda,T}=\frac{\int_{\lambda_1}^{\lambda_2}\varepsilon(\lambda,T)S(\lambda)E(\lambda,T)d\lambda}{\int_{\lambda_1}^{\lambda_2}S(\lambda)E(\lambda,T)d\lambda} \quad (4)$$

where $\varepsilon_{\lambda,T}$ is the radiation coefficient at wavelength λ for temperature T, $\varepsilon(\lambda,T)$ is the spectral emissivity of the object; $S(\lambda)$ is the spectral characteristic of the pyrometer sensitivity; $E(\lambda, T)$ is the Planck function; λ_1 and λ_2 are the lower and upper limits of spectral sensitivity.

Since (4) represents the ratio of two definite integrals that are practically insoluble analytically, its use in practice by metrologists and technologists of enterprises is hardly possible – for this, a specialist must have a legally purchased package such as MathCad or Mathlab and be able to use it. Therefore, it is necessary to develop simple and freely distributed programs with which users with minimal computer skills could determine the radiation coefficient according to (4). One of the variants of the set of such programs is given in [17].

Further, since $\varepsilon(\lambda,T)$ and $E(\lambda, T)$ depend on the temperature of the object, the coefficient $\varepsilon_{\lambda,T}$ also depends on temperature. That is, the radiation coefficient found using (4) depends on the temperature. In this case, a vicious circle arises – in order to measure the temperature correctly with an energy pyrometer, you need to enter the correct value of the radiation coefficient into it. But to find the correct value of the radiation coefficient, you need to know the temperature

of the object, which we are still only going to measure. The established practice of adjusting the radiation coefficient to the correct result, if this correct result is unknown in advance, does not solve the problem.

It follows from the above that for the accurate correction of energy pyrometers for emissivity, not only the ratio (4) is required, but also a preliminary knowledge of the temperature to be measured, because without this it is impossible to correctly select those $\varepsilon(\lambda,T)$ and $E(\lambda, T)$ that are necessary to calculate $\varepsilon_{\lambda,T}$ according to (4).

Therefore, the task can be formulated as follows: for energy pyrometers, it is necessary to develop a method of correction for emissivity, different from the one currently used, in which there is no need for prior knowledge of the temperature to be measured in order to correctly use the temperature-dependent radiation coefficient $\varepsilon_{\lambda,T}$ i.e. it is necessary to break this vicious circle when you need to know its correct value to measure temperature, and in order to calculate it correctly in accordance with (4), we need to know this temperature, which is still unknown to us. The current method of correction is not capable of breaking it without some additional information.

It is the above-mentioned method of correction, which differs from the currently used one, in combination with knowledge of temperature-dependent spectral emissivity, that will be the necessary and sufficient means to minimize/exclude methodical errors in the method of energy pyrometry.

The solution of the mentioned problem is planned by the author to be published in one of the next issues of one of the periodicals covering measuring topics. A general approach to solving this problem is formulated in [18].

The implementation of solutions to the formulated tasks will dramatically reduce the methodical errors in pyrometry to a level comparable to the level achieved by instrumental errors.

IX. Conclusion

1. The main methodological postulate specific to pyrometry is formulated – the implicitly postulated priority of radiation laws in this branch over all other laws and patterns used to determine the temperature of heated bodies. It is shown that it is the unconscious adherence to this postulate that does not allow for half a century to solve the problem of reducing/eliminating methodical errors in non-contact temperature control methods.
2. A new, alternative to the above, basic methodological postulate specific to pyrometry is formulated. He proclaims that without knowledge and use of the real (not generalized or averaged!) the temperature-spectral emissivity of a particular measured object it is impossible to exclude methodical errors in the non-contact measurement of its temperature.
3. Since to date there has not been a theory that adequately connects the temperature-spectral emissivity with the physico-chemical constants of the object's material, it is argued that it will be necessary to obtain the necessary information about the spectral emissivity experimentally. At the same time, it should be noted that at the moment there are no specialized measuring instruments for spectral emissivity on the market. Nevertheless, in a number of the author's works, the technical possibility of their creation is demonstrated, two such devices are described, one of which is protected by a patent of the Russian Federation.
4. However, knowledge of the spectral emissivity is only a necessary condition for reducing or completely eliminating large methodical errors inherent in pyrometry methods. For sufficiency, it is necessary to develop algorithms and methods for accounting for the effect on the spectral emissivity of the temperature of the measured object, which are now either insufficiently developed or completely absent.
5. References are given to the algorithms developed by the author of this article for taking into account the influence of temperature on the spectral emissivity of an object used in the methods of spectral ratio pyrometry and energy pyrometry.
6. The algorithms noted in paragraph 5 (recognition of temperature-spectral emissivity), when implemented, will reduce the methodical errors of pyrometry methods to a level comparable to the level achieved by instrumental errors.

References Références Referencias

1. *A. V. Frunze,* The development of pyrometry methodology, Scientific Review, 2014, No. 10, pp. 78-81.
2. *A. Ya. Baskakov and N. V. Tulenkov,* Methodology of scientific research: Textbook. The manual, Kiev, 2004, 216 p.
3. *D. Ya. Svet,* Objective methods of high-temperature pyrometry with a continuous radiation spectrum, Moscow, Nauka, 1968, 240 p.
4. *A. M. Belenky, M. Y. Dubinsky, M. G. Ladygichev, V. G. Lisienko,* Temperature measurement: theory, practice, experiment, Reference edition, in 3 volumes, Vol. 2, Moscow, Teplotekhnik, 2007, 736 p.
5. *A. N. Magunov,* Spectral pyrometry, Moscow, FIZMATLIT, 2012, 248 p.
6. *A. V. Frunze,* A numerical method of determining the spectral-ratio temperature, Measurement Techniques, 2010, Vol. 53, No. 6, pp. 664-667.

7. *A. V. Frunze,* Patent of the Russian Federation No. 2403539 (Russian Federation). A device for determining the spectral emissivity of heated objects. Declared on 06/23/2009.
8. *A. V. Frunze,* Development of an optoelectronic method for measuring temperature with two-spectral photodiodes based on the study on the spectral emissivity of magnetic, composite and refractory materials, abstract of the dissertation for the degree of Candidate of Technical Sciences, Russian State Technical University, K.E. Tsiolkovsky University (MATI), Moscow, 2011.
9. *A. V. Frunze,* On the need to create a primary standard of emissivity, Metrology, 2012, No. 6, pp. 22-27.
10. *A. V. Frunze,* Metrological problems of modern spectral pyrometry, Measurement Techniques, 2018, Vol. 61, No. 6, pp. 621-626.
11. *A. V. Frunze,* About one little-known feature of spectral ratio pyrometers today, Photonics, 2013, No. 3, pp. 86–94.
12. *M. L. Samoilov and A. V. Frunze,* Improving the accuracy of temperature measurements of "non–gray bodies" with a broadband pyrometer of spectral ratio, Metrology, 2010, No. 6, pp. 23–31.
13. *A. V. Frunze,* Improving the accuracy of temperature measurement by a spectral ratio pyrometer // Thermophysics and Aeromechanics, 2023, Vol. 30, No. 3. pp. 581-588.
14. *A. V. Frunze,* Metrological problems of modern energy-controlled pyrometry, Measurement Techniques, 2018, Vol. 61, No. 3, pp. 271–277.
15. *A. V. Frunze,* Methodological errors of modern pyrometers and ways to minimize them, Metrology, 2012, No. 7, pp. 25-38.
16. *D. Ya. Svet,* Optical methods for measuring true temperatures, Moscow, Nauka, 1982, 296 p.
17. *Frunze A. V., Gorbunov R. A., Simakov D. S.,* A set of low-level programs for calculating the temperature of the spectral ratio when measuring the temperature of "non-gray" bodies with two-spectral broadband pyrometers, In the collection: Current problems and prospects for the development of radio engineering and infocommunication systems "RADIOINFOCOM-2021". Collection of scientific articles of the V international scientific and practical conference, Moscow, 2021. pp. 420-426.
18. *Frunze A. V.,* An algorithm for determining the actual temperature of an object, taking into account the temperature dependence of its emissivity, In the collection: Energy-saving technologies in industry. Furnace units, ecology. Proceedings of the VII International Scientific and Practical Conference, National Research Technological University "MISIS"; Compiled by: A. M. Belenky, A. N. Bursin, N. A. Korotchenko, I. V. Korochantseva. 2014. pp. 418-424.

This page is intentionally left blank

Global Journal of Researches in Engineering: A
Mechanical and Mechanics Engineering
Volume 24 Issue 1 Version 1.0 Year 2024
Type: Double Blind Peer Reviewed International Research Journal
Publisher: Global Journals
Online ISSN: 2249-4596 & Print ISSN: 0975-5861

Studies of the Mechanism of Adhesion of Polymer Coatings on the Oxidized Surface of Aluminum and Magnesium Alloys

By Makarychev Yu. B., Kuzenkov Yu. A., Chugunov D. O. & Grafov O. Yu.

Abstract- The adhesion of the polymer paint Lakroten E-244 was investigated on oxidized aluminum A5154 and magnesium MA-20 alloys. It is shown that the adhesion of the polymer coating on the chemically oxidized surface of the aluminum alloy is significantly greater than on the anodic film of the magnesium alloy. Using photoelectron XPS spectroscopy and SEM analysis, the chemical composition and morphology of the alloys have been investigated. The dependence of these factors on the adhesion force of the polymer coating to the oxidized surface of aluminum and magnesium alloys has been established. Methods of modification of conversion coatings with ethylen glycol, which significantly improve the adhesion of polymer layers, have been proposed. The chemical composition and morphology of these coatings have been investigated. An explanation of the mechanism of improvement of adhesion properties of modified coatings on aluminum and magnesium alloys is given. The mechanism of improving the adhesive properties of modified coatings on aluminum and magnesium alloys is explained.

Keywords: adhesion strength, x-ray photoelectron spectroscopy, conversion coatings, paints.

GJRE-A Classification: LCC: TP1180, QD549

Strictly as per the compliance and regulations of:

Studies of the Mechanism of Adhesion of Polymer Coatings on the Oxidized Surface of Aluminum and Magnesium Alloys

Makarychev Yu. B. [α], Kuzenkov Yu. A. [σ], Chugunov D. O. [ρ] & Grafov O. Yu. [ω]

Abstract- The adhesion of the polymer paint Lakroten E-244 was investigated on oxidized aluminum A5154 and magnesium MA-20 alloys. It is shown that the adhesion of the polymer coating on the chemically oxidized surface of the aluminum alloy is significantly greater than on the anodic film of the magnesium alloy. Using photoelectron XPS spectroscopy and SEM analysis, the chemical composition and morphology of the alloys have been investigated. The dependence of these factors on the adhesion force of the polymer coating to the oxidized surface of aluminum and magnesium alloys has been established. Methods of modification of conversion coatings with ethylen glycol, which significantly improve the adhesion of polymer layers, have been proposed. The chemical composition and morphology of these coatings have been investigated. An explanation of the mechanism of improvement of adhesion properties of modified coatings on aluminum and magnesium alloys is given. The mechanism of improving the adhesive properties of modified coatings on aluminum and magnesium alloys is explained.

Keywords: adhesion strength, x-ray photoelectron spectroscopy, conversion coatings, paints.

I. Introduction

Aluminum and magnesium alloys are widely used as structural materials in the aerospace, electronics and automotive industries due to their low density and high strength. The disadvantage of these alloys is their low corrosion resistance in aqueous electrolytes, which limits their use without special preparation. To protect aluminum and magnesium alloys from corrosion, paints and varnishes are commonly used, which are applied to conversion coatings. To improve the adhesion of aluminum and magnesium alloys to paints, alkaline treatment is often recommended to increase the concentration of -Me-OH atomic groups on their surface. To enhance the adhesive activity of aluminum and magnesium alloys to paints, alkaline treatment is often recommended in order to increase the concentration of Me-OH groups of atoms on their surface. At the same time, an increase in the adhesive force is associated with the chemical interaction of surface metal hydroxides with paintwork components. Most coatings in their composition contain monomers with the general formula R-OH and R-COOH, where R is aliphatic or cyclic hydrocarbons. In this case, the chemical interaction of the paint with metal occurs as a result of the condensation reaction, which can be represented in the form of equations:

$$Me\text{-}OH + R\text{-}OH = Me\text{-}OR + H_2O \quad (1)$$

$$Me\text{-}OH + R\text{-}COOH = MeOCOR + H_2O \quad (2)$$

Thus, for the paint to form chemical bonds with the conversion coating, chemically active hydroxyl groups of atoms must be present in its composition. Most studies on the modification of conversion coatings are aimed at changing their structure rather than their chemical composition, based on the assumption that the main factor that increases adhesion is the mechanical bonding of the paint to the pore walls. However, the rapid development of technologies based on the use of organosilane primers indicates the significant role of chemical interaction in the formation of strong bonds of coating materials with the surface of metals. Conversion coatings on aluminum and magnesium alloys consist mainly of metal oxides and hydroxides. Only metal hydroxides participate in the formation of chemical bonds by the mechanism of hydrolytic condensation, so the adhesion strength should depend on the MeO/MeOH ratio in the conversion coating. In this work, the chemical compositions of anodized layers on aluminum A5154 and magnesium MA-20 alloys will be investigated by XPS methods in order to determine the influence of the chemical composition of conversion coatings on the adhesion force to paints. The coatings impregnation was carried out with acrylic paint based on Lakroten E-244 dispersion. The copolymer of this dispersion is acrylic acid which can interact with metal hydroxides by reaction (2).

II. Material and Methods

The work used samples of aluminum and magnesium alloys, the composition of which is shown in Table 1.

Author α σ ρ ω: A.N. Frumkin Institute of Physical Chemistry and Electrochemistry, Russian Academy of Sciences, Leninsky pr. 31, Moscow, Russian. e-mail: makarychev-1949@mail.ru

Table 1: Compositions of aluminum alloy A 5154 and magnesium alloy MA-20

	Mass fraction of elements, %							
Alloy grade	Fe	Cu	Mn	Mg	Cr	Zn	Ce	Al
A5154	0.25	0.4	0.1	0.1	3.1	15	0.2	93.8
MA20	0.05	0.03	0.04	97.94	1.5	0.12	0.02	0.2

The following substances were used to compose inhibitory compositions:

- Ethylene glycol (EG), HO-CH_2-CH_2-OH (Chem.Russia);
- Vinyltrimethoxysilane (VS) (WitcoCo);

Compositions of oxidation electrolytes of aluminum alloy A 5154 and magnesium alloy MA-20 is shown in Table 2.

Table 2: Compositions of oxidation electrolytes of aluminum alloy A 5154 and magnesium alloy MA-20

Sample	Conversion Coating	Modified Conversion Coating
A5154	35g/l NaH_2PO_4,10gl $AlNO_3$, 5 г/л NaOH	35g/l NaH_2PO_4,10gl $AlNO_3$, 5 г/л NaOH,50 г/л EG
MA20	55g/l NaOH, 35g/l Na_2HPO_4, 10g/l $Al(NO_3)_3$	55g/l NaOH, 35g/l Na_2HPO_4 10g/l $Al(NO_3)_3$,50 г/л EG

a) Adhesion Measurement

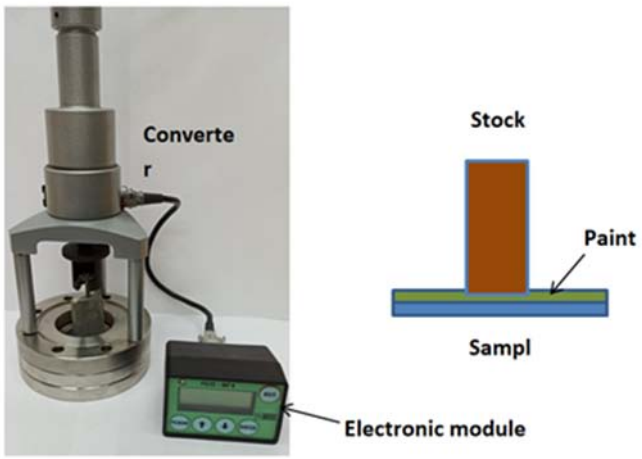

Fig. 1: Electronic adhesion meter PSO-MG4g

The coating adhesion test during separation was carried out using an electronic adhesion meter PSP-MP4 (Russia), shown in Fig. 1. Samples with conversion coating were placed in a fixed holder. Super glue was applied to the surface of an aluminum rod with a diameter of 10 mm and then brought into contact with the test samples. After curing the glue, the joint was stretched at a constant speed of 5 mm/min. For each test, five repeating samples with the specified mean value were used.

b) X-ray Photoelectron Spectroscopy (XPS) Study

X-ray photoelectronic spectra (XPS) were recorded using the Omicron+ X-ray photoelectron spectrometer (FRG). The pressure in the analyzer chamber did not exceed 10-8 Torr. The radiation of an X-ray Al-anode (radiation energy 1486.6 eV, power 200 W) was used as a source. The transmission energy of the analyzer is set to 20 eV. The binding energy of the electrons was calibrated according to the XPS peak of C1s electrons, the binding energy of which was assumed to be 285.0 eV and which is due to the settled layers of diffusion oil vapor. Photoionization cross sections of the corresponding electron shells taken from [19] were used for quantitative evaluation. The integral peak intensities were obtained after subtracting the background using the Shirley method [20] and by fitting the observed peaks with Gauss curves with the contribution of the Lorentz component. To obtain information about the thicknesses of the layers formed on the surface, the MultiQuant program was used [21], the photoionization sections of the corresponding electron shells given by Schofield [22] were selected. To calculate the thicknesses of the layers, the values of electron free path lengths (or average attenuation

coefficients) calculated by the method proposed by Kampson and Sih were used [23].

c) SEM of the Study

SEM images were obtained by a JSM-6400 scanning microscope with an electron-beam intensity of 20 keV, unless otherwise written. Analysis of the elements was performed with SEM equipped with energy-dispersive X-ray analysis (EDX) with a WinEDS EUMEX analyzer (Germany). The thickness of the polymer siloxane coatings was determined using the ZAF correction algorithm for Ka-ratios samples with a known coating thickness.

d) EIS Study

An electrochemical complex consisting of a potentiostat with a frequency analyzer (FRA) is used to measure the impedance. The measurements were carried out in a three-electrode electrochemical cell with a corrosion potential using the Solartron electrochemical complex with a change in the frequency of alternating current from 60,000 to 0.1 Hz (ΔE = 10 Mv).. The impedance data was analyzed using ZView® electrochemical impedance software (version Scribner Associates, Inc., USA).

III. Experimental

The adhesion of coating materials to metal surfaces depends mainly on the chemical composition of the surface, the thickness and porosity of the adhesion layer. The thickness and porosity of conversion coatings for aluminum and magnesium alloys differ to a lesser extent than the chemical composition. Anodic coatings on magnesium alloy AZ91D contain mainly MgO, Al_2O_3 and $MgAl_2O_4$ [24,25]. The adhesion of the paint to such a surface should depend on the thickness and porosity of the conversion coating, since the chemical interaction is minimized. The addition of reagents to anodizing electrolytes that are susceptible to hydrolysis increases the hydroxide ion content of the conversion coating and thus, according to equation (1.2), the adhesion of the coating to the alloy surface. Since the adhesive strength of the coating depends on the chemical composition of the substrate, XPS studies of conversion coatings were carried out.

a) XPS and SEM Investigation of the Chemical Composition of the Conversion Coating on the MA-20 Alloy

The elemental composition of the conversion coating obtained by anodizing the MA-20 alloy in an alkaline solution is shown in Table 3.

Table 3: The elemental composition of the conversion coating on the MA-20 alloy

Sample	Mg,% at	Al,% at	C,% at	O,% at	Thickness, mkm
MA-20	30.3	8.4	19.2	42.1	23.0±5.0

From the results of the chemical analysis given in Table 2, it can be seen that the composition of the conversion coating includes significant amounts of aluminum compounds that fall into the coating from the substrate or electrolyte during oxidation. Figure 2 shows the XPS spectra of Mg2p and Al2p in the conversion coating. After decomposition of the spectra into components, it is seen that the conversion coating consists mainly of magnesium and aluminum oxides. A study of the adhesion of acrylic paint on anodised magnesium alloy surfaces showed extremely low adhesion strength. To increase the adhesive strength of aluminium and magnesium alloys, it is often recommended to hydroxylate the surface by treatment in alkaline solutions. It is possible to increase the concentration of adhesively active R–OH radicals in the conversion coating by adding polyfunctional alcohols to the anodizing electrolytes.

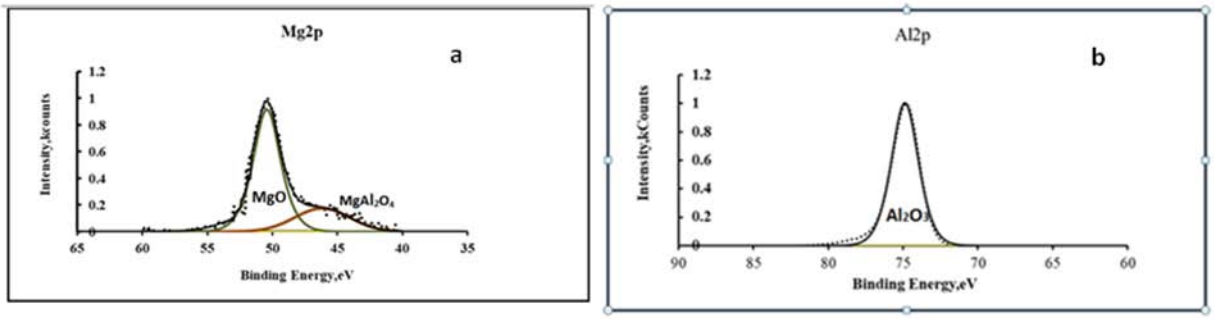

Fig. 2: X-ray spectra of Mg2p (a) and C1s (b) in the conversion coating

In the articles [26,27], studies were carried out on the anodizing of magnesium alloys in aqueous solutions of ethylene glycol and glycerin. The authors of these works found that the conversion coatings obtained in these solutions are formed at sufficiently high speeds, have a porous structure, have high hardness and wear resistance. However, studies of the chemical composition and adhesive strength were not carried out in these works. Morphology and chemical composition of the magnesium layers obtained with ethylene glycol additives in anodizing solutions were studied. Figure 4 shows SEM images of the surface of the anodized alloy before and after modification with ethylene glycol.

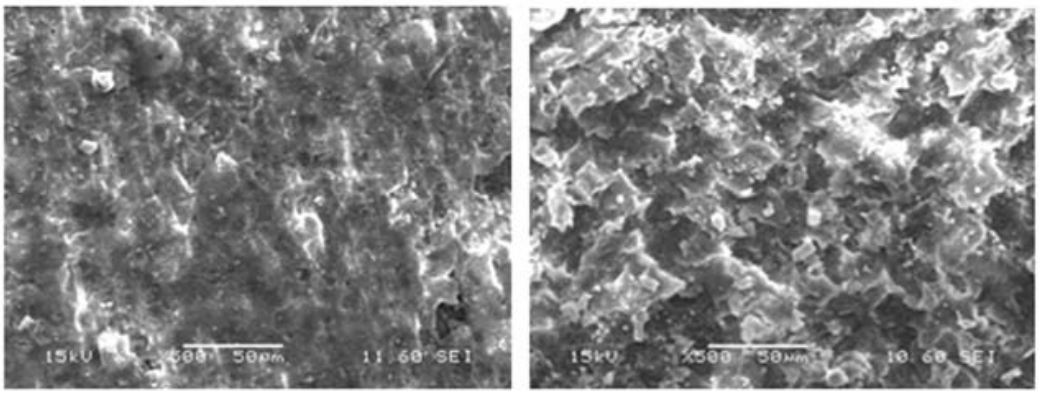

Fig. 3: SEM images of the surface of the anodized alloy before and after modification with ethylene glycol

The addition of ethylene glycol to the electrolyte leads to an increase in the roughness and thickness of the coating. The increase in roughness is apparently due to the formation of magnesium glycolate macromolecules [29] linked together by a bridging bond. Table 4 shows the chemical composition of the modified composite coating.

Table 4: Elemental composition of the modified composite coating

Sample	Mg, % ат.	Al, % ат.	C, % ат.	O, % ат.	Thickness, mkm
MA-20	22,3	2.4	43.2	32,1	32.4.0±5.0

The results of chemical analysis show that the composite coating contains a significant amount of carbon. According to [29], magnesium hydroxide molecules interact with ethylene glycol to form magnesium ethylene glycolate by reaction (3). Magnesium glycolates can interact with each other to form macromolecules by reaction (4).

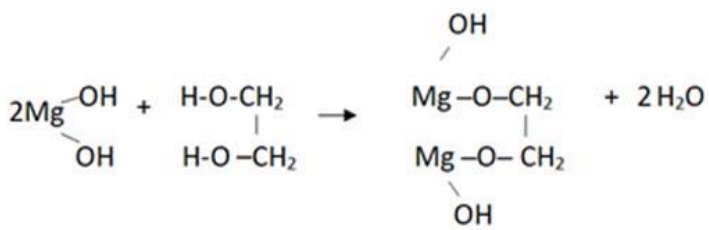

(3)

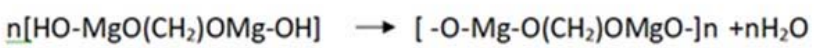

(4)

Macromolecules, together with magnesium oxides, are embedded in the structure of globules that make up conversion coating [29,30]. Polyglycolates contain in their composition adhesive active groups –OH, through which interaction with paints and individual globules with each other is carried out. On the XPS spectra of Mg2, magnesium ethylene glycolates can be observed by the appearance of a peak with E_b= 53.5 eV (Fig. 5), and on the spectra of C1s with E_b = 288.2 eV (Fig. 6).

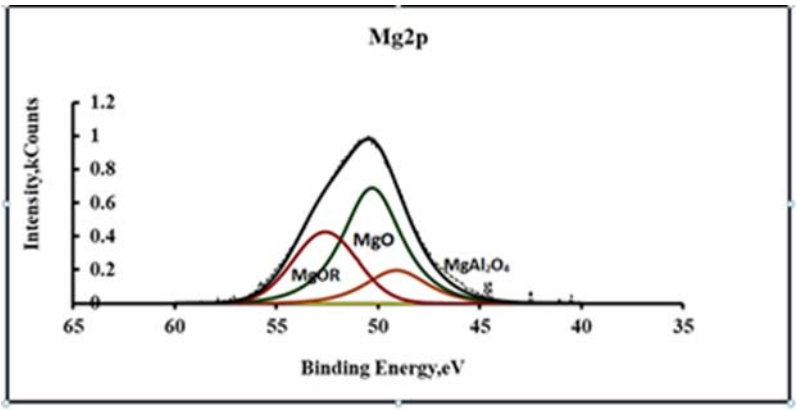

Fig. 4: XPS spectra of Mg2p in a modified inversion coating

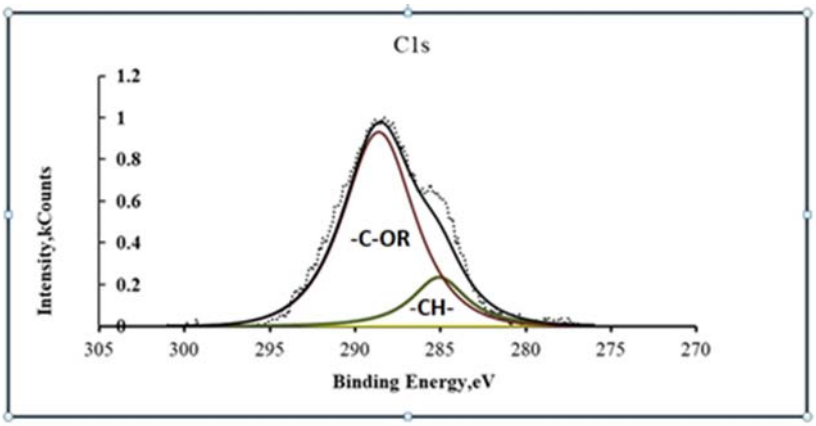

Fig. 5: XPS spectra of C1S carbon in a modified conversion coating

The amounts of ethylene glycolates and magnesium hydroxides in the original and modified conversion coating are shown in Table 5.

Table 5: Chemical composition and tensile strength of the initial and modified MA-20 alloy

Type of coating	MgO, % ат.	Mg glycolate% ат.	$MgAlO_4$ % ат.	Adhesion strength KPa
1. Initial coating	84,6	-	15.4	300±50
2. Modified	57.2	36.2	18.6	1180±50

The inclusion of magnesium glycolates in the conversion coating should change the concentration of chemically active groups -OH. Figure 6 shows the XPS spectra of O1s oxygen in the modified conversion coating.

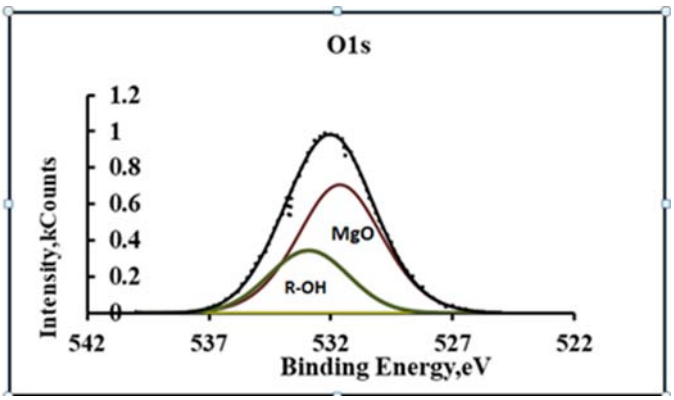

Fig. 6: XPS-spectra of O1s oxygen in the modified conversion coating

Quantitative calculations have shown that the ratio of [O]/[OH] concentrations in the conversion coating changes towards an increase in hydroxide ions mainly due to magnesium ethylene glycolate. An increase in the adhesive strength of the modified conversion coating may be due to an increase in roughness or due to the formation of chemical bonds with the paint. With the help of vapor-gas deposition of vinyltrimethoxysilane (VS) [31], its roughness was reduced on the surface of the modified conversion coating. The coating thickness was 150-200 nm. To assess the roughness of the conversion coating, EIS studies were conducted.

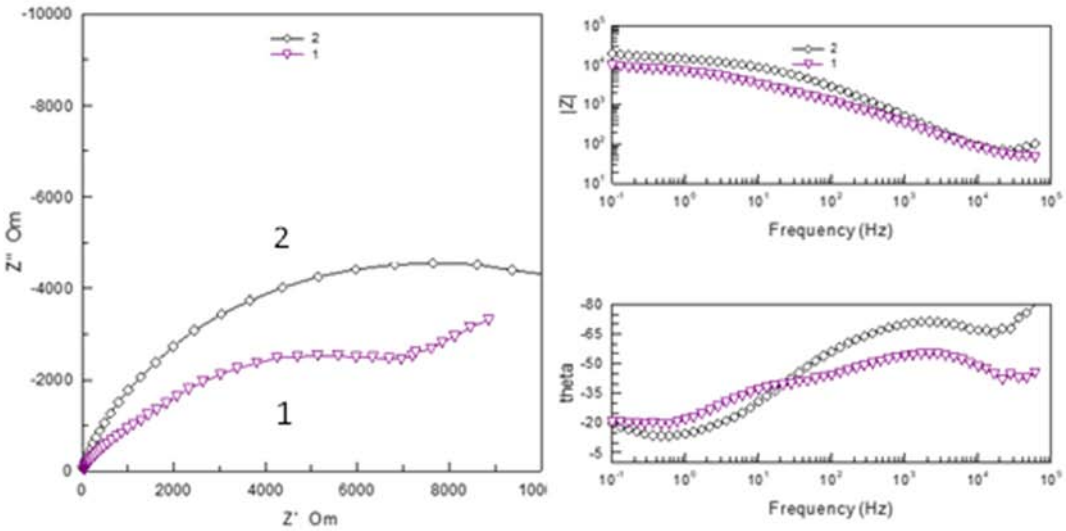

Fig. 7: Nyquist and Bode plots for modified conversion coating (plot 1) and after VS impregnation (plot 2)

In plot 1 (Fig. 7), there is a rectilinear section with an angle of 45° in the high frequency region. This form of the Nyquist graph is characteristic of mass transfer in porous systems. After impregnation, the Nyquist graph has the form of a hemisphere, characteristic of a smoothed surface. The Bode graphs for the initial conversion coverage show the presence of two well-defined time constants. In the high frequency range the time constant can be explained by the barrier properties of coatings. In the low-frequency region, 10-50 Hz is attributed to corrosion processes at the boundary of the coating and metal. After the vapor-gas modification of the conversion coverage, the through pores are filled with polymer and a wide area of change in the phase angle of the barrier coating remains. Silane coating practically does not change $|Z|$, which indicates partial filling of the pores and a slight change in the structure of the coating. The decrease in the roughness and pore volume of the conversion coverage should have reduced the adhesive force at the same time, it increased after steam-gas treatment by ~ 20-30%, which indicates the predominant influence of chemical interaction over mechanical. Impregnation of the coatings with vinylsilane increases the number of functional groups involved in the formation of chemical bonds in connection with which it can be used to enhance the adhesion of the coating with paint. Table 6 shows the adhesion strength of Lakroten E-244 to oxidized alloys MA-20 and A5154.with paint.

Table 6: Adhesive strength of Lakroten E-244 to oxidized alloys MA-20 and A5154

Conversion coverage on MA-20	Adhesion strength, KPa
1. Initial	300±50
2. Modified with ethylene glycol	1180±50
3. Modified with ethylene glycol+VS	1350±100
Conversion coverage on A 5154	
4. Initial	1600±100
5. Conversion coverage on A 5154	1850±100

From the data given in Table 6, it can be seen that the adhesion of Lakroten E-244 on the modified chemically oxidized alloy A5154 is maximum. To clarify the influence of the morphology and chemical composition of the aluminum alloy on the adhesion of the paint, XPS and SEM studies were conducted.

b) XPS and SEM Study of the Chemical Composition of the Conversion Coating on Aluminum Alloy A5154

The conversion coating on chemically oxidized alloy A5154 consists mainly of $Al(OH)_4$, which is obtained by the equation:

$$Al_2O_3+2OH^-+3H_2O \rightarrow 2\ Al(OH)_4 \quad (5)$$

This explains the high adhesion of coatings to these alloys. Chemical oxidation is used along with electrochemical, but is inferior to the latter in terms of performance characteristics, primarily mechanical strength and wear resistance. Modification of a chemically oxidized conversion coating with ethylene glycol can increase its mechanical properties due to additional chemical bonds between individual amorphous $Al(OH)_4$ globules of which conversion coating consists [32]. Along with high adhesive activity, such coatings could significantly expand their application areas.

The conversion coating on alloy A 5154 was modified with ethylene glycol by adding it to oxidation solutions. Figure 8 shows a SEM images of the surface of the conversion coating on the original and modified alloy.

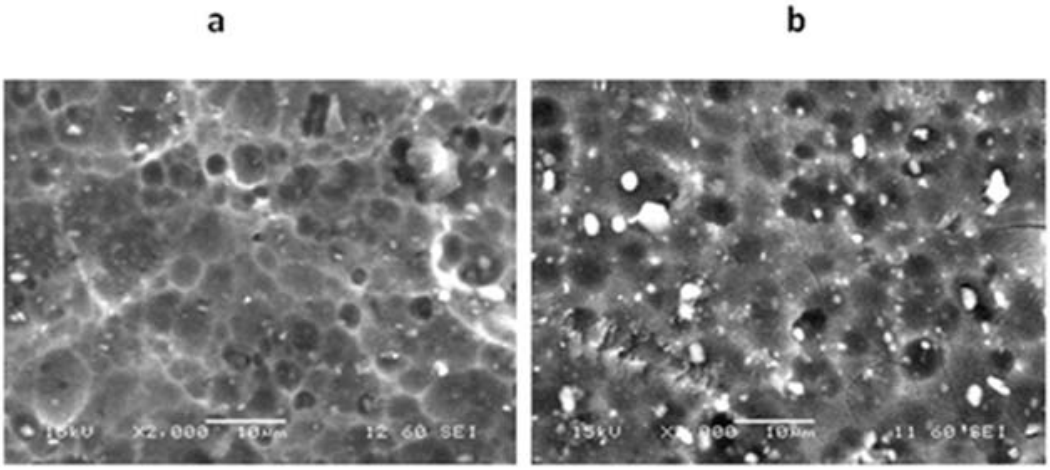

Fig. 8: SEM images of the surface of the conversion coating on the original (a) and modified (b) alloy

It can be seen that the structure of conversion coating A5154 is fine-grained with vertical pores of 5-10 microns in size, in contrast to magnesium MA-20. On the modified alloy the structure is also granular but the number and diameter of the pores are larger. Inclusions of white colour according to X-ray microanalysis data are microphases of magnesium glycolate. The chemical composition of the alloys is given in Table 7.

Table 7: Chemical composition of the initial and modified conversion coating on alloy A5154

Conversion coating on alloy A5154	Mg, % ат.	Al, % ат.	C, % ат.	O, % ат.	Thickness, mKm
Initial	2,3	14.4	25.1	58.2	3.2
Modified	1.8	11.6	42.8	43.8	2.8

Comparing the chemical analysis data of the original and modified coating, it is clear that the latter contains a significant amount of carbon belonging to magnesium and aluminum glycolates. Aluminum glycolates can be detected by the appearance of a peak on the Al 2p spectra with an energy of 71.4 eV and a peak with an energy of 288.2 eV on the C1s spectra (Fig. 9).

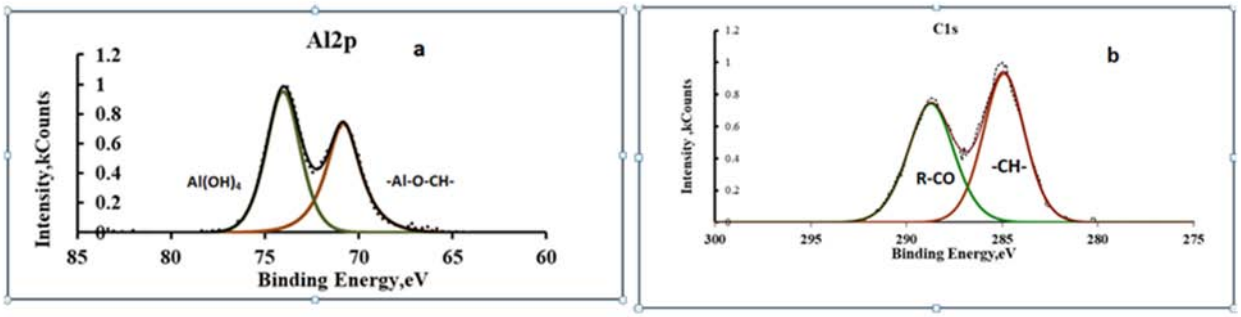

Fig. 9: XPS spectra of Al 2p(a) and C1s (b) for a modified conversion coating on alloy A 5154

A symmetrical doublet on the Al2p spectrum indicates the existence of two types of chemical compounds of aluminum distributed in the conversion coating as separate phases. One of these phases is $Al(OH_{)4}$, the other is aluminum glycolate. Quantitative calculations of the XPS spectra belonging to aluminum hycolates have shown that two aluminum atoms account for approximately the same number of carbon atoms. This ratio corresponds to the reaction of the formation of aluminum glycolate according to equation (6).

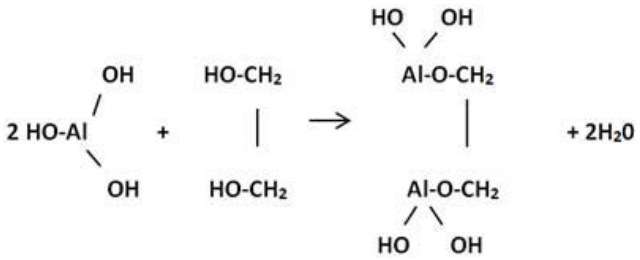

(6)

Aluminum glycolate molecules can interact with each other to form macromolecules and individual phases in the conversion coating. A significant amount of aluminum glycolate in the coating indicates a high chemical activity of ethylene glycol to aluminum hydroxides. The inclusion of aluminum glycolate in the composition of the conversion coating changes its structure and possibly mechanical properties in the direction of increasing strength due to the formation of new chemical bond. The adhesive strength of the modified conversion coating is slightly higher than the initial one due to mechanical adhesion, since the concentration of chemically active –OH groups varies slightly.

IV. Results and Discussion

Published studies of paint adhesion to aluminium and magnesium alloys are random and adhesion strength is mainly attributed to mechanical adhesion in the pore volume. At the same time, our studies have shown that the adhesion strength of paint to the surface of these alloys can vary by an order of magnitude. In this work, the surface of the alloys was subjected to chemical and anodic oxidation. Conversion coatings on aluminium alloy A5154 were obtained by chemical oxidation in alkaline solutions. Oxide coatings on magnesium alloys Ma-20 were obtained by anodising in alkaline solutions. From the point of view of the theory of mechanical adhesion of paints with the alloy surface, conversion coatings on Ma-20 alloy are more preferable because they have a more developed structure on the surface and inside the oxide layer. However, studies have shown that the adhesion force on aluminium alloys is 5-6 times greater than on magnesium alloys. It has been suggested that this is due to the chemical composition of the conversion layers. On aluminium alloys they consist of aluminium hydroxides $Al(OH)_4$ and on magnesium alloys of oxides. According to equations (1,2) the formation of strong chemical bonds with paints is possible only on aluminium alloy. Modification of the conversion coating with ethylene glycol leads to an increase in its concentration of -OH groups capable of chemical interaction with paintwork materials, as a result of which the adhesive force increases. It is possible to increase the concentration of hydroxides in the coating by introducing compounds that form -R-OH groups of atoms as a result of hydrolysis, such as organosilanes,

into the anodising electrolyte. Modification of aluminium alloys with ethylene glycol does not lead to a significant increase in adhesion strength because the conversion coating consists of aluminium hydroxides. However, there is an increase in the number and size of pores, which increases the adhesive strength.

V. Conclusions

Studies of the adhesion of the acrylic paint Lakroten E-244 to aluminum A5154 and magnesium Ma-20 alloys have been carried out. Significant differences in the adhesive activity of these alloys to polymer coatings were found. With the help of XPS and SEM, studies of the chemical composition and morphology of alloys were carried out. It is shown that the adhesion of coatings to the surface of alloys depends mainly on the ratio of MeO/MeO in the conversion coating. Modification of the conversion coating on a magnesium alloy with ethylene glycol significantly increases the adhesive strength of the alloy to paints. The chemical composition of magnesium ethylene glycolate macromolecules and their amount in the conversion coating were determined with the help of XPS studies. The addition of ethylene glycol increases the thickness of the conversion coating and its strength due to the formation of additional chemical bonds of magnesium ethylene glycol macromelecules with inside and on the border of globules. Studies of the chemical composition, morphology and adhesive activity of conversion coatings on the surface of aluminum alloys modified with ethylene glycol have been carried out. It is shown that the increase in the adhesive activity of modified aluminum alloys is mainly due to an increase in the number and size of pores. The chemical composition and quantity have been established macromolecules of aluminum ethylene glycolate in the conversion coating of aluminum alloy. Modification of the ethylene glycol conversion coating on magnesium and aluminum alloys changes their structure and chemical composition, which contributes to a significant increase in their adhesive activity.

References Références Referencias

1. S. A. Kulinicha, b and A. S. Akhtara, On Conversion Coating Treatments to Replace Chromating for Al Alloys: Recent Developments and Possible Future Directions, Russian Journal of NonFerrous Metals, 2012, Vol. 53, No. 2, pp. 176–203. © Allerton Press, Inc., 2012.
2. J.-P. Dasquet a, U, D. Caillardb, Investigation of the anodic oxide layer on 1050 and 2024T3 aluminium alloys by electron microscopy and electrochemical impedance spectroscopy Thin Solid Films 371 2000 183-190.
3. Yoganandan, J. N. Balaraju*, Synergistic effect of V and Mn oxyanions for the corrosion protection of anodized aerospace aluminum alloy, Surface Engineering Division, CSIR National Aerospace Laboratories, Post Bag No. 1779 Bangalore 560017, Karnataka, India a.
4. Golru SS, Attar M, Ramezanzadeh B (2015) Effects of surface treatment of aluminium alloy 1050 on the adhesion and anticorrosion properties of the epoxy coating. Appl Surf Sci 345:360–36.
5. Zhu W, Li W, Mu S, Fu N, Liao Z (2017) Comparative study on Ti/Zr/V and chromate conversion treated aluminum alloys: anticorrosion performance and epoxy coating adhesion properties. Appl Surf Sci 405:157–168.
6. Li Y, Zhang P, Bai P, Wu L, Liu B, Zhao Z (2018) Microstructure and properties of Ti/TiBCN coating on 7075 aluminum alloy by laser cladding. Surf Coat Technol 334:142–149.
7. Sabouri M, Khoei SM (2018) Plasma electrolytic oxidation in the presence of multiwall carbon nanotubes on aluminum substrate: morphological and corrosion studies. Surf Coat Technol 334:543–555.
8. Meis N, van der Ven L, van Benthem R (2014) Extreme wet adhesion of a novel epoxy-amine coating on aluminum alloy 2024-T3. Prog Org Coat 77(1):176–183.
9. Fabiola Pinedac, Carola Martínezb,d, Mamié Sancyb, Marcela UrzuaeMarcos Floresf, María V. Encinasg, Maritza A. Páeza. Improving the interaction between aluminum surfaces and polymer coating, Surface and Coatings Technology. Volume 358, 25 January 2019, Pages 435-442.
10. Ruiyue Zhanga, Shu Cai a,∗, Guohua Xub,∗∗, Huan Zhaoa, Yan Li a, Xuexin Wanga, Kai Huanga, Mengguo Rena, Xiaodong Wub. Crack self-healing of phytic acid conversion coating on AZ31magnesium alloy by heat treatment and the corrosion resistance. Applied Surface Science,V3,2014 p.831-836.
11. R. F Zhang, J. Bu, C. Lin, G. Song, Recent progress in corrosion protection of magnesium alloys by organic coatings, Prog. Org. Coat. 73 (2012) 129–141.
12. R. F. Zhang, S. F. Zhang a b, N. Yang b, L.J. Yao b, F.X. He b, Y.P. Zhou b, X. Xu b, L. Chang b, S.J. Bai b Journal of Alloys and Compounds Influence of 8-hydroxyquinoline on properties of anodic coatings obtained by micro arc oxidation on AZ91 magnesium alloys. Volume 539, 25 October 2012, Pages 249-255.
13. Srinivasan PB, Liang J, Blawert C, Störmer M, Dietzel W. Characterization of calcium containing plasma electrolytic oxidation coatings on AM50 magnesium alloy. Appl Surf Sci 2010; 256:4017–22.
14. Ximei Wang, Liqun Zhu, Weiping Li, Huicong Liu, Yihong Li, Effects of half-wave and full-wave power source on the anodic oxidation process on AZ91D

magnesium alloy, Volume 255, Issue 11, 15 March 2009, Pages 5721-5728.
15. R. F. Zhang a b, Yu Zuo a, Guochao Nie, The enhanced properties of anodic films on AZ91D magnesium alloy by addition of oxide nanoparticles, Journal of Alloys and Compounds, Volume 834, 5 September 2020, 1550.
16. Gen Zhang a, Aitao Tang a b, Liang Wu a b, Zeyu Zhang a, Hongxin Liao a, Ying Long a, Lingjie Li c, Andrej Atrens d, Fusheng Pan a b, In-situ grown super- or hydrophobic Mg-Al layered double hydroxides films on the anodized magnesium alloy to improve corrosion properties, Surface and Coatings Technology Volume 366, 25 May 2019, Pages 238-247.
17. Jothi a, Akeem Yusuf Adesina b, A. Madhan Kumar b, Mohammad Mizanur Rahman b, J.S. Nirmal Ram, Enhancing the biodegradability and surface protective performance of AZ31 Mg alloy using polypyrrole/gelatin composite coatings with anodized Mg surface, Surface and Coatings Technology Volume 381, 15 January 2020, 125139.
18. Y. R. Ding, X. W. Guo, Y. F. Jiang, et al., Effects of triethanolamine on the performances of the anodicing film of AZ31B magnesium alloy, Mater. Sci. Forum, 488e489 (2005) 657e660.
19. D. A. Shirley, High-resolution X-ray photoemission spectrum of the valence bands of gold, Phys. Rev. B 5 (1972) 4709–4713.
20. M. Mohai, XPS MultiQuant: multimodel XPS quantification software, Surf. Interface Anal. 36 (2004) 828–832. DOI
21. R. A. Waldo, An Iteration Procedure to Calculate Film Compositions and Thicknesses in Electron-Probe Microanalysis, San Francisco Press, San-Francisco, 1988.
22. Cumpson P. J., Seah M. P. Elastic Scattering Correction in AES and XPS. II. Estimating Attenuation Lengths and Conditions Required for their Valid Use on Overlayer/Substrate Experiments. // Surf. Interface Anal., 1997, V. 25, № 6, P. 430-446.
23. Pei Zhang a, b, Yu Zuo a, *, Guochao Nie c The enhanced properties of anodic films on AZ91D magnesium alloby addition of oxide nanoparticles Journal of Alloys and Compounds 834 (2020) 155041.
24. H. Y. Hsiao, W. T. Tsai, Characterization of anodic films formed on AZ91D magnesium alloy, Surf. Coating. Technol. 190 (2005) 299e308.
25. Hiroki Habazaki a b, Fumitaka Kataoka a, Khurram Shahzad a, Etsushi Tsuji a b, Yoshitaka Aoki a b, Shinji Nagata c, Peter Skeldon d, George E. Thompson d, Growth of barrier-type anodic films on magnesium in ethylene glycol electrolytes containing fluoride and water, Electrochimica Acta, Volume 179, 10 October 2015, Pages 402-413.
26. A. Němcová a, O. Galal a, P. Skeldon a, I. Kuběna b, M. Šmíd c, E. Briand d, I. Vickridge d, J-J. Ganem d, H. Habazaki, Film growth and alloy enrichment during anodizing AZ31 magnesium alloy in fluoride/glycerol electrolytes of a range of water contents, Electrochimica Acta Volume 219, 20 November 2016, Pages 28-37.
27. Makarychev Yu. B., Kuzenkov Yu. A., Chugunov D. O., Grafov O. Yu., Aliev A. D., Vapor-phase deposition of polymer siloxane coatings on aluminum and magnesium alloys Prog. Org. Coat. Volume 183, October 2023, 107755.
28. Santamaria M, DiQuarto F, Zanna S, Marcus P. Initial surface film on magnesium metal: a characterization by X-ray photoelectron spectroscopy (XPS) and photocurrent spectroscopy (PCS). Electrochimica 2007;53(3):1315–25.
29. Zhou W, Shan D, Han E, Ke W. Structure and formation mechanism ophosphate conversion coating on die-cast AZ91D magnesium alloy. Corros Sci. 2008;50:329–37.
30. Makarychev Yu B., Luchkin A. Yu, Grafov O. Yu, Andreev N. N, Vapor-phase deposition of polymer siloxane coatings on the surface of copper and low-carbon steel. International Journal of Corrosion and Scale Inhibition, V 11, № 3, c. 980-1000 DOI.
31. Synergistic effect of V and Mn oxyanions for the corrosion protection of anodized aerospace aluminum alloy G. Yoganandan, J. N. Balaraju*, Surface Engineering Division, CSIR National Aerospace Laboratories, Post Bag No. 1779 Bangalore 560017, Karnataka, India.

Global Journals Guidelines Handbook 2024

www.GlobalJournals.org

Memberships

Fellows/Associates of Engineering Research Council

FERC/AERC Memberships

Introduction

FERC/AERC is the most prestigious membership of Global Journals accredited by Open Association of Research Society, U.S.A (OARS). The credentials of Fellow and Associate designations signify that the researcher has gained the knowledge of the fundamental and high-level concepts, and is a subject matter expert, proficient in an expertise course covering the professional code of conduct, and follows recognized standards of practice. The credentials are designated only to the researchers, scientists, and professionals that have been selected by a rigorous process by our Editorial Board and Management Board.

Associates of FERC/AERC are scientists and researchers from around the world are working on projects/researches that have huge potentials. Members support Global Journals' mission to advance technology for humanity and the profession.

FERC

Fellow of Engineering Research Council

FELLOW OF ENGINEERING RESEARCH COUNCIL is the most prestigious membership of Global Journals. It is an award and membership granted to individuals that the Open Association of Research Society judges to have made a 'substantial contribution to the improvement of computer science, technology, and electronics engineering.

The primary objective is to recognize the leaders in research and scientific fields of the current era with a global perspective and to create a channel between them and other researchers for better exposure and knowledge sharing. Members are most eminent scientists, engineers, and technologists from all across the world. Fellows are elected for life through a peer review process on the basis of excellence in the respective domain. There is no limit on the number of new nominations made in any year. Each year, the Open Association of Research Society elect up to 12 new Fellow Members.

Benefits

To the institution

Get letter of appreciation

Global Journals sends a letter of appreciation of author to the Dean or CEO of the University or Company of which author is a part, signed by editor in chief or chief author.

Exclusive Network

Get access to a closed network

A FERC member gets access to a closed network of Tier 1 researchers and scientists with direct communication channel through our website. Fellows can reach out to other members or researchers directly. They should also be open to reaching out by other.

Career | Credibility | Exclusive | Reputation

Certificate

Certificate, LoR and Laser-Momento

Fellows receive a printed copy of a certificate signed by our Chief Author that may be used for academic purposes and a personal recommendation letter to the dean of member's university.

Career | Credibility | Exclusive | Reputation

Designation

Get honored title of membership

Fellows can use the honored title of membership. The “FERC” is an honored title which is accorded to a person’s name viz. Dr. John E. Hall, Ph.D., FERC or William Walldroff, M.S., FERC.

Career | Credibility | Exclusive | Reputation

Recognition on the Platform

Better visibility and citation

All the Fellow members of FERC get a badge of "Leading Member of Global Journals" on the Research Community that distinguishes them from others. Additionally, the profile is also partially maintained by our team for better visibility and citation. All fellows get a dedicated page on the website with their biography.

Career | Credibility | Reputation

Future Work

Get discounts on the future publications

Fellows receive discounts on the future publications with Global Journals up to 60%. Through our recommendation programs, members also receive discounts on publications made with OARS affiliated organizations.

Career | Financial

GJ Account

Unlimited forward of Emails

Fellows get secure and fast GJ work emails with unlimited storage of emails that they may use them as their primary email. For example, john [AT] globaljournals [DOT] org.

Career | Credibility | Reputation

Premium Tools

Access to all the premium tools

To take future researches to the zenith, fellows receive access to all the premium tools that Global Journals have to offer along with the partnership with some of the best marketing leading tools out there.

Financial

Conferences & Events

Organize seminar/conference

Fellows are authorized to organize symposium/seminar/conference on behalf of Global Journal Incorporation (USA). They can also participate in the same organized by another institution as representative of Global Journal. In both the cases, it is mandatory for him to discuss with us and obtain our consent. Additionally, they get free research conferences (and others) alerts.

Career | Credibility | Financial

Early Invitations

Early invitations to all the symposiums, seminars, conferences

All fellows receive the early invitations to all the symposiums, seminars, conferences and webinars hosted by Global Journals in their subject.

Exclusive

Publishing Articles & Books

Earn 60% of sales proceeds

Fellows can publish articles (limited) without any fees. Also, they can earn up to 70% of sales proceeds from the sale of reference/review books/literature/publishing of research paper. The FERC member can decide its price and we can help in making the right decision.

Exclusive | Financial

Reviewers

Get a remuneration of 15% of author fees

Fellow members are eligible to join as a paid peer reviewer at Global Journals Incorporation (USA) and can get a remuneration of 15% of author fees, taken from the author of a respective paper.

Financial

Access to Editorial Board

Become a member of the Editorial Board

Fellows may join as a member of the Editorial Board of Global Journals Incorporation (USA) after successful completion of three years as Fellow and as Peer Reviewer. Additionally, Fellows get a chance to nominate other members for Editorial Board.

Career | Credibility | Exclusive | Reputation

And Much More

Get access to scientific museums and observatories across the globe

All members get access to 5 selected scientific museums and observatories across the globe. All researches published with Global Journals will be kept under deep archival facilities across regions for future protections and disaster recovery. They get 10 GB free secure cloud access for storing research files.

AERC

ASSOCIATE OF ENGINEERING RESEARCH COUNCIL

ASSOCIATE OF ENGINEERING RESEARCH COUNCIL is the membership of Global Journals awarded to individuals that the Open Association of Research Society judges to have made a 'substantial contribution to the improvement of computer science, technology, and electronics engineering.

The primary objective is to recognize the leaders in research and scientific fields of the current era with a global perspective and to create a channel between them and other researchers for better exposure and knowledge sharing. Members are most eminent scientists, engineers, and technologists from all across the world. Associate membership can later be promoted to Fellow Membership. Associates are elected for life through a peer review process on the basis of excellence in the respective domain. There is no limit on the number of new nominations made in any year. Each year, the Open Association of Research Society elect up to 12 new Associate Members.

Benefits

To the institution

Get letter of appreciation

Global Journals sends a letter of appreciation of author to the Dean or CEO of the University or Company of which author is a part, signed by editor in chief or chief author.

Exclusive Network

Get access to a closed network

A AERC member gets access to a closed network of Tier 1 researchers and scientists with direct communication channel through our website. Associates can reach out to other members or researchers directly. They should also be open to reaching out by other.

Career | Credibility | Exclusive | Reputation

Certificate

Certificate, LoR and Laser-Momento

Associates receive a printed copy of a certificate signed by our Chief Author that may be used for academic purposes and a personal recommendation letter to the dean of member's university.

Career | Credibility | Exclusive | Reputation

Designation

Get honored title of membership

Associates can use the honored title of membership. The “AERC” is an honored title which is accorded to a person’s name viz. Dr. John E. Hall, Ph.D., AERC or William Walldroff, M.S., AERC.

Career | Credibility | Exclusive | Reputation

Recognition on the Platform

Better visibility and citation

All the Associate members of AERC get a badge of "Leading Member of Global Journals" on the Research Community that distinguishes them from others. Additionally, the profile is also partially maintained by our team for better visibility and citation. All associates get a dedicated page on the website with their biography.

Career | Credibility | Reputation

Future Work

Get discounts on the future publications

Associates receive discounts on the future publications with Global Journals up to 60%. Through our recommendation programs, members also receive discounts on publications made with OARS affiliated organizations.

Career | Financial

GJ Account

Unlimited forward of Emails

Associates get secure and fast GJ work emails with unlimited storage of emails that they may use them as their primary email. For example, john [AT] globaljournals [DOT] org..

Career | Credibility | Reputation

Premium Tools

Access to all the premium tools

To take future researches to the zenith, associates receive access to all the premium tools that Global Journals have to offer along with the partnership with some of the best marketing leading tools out there.

Financial

Conferences & Events

Organize seminar/conference

Associates are authorized to organize symposium/seminar/conference on behalf of Global Journal Incorporation (USA). They can also participate in the same organized by another institution as representative of Global Journal. In both the cases, it is mandatory for him to discuss with us and obtain our consent. Additionally, they get free research conferences (and others) alerts.

Career | Credibility | Financial

Early Invitations

Early invitations to all the symposiums, seminars, conferences

All associates receive the early invitations to all the symposiums, seminars, conferences and webinars hosted by Global Journals in their subject.

Exclusive

Publishing Articles & Books

Earn 30-40% of sales proceeds

Associates can publish articles (limited) without any fees. Also, they can earn up to 30-40% of sales proceeds from the sale of reference/review books/literature/publishing of research paper.

Exclusive | Financial

Reviewers

Get a remuneration of 15% of author fees

Associate members are eligible to join as a paid peer reviewer at Global Journals Incorporation (USA) and can get a remuneration of 15% of author fees, taken from the author of a respective paper.

Financial

And Much More

Get access to scientific museums and observatories across the globe

All members get access to 2 selected scientific museums and observatories across the globe. All researches published with Global Journals will be kept under deep archival facilities across regions for future protections and disaster recovery. They get 5 GB free secure cloud access for storing research files.

Associate	Fellow	Research Group	Basic
$4800 **lifetime designation**	$6800 **lifetime designation**	$12500.00 **organizational**	APC **per article**
Certificate, LoR and Momento **2** discounted publishing/year **Gradation** of Research **10** research contacts/day **1 GB** Cloud Storage **GJ** Community Access	**Certificate,** LoR and Momento **Unlimited** discounted publishing/year **Gradation** of Research **Unlimited** research contacts/day **5 GB** Cloud Storage **Online Presense** Assistance **GJ** Community Access	**Certificates,** LoRs and Momentos **Unlimited** free publishing/year **Gradation** of Research **Unlimited** research contacts/day **Unlimited** Cloud Storage **Online Presense** Assistance **GJ** Community Access	**GJ** Community Access

We accept the manuscript submissions in any standard (generic) format.

We typeset manuscripts using advanced typesetting tools like Adobe In Design, CorelDraw, TeXnicCenter, and TeXStudio. We usually recommend authors submit their research using any standard format they are comfortable with, and let Global Journals do the rest.

Alternatively, you can download our basic template from https://globaljournals.org/Template.zip

Authors should submit their complete paper/article, including text illustrations, graphics, conclusions, artwork, and tables. Authors who are not able to submit manuscript using the form above can email the manuscript department at submit@globaljournals.org or get in touch with chiefeditor@globaljournals.org if they wish to send the abstract before submission.

Before and during Submission

Authors must ensure the information provided during the submission of a paper is authentic. Please go through the following checklist before submitting:

1. Authors must go through the complete author guideline and understand and *agree to Global Journals' ethics and code of conduct,* along with author responsibilities.
2. Authors must accept the privacy policy, terms, and conditions of Global Journals.
3. Ensure corresponding author's email address and postal address are accurate and reachable.
4. Manuscript to be submitted must include keywords, an abstract, a paper title, co-author(s') names and details (email address, name, phone number, and institution), figures and illustrations in vector format including appropriate captions, tables, including titles and footnotes, a conclusion, results, acknowledgments and references.
5. Authors should submit paper in a ZIP archive if any supplementary files are required along with the paper.
6. Proper permissions must be acquired for the use of any copyrighted material.
7. Manuscript submitted *must not have been submitted or published elsewhere* and all authors must be aware of the submission.

Declaration of Conflicts of Interest

It is required for authors to declare all financial, institutional, and personal relationships with other individuals and organizations that could influence (bias) their research.

Policy on Plagiarism

Plagiarism is not acceptable in Global Journals submissions at all.

Plagiarized content will not be considered for publication. We reserve the right to inform authors' institutions about plagiarism detected either before or after publication. If plagiarism is identified, we will follow COPE guidelines:

Authors are solely responsible for all the plagiarism that is found. The author must not fabricate, falsify or plagiarize existing research data. The following, if copied, will be considered plagiarism:

- Words (language)
- Ideas
- Findings
- Writings
- Diagrams
- Graphs
- Illustrations
- Lectures

- Printed material
- Graphic representations
- Computer programs
- Electronic material
- Any other original work

Authorship Policies

Global Journals follows the definition of authorship set up by the Open Association of Research Society, USA. According to its guidelines, authorship criteria must be based on:

1. Substantial contributions to the conception and acquisition of data, analysis, and interpretation of findings.
2. Drafting the paper and revising it critically regarding important academic content.
3. Final approval of the version of the paper to be published.

Changes in Authorship

The corresponding author should mention the name and complete details of all co-authors during submission and in manuscript. We support addition, rearrangement, manipulation, and deletions in authors list till the early view publication of the journal. We expect that corresponding author will notify all co-authors of submission. We follow COPE guidelines for changes in authorship.

Copyright

During submission of the manuscript, the author is confirming an exclusive license agreement with Global Journals which gives Global Journals the authority to reproduce, reuse, and republish authors' research. We also believe in flexible copyright terms where copyright may remain with authors/employers/institutions as well. Contact your editor after acceptance to choose your copyright policy. You may follow this form for copyright transfers.

Appealing Decisions

Unless specified in the notification, the Editorial Board's decision on publication of the paper is final and cannot be appealed before making the major change in the manuscript.

Acknowledgments

Contributors to the research other than authors credited should be mentioned in Acknowledgments. The source of funding for the research can be included. Suppliers of resources may be mentioned along with their addresses.

Declaration of funding sources

Global Journals is in partnership with various universities, laboratories, and other institutions worldwide in the research domain. Authors are requested to disclose their source of funding during every stage of their research, such as making analysis, performing laboratory operations, computing data, and using institutional resources, from writing an article to its submission. This will also help authors to get reimbursements by requesting an open access publication letter from Global Journals and submitting to the respective funding source.

Preparing your Manuscript

Authors can submit papers and articles in an acceptable file format: MS Word (doc, docx), LaTeX (.tex, .zip or .rar including all of your files), Adobe PDF (.pdf), rich text format (.rtf), simple text document (.txt), Open Document Text (.odt), and Apple Pages (.pages). Our professional layout editors will format the entire paper according to our official guidelines. This is one of the highlights of publishing with Global Journals—authors should not be concerned about the formatting of their paper. Global Journals accepts articles and manuscripts in every major language, be it Spanish, Chinese, Japanese, Portuguese, Russian, French, German, Dutch, Italian, Greek, or any other national language, but the title, subtitle, and abstract should be in English. This will facilitate indexing and the pre-peer review process.

The following is the official style and template developed for publication of a research paper. Authors are not required to follow this style during the submission of the paper. It is just for reference purposes.

Manuscript Style Instruction (Optional)

- Microsoft Word Document Setting Instructions.
- Font type of all text should be Swis721 Lt BT.
- Page size: 8.27" x 11'", left margin: 0.65, right margin: 0.65, bottom margin: 0.75.
- Paper title should be in one column of font size 24.
- Author name in font size of 11 in one column.
- Abstract: font size 9 with the word "Abstract" in bold italics.
- Main text: font size 10 with two justified columns.
- Two columns with equal column width of 3.38 and spacing of 0.2.
- First character must be three lines drop-capped.
- The paragraph before spacing of 1 pt and after of 0 pt.
- Line spacing of 1 pt.
- Large images must be in one column.
- The names of first main headings (Heading 1) must be in Roman font, capital letters, and font size of 10.
- The names of second main headings (Heading 2) must not include numbers and must be in italics with a font size of 10.

Structure and Format of Manuscript

The recommended size of an original research paper is under 15,000 words and review papers under 7,000 words. Research articles should be less than 10,000 words. Research papers are usually longer than review papers. Review papers are reports of significant research (typically less than 7,000 words, including tables, figures, and references)

A research paper must include:

a) A title which should be relevant to the theme of the paper.
b) A summary, known as an abstract (less than 150 words), containing the major results and conclusions.
c) Up to 10 keywords that precisely identify the paper's subject, purpose, and focus.
d) An introduction, giving fundamental background objectives.
e) Resources and techniques with sufficient complete experimental details (wherever possible by reference) to permit repetition, sources of information must be given, and numerical methods must be specified by reference.
f) Results which should be presented concisely by well-designed tables and figures.
g) Suitable statistical data should also be given.
h) All data must have been gathered with attention to numerical detail in the planning stage.

Design has been recognized to be essential to experiments for a considerable time, and the editor has decided that any paper that appears not to have adequate numerical treatments of the data will be returned unrefereed.

i) Discussion should cover implications and consequences and not just recapitulate the results; conclusions should also be summarized.
j) There should be brief acknowledgments.
k) There ought to be references in the conventional format. Global Journals recommends APA format.

Authors should carefully consider the preparation of papers to ensure that they communicate effectively. Papers are much more likely to be accepted if they are carefully designed and laid out, contain few or no errors, are summarizing, and follow instructions. They will also be published with much fewer delays than those that require much technical and editorial correction.

The Editorial Board reserves the right to make literary corrections and suggestions to improve brevity.

Format Structure

It is necessary that authors take care in submitting a manuscript that is written in simple language and adheres to published guidelines.

All manuscripts submitted to Global Journals should include:

Title

The title page must carry an informative title that reflects the content, a running title (less than 45 characters together with spaces), names of the authors and co-authors, and the place(s) where the work was carried out.

Author details

The full postal address of any related author(s) must be specified.

Abstract

The abstract is the foundation of the research paper. It should be clear and concise and must contain the objective of the paper and inferences drawn. It is advised to not include big mathematical equations or complicated jargon.

Many researchers searching for information online will use search engines such as Google, Yahoo or others. By optimizing your paper for search engines, you will amplify the chance of someone finding it. In turn, this will make it more likely to be viewed and cited in further works. Global Journals has compiled these guidelines to facilitate you to maximize the web-friendliness of the most public part of your paper.

Keywords

A major lynchpin of research work for the writing of research papers is the keyword search, which one will employ to find both library and internet resources. Up to eleven keywords or very brief phrases have to be given to help data retrieval, mining, and indexing.

One must be persistent and creative in using keywords. An effective keyword search requires a strategy: planning of a list of possible keywords and phrases to try.

Choice of the main keywords is the first tool of writing a research paper. Research paper writing is an art. Keyword search should be as strategic as possible.

One should start brainstorming lists of potential keywords before even beginning searching. Think about the most important concepts related to research work. Ask, “What words would a source have to include to be truly valuable in a research paper?” Then consider synonyms for the important words.

It may take the discovery of only one important paper to steer in the right keyword direction because, in most databases, the keywords under which a research paper is abstracted are listed with the paper.

Numerical Methods

Numerical methods used should be transparent and, where appropriate, supported by references.

Abbreviations

Authors must list all the abbreviations used in the paper at the end of the paper or in a separate table before using them.

Formulas and equations

Authors are advised to submit any mathematical equation using either MathJax, KaTeX, or LaTeX, or in a very high-quality image.

Tables, Figures, and Figure Legends

Tables: Tables should be cautiously designed, uncrowned, and include only essential data. Each must have an Arabic number, e.g., Table 4, a self-explanatory caption, and be on a separate sheet. Authors must submit tables in an editable format and not as images. References to these tables (if any) must be mentioned accurately.

Figures

Figures are supposed to be submitted as separate files. Always include a citation in the text for each figure using Arabic numbers, e.g., Fig. 4. Artwork must be submitted online in vector electronic form or by emailing it.

Preparation of Eletronic Figures for Publication

Although low-quality images are sufficient for review purposes, print publication requires high-quality images to prevent the final product being blurred or fuzzy. Submit (possibly by e-mail) EPS (line art) or TIFF (halftone/ photographs) files only. MS PowerPoint and Word Graphics are unsuitable for printed pictures. Avoid using pixel-oriented software. Scans (TIFF only) should have a resolution of at least 350 dpi (halftone) or 700 to 1100 dpi (line drawings). Please give the data for figures in black and white or submit a Color Work Agreement form. EPS files must be saved with fonts embedded (and with a TIFF preview, if possible).

For scanned images, the scanning resolution at final image size ought to be as follows to ensure good reproduction: line art: >650 dpi; halftones (including gel photographs): >350 dpi; figures containing both halftone and line images: >650 dpi.

Color charges: Authors are advised to pay the full cost for the reproduction of their color artwork. Hence, please note that if there is color artwork in your manuscript when it is accepted for publication, we would require you to complete and return a Color Work Agreement form before your paper can be published. Also, you can email your editor to remove the color fee after acceptance of the paper.

Tips for Writing a Good Quality Engineering Research Paper

Techniques for writing a good quality engineering research paper:

1. Choosing the topic: In most cases, the topic is selected by the interests of the author, but it can also be suggested by the guides. You can have several topics, and then judge which you are most comfortable with. This may be done by asking several questions of yourself, like "Will I be able to carry out a search in this area? Will I find all necessary resources to accomplish the search? Will I be able to find all information in this field area?" If the answer to this type of question is "yes," then you ought to choose that topic. In most cases, you may have to conduct surveys and visit several places. Also, you might have to do a lot of work to find all the rises and falls of the various data on that subject. Sometimes, detailed information plays a vital role, instead of short information. Evaluators are human: The first thing to remember is that evaluators are also human beings. They are not only meant for rejecting a paper. They are here to evaluate your paper. So present your best aspect.

2. Think like evaluators: If you are in confusion or getting demotivated because your paper may not be accepted by the evaluators, then think, and try to evaluate your paper like an evaluator. Try to understand what an evaluator wants in your research paper, and you will automatically have your answer. Make blueprints of paper: The outline is the plan or framework that will help you to arrange your thoughts. It will make your paper logical. But remember that all points of your outline must be related to the topic you have chosen.

3. Ask your guides: If you are having any difficulty with your research, then do not hesitate to share your difficulty with your guide (if you have one). They will surely help you out and resolve your doubts. If you can't clarify what exactly you require for your work, then ask your supervisor to help you with an alternative. He or she might also provide you with a list of essential readings.

4. Use of computer is recommended: As you are doing research in the field of research engineering then this point is quite obvious. Use right software: Always use good quality software packages. If you are not capable of judging good software, then you can lose the quality of your paper unknowingly. There are various programs available to help you which you can get through the internet.

5. Use the internet for help: An excellent start for your paper is using Google. It is a wondrous search engine, where you can have your doubts resolved. You may also read some answers for the frequent question of how to write your research paper or find a model research paper. You can download books from the internet. If you have all the required books, place importance on reading, selecting, and analyzing the specified information. Then sketch out your research paper. Use big pictures: You may use encyclopedias like Wikipedia to get pictures with the best resolution. At Global Journals, you should strictly follow here.

6. Bookmarks are useful: When you read any book or magazine, you generally use bookmarks, right? It is a good habit which helps to not lose your continuity. You should always use bookmarks while searching on the internet also, which will make your search easier.

7. Revise what you wrote: When you write anything, always read it, summarize it, and then finalize it.

8. Make every effort: Make every effort to mention what you are going to write in your paper. That means always have a good start. Try to mention everything in the introduction—what is the need for a particular research paper. Polish your work with good writing skills and always give an evaluator what he wants. Make backups: When you are going to do any important thing like making a research paper, you should always have backup copies of it either on your computer or on paper. This protects you from losing any portion of your important data.

9. Produce good diagrams of your own: Always try to include good charts or diagrams in your paper to improve quality. Using several unnecessary diagrams will degrade the quality of your paper by creating a hodgepodge. So always try to include diagrams which were made by you to improve the readability of your paper. Use of direct quotes: When you do research relevant to literature, history, or current affairs, then use of quotes becomes essential, but if the study is relevant to science, use of quotes is not preferable.

10. Use proper verb tense: Use proper verb tenses in your paper. Use past tense to present those events that have happened. Use present tense to indicate events that are going on. Use future tense to indicate events that will happen in the future. Use of wrong tenses will confuse the evaluator. Avoid sentences that are incomplete.

11. Pick a good study spot: Always try to pick a spot for your research which is quiet. Not every spot is good for studying.

12. Know what you know: Always try to know what you know by making objectives, otherwise you will be confused and unable to achieve your target.

13. Use good grammar: Always use good grammar and words that will have a positive impact on the evaluator; use of good vocabulary does not mean using tough words which the evaluator has to find in a dictionary. Do not fragment sentences. Eliminate one-word sentences. Do not ever use a big word when a smaller one would suffice.

Verbs have to be in agreement with their subjects. In a research paper, do not start sentences with conjunctions or finish them with prepositions. When writing formally, it is advisable to never split an infinitive because someone will (wrongly) complain. Avoid clichés like a disease. Always shun irritating alliteration. Use language which is simple and straightforward. Put together a neat summary.

14. Arrangement of information: Each section of the main body should start with an opening sentence, and there should be a changeover at the end of the section. Give only valid and powerful arguments for your topic. You may also maintain your arguments with records.

15. Never start at the last minute: Always allow enough time for research work. Leaving everything to the last minute will degrade your paper and spoil your work.

16. Multitasking in research is not good: Doing several things at the same time is a bad habit in the case of research activity. Research is an area where everything has a particular time slot. Divide your research work into parts, and do a particular part in a particular time slot.

17. Never copy others' work: Never copy others' work and give it your name because if the evaluator has seen it anywhere, you will be in trouble. Take proper rest and food: No matter how many hours you spend on your research activity, if you are not taking care of your health, then all your efforts will have been in vain. For quality research, take proper rest and food.

18. Go to seminars: Attend seminars if the topic is relevant to your research area. Utilize all your resources.

19. Refresh your mind after intervals: Try to give your mind a rest by listening to soft music or sleeping in intervals. This will also improve your memory. Acquire colleagues: Always try to acquire colleagues. No matter how sharp you are, if you acquire colleagues, they can give you ideas which will be helpful to your research.

20. Think technically: Always think technically. If anything happens, search for its reasons, benefits, and demerits. Think and then print: When you go to print your paper, check that tables are not split, headings are not detached from their descriptions, and page sequence is maintained.

21. Adding unnecessary information: Do not add unnecessary information like "I have used MS Excel to draw graphs." Irrelevant and inappropriate material is superfluous. Foreign terminology and phrases are not apropos. One should never take a broad view. Analogy is like feathers on a snake. Use words properly, regardless of how others use them. Remove quotations. Puns are for kids, not grunt readers. Never oversimplify: When adding material to your research paper, never go for oversimplification; this will definitely irritate the evaluator. Be specific. Never use rhythmic redundancies. Contractions shouldn't be used in a research paper. Comparisons are as terrible as clichés. Give up ampersands, abbreviations, and so on. Remove commas that are not necessary. Parenthetical words should be between brackets or commas. Understatement is always the best way to put forward earth-shaking thoughts. Give a detailed literary review.

22. Report concluded results: Use concluded results. From raw data, filter the results, and then conclude your studies based on measurements and observations taken. An appropriate number of decimal places should be used. Parenthetical remarks are prohibited here. Proofread carefully at the final stage. At the end, give an outline to your arguments. Spot perspectives of further study of the subject. Justify your conclusion at the bottom sufficiently, which will probably include examples.

23. Upon conclusion: Once you have concluded your research, the next most important step is to present your findings. Presentation is extremely important as it is the definite medium though which your research is going to be in print for the rest of the crowd. Care should be taken to categorize your thoughts well and present them in a logical and neat manner. A good quality research paper format is essential because it serves to highlight your research paper and bring to light all necessary aspects of your research.

Informal Guidelines of Research Paper Writing

Key points to remember:

- Submit all work in its final form.
- Write your paper in the form which is presented in the guidelines using the template.
- Please note the criteria peer reviewers will use for grading the final paper.

Final points:

One purpose of organizing a research paper is to let people interpret your efforts selectively. The journal requires the following sections, submitted in the order listed, with each section starting on a new page:

The introduction: This will be compiled from reference matter and reflect the design processes or outline of basis that directed you to make a study. As you carry out the process of study, the method and process section will be constructed like that. The results segment will show related statistics in nearly sequential order and direct reviewers to similar intellectual paths throughout the data that you gathered to carry out your study.

The discussion section:

This will provide understanding of the data and projections as to the implications of the results. The use of good quality references throughout the paper will give the effort trustworthiness by representing an alertness to prior workings.

Writing a research paper is not an easy job, no matter how trouble-free the actual research or concept. Practice, excellent preparation, and controlled record-keeping are the only means to make straightforward progression.

General style:

Specific editorial column necessities for compliance of a manuscript will always take over from directions in these general guidelines.

To make a paper clear: Adhere to recommended page limits.

Mistakes to avoid:

- Insertion of a title at the foot of a page with subsequent text on the next page.
- Separating a table, chart, or figure—confine each to a single page.
- Submitting a manuscript with pages out of sequence.
- In every section of your document, use standard writing style, including articles ("a" and "the").
- Keep paying attention to the topic of the paper.

- Use paragraphs to split each significant point (excluding the abstract).
- Align the primary line of each section.
- Present your points in sound order.
- Use present tense to report well-accepted matters.
- Use past tense to describe specific results.
- Do not use familiar wording; don't address the reviewer directly. Don't use slang or superlatives.
- Avoid use of extra pictures—include only those figures essential to presenting results.

Title page:

Choose a revealing title. It should be short and include the name(s) and address(es) of all authors. It should not have acronyms or abbreviations or exceed two printed lines.

Abstract: This summary should be two hundred words or less. It should clearly and briefly explain the key findings reported in the manuscript and must have precise statistics. It should not have acronyms or abbreviations. It should be logical in itself. Do not cite references at this point.

An abstract is a brief, distinct paragraph summary of finished work or work in development. In a minute or less, a reviewer can be taught the foundation behind the study, common approaches to the problem, relevant results, and significant conclusions or new questions.

Write your summary when your paper is completed because how can you write the summary of anything which is not yet written? Wealth of terminology is very essential in abstract. Use comprehensive sentences, and do not sacrifice readability for brevity; you can maintain it succinctly by phrasing sentences so that they provide more than a lone rationale. The author can at this moment go straight to shortening the outcome. Sum up the study with the subsequent elements in any summary. Try to limit the initial two items to no more than one line each.

Reason for writing the article—theory, overall issue, purpose.

- Fundamental goal.
- To-the-point depiction of the research.
- Consequences, including definite statistics—if the consequences are quantitative in nature, account for this; results of any numerical analysis should be reported. Significant conclusions or questions that emerge from the research.

Approach:

- Single section and succinct.
- An outline of the job done is always written in past tense.
- Concentrate on shortening results—limit background information to a verdict or two.
- Exact spelling, clarity of sentences and phrases, and appropriate reporting of quantities (proper units, important statistics) are just as significant in an abstract as they are anywhere else.

Introduction:

The introduction should "introduce" the manuscript. The reviewer should be presented with sufficient background information to be capable of comprehending and calculating the purpose of your study without having to refer to other works. The basis for the study should be offered. Give the most important references, but avoid making a comprehensive appraisal of the topic. Describe the problem visibly. If the problem is not acknowledged in a logical, reasonable way, the reviewer will give no attention to your results. Speak in common terms about techniques used to explain the problem, if needed, but do not present any particulars about the protocols here.

The following approach can create a valuable beginning:

- Explain the value (significance) of the study.
- Defend the model—why did you employ this particular system or method? What is its compensation? Remark upon its appropriateness from an abstract point of view as well as pointing out sensible reasons for using it.
- Present a justification. State your particular theory(-ies) or aim(s), and describe the logic that led you to choose them.
- Briefly explain the study's tentative purpose and how it meets the declared objectives.

Approach:

Use past tense except for when referring to recognized facts. After all, the manuscript will be submitted after the entire job is done. Sort out your thoughts; manufacture one key point for every section. If you make the four points listed above, you will need at least four paragraphs. Present surrounding information only when it is necessary to support a situation. The reviewer does not desire to read everything you know about a topic. Shape the theory specifically—do not take a broad view.

As always, give awareness to spelling, simplicity, and correctness of sentences and phrases.

Procedures (methods and materials):

This part is supposed to be the easiest to carve if you have good skills. A soundly written procedures segment allows a capable scientist to replicate your results. Present precise information about your supplies. The suppliers and clarity of reagents can be helpful bits of information. Present methods in sequential order, but linked methodologies can be grouped as a segment. Be concise when relating the protocols. Attempt to give the least amount of information that would permit another capable scientist to replicate your outcome, but be cautious that vital information is integrated. The use of subheadings is suggested and ought to be synchronized with the results section.

When a technique is used that has been well-described in another section, mention the specific item describing the way, but draw the basic principle while stating the situation. The purpose is to show all particular resources and broad procedures so that another person may use some or all of the methods in one more study or referee the scientific value of your work. It is not to be a step-by-step report of the whole thing you did, nor is a methods section a set of orders.

Materials:

Materials may be reported in part of a section or else they may be recognized along with your measures.

Methods:

- Report the method and not the particulars of each process that engaged the same methodology.
- Describe the method entirely.
- To be succinct, present methods under headings dedicated to specific dealings or groups of measures.
- Simplify—detail how procedures were completed, not how they were performed on a particular day.
- If well-known procedures were used, account for the procedure by name, possibly with a reference, and that's all.

Approach:

It is embarrassing to use vigorous voice when documenting methods without using first person, which would focus the reviewer's interest on the researcher rather than the job. As a result, when writing up the methods, most authors use third person passive voice.

Use standard style in this and every other part of the paper—avoid familiar lists, and use full sentences.

What to keep away from:

- Resources and methods are not a set of information.
- Skip all descriptive information and surroundings—save it for the argument.
- Leave out information that is immaterial to a third party.

Results:

The principle of a results segment is to present and demonstrate your conclusion. Create this part as entirely objective details of the outcome, and save all understanding for the discussion.

The page length of this segment is set by the sum and types of data to be reported. Use statistics and tables, if suitable, to present consequences most efficiently.

You must clearly differentiate material which would usually be incorporated in a study editorial from any unprocessed data or additional appendix matter that would not be available. In fact, such matters should not be submitted at all except if requested by the instructor.

Content:

- Sum up your conclusions in text and demonstrate them, if suitable, with figures and tables.
- In the manuscript, explain each of your consequences, and point the reader to remarks that are most appropriate.
- Present a background, such as by describing the question that was addressed by creation of an exacting study.
- Explain results of control experiments and give remarks that are not accessible in a prescribed figure or table, if appropriate.
- Examine your data, then prepare the analyzed (transformed) data in the form of a figure (graph), table, or manuscript.

What to stay away from:

- Do not discuss or infer your outcome, report surrounding information, or try to explain anything.
- Do not include raw data or intermediate calculations in a research manuscript.
- Do not present similar data more than once.
- A manuscript should complement any figures or tables, not duplicate information.
- Never confuse figures with tables—there is a difference.

Approach:

As always, use past tense when you submit your results, and put the whole thing in a reasonable order.

Put figures and tables, appropriately numbered, in order at the end of the report.

If you desire, you may place your figures and tables properly within the text of your results section.

Figures and tables:

If you put figures and tables at the end of some details, make certain that they are visibly distinguished from any attached appendix materials, such as raw facts. Whatever the position, each table must be titled, numbered one after the other, and include a heading. All figures and tables must be divided from the text.

Discussion:

The discussion is expected to be the trickiest segment to write. A lot of papers submitted to the journal are discarded based on problems with the discussion. There is no rule for how long an argument should be.

Position your understanding of the outcome visibly to lead the reviewer through your conclusions, and then finish the paper with a summing up of the implications of the study. The purpose here is to offer an understanding of your results and support all of your conclusions, using facts from your research and generally accepted information, if suitable. The implication of results should be fully described.

Infer your data in the conversation in suitable depth. This means that when you clarify an observable fact, you must explain mechanisms that may account for the observation. If your results vary from your prospect, make clear why that may have happened. If your results agree, then explain the theory that the proof supported. It is never suitable to just state that the data approved the prospect, and let it drop at that. Make a decision as to whether each premise is supported or discarded or if you cannot make a conclusion with assurance. Do not just dismiss a study or part of a study as "uncertain."

Research papers are not acknowledged if the work is imperfect. Draw what conclusions you can based upon the results that you have, and take care of the study as a finished work.

- You may propose future guidelines, such as how an experiment might be personalized to accomplish a new idea.
- Give details of all of your remarks as much as possible, focusing on mechanisms.
- Make a decision as to whether the tentative design sufficiently addressed the theory and whether or not it was correctly restricted. Try to present substitute explanations if they are sensible alternatives.
- One piece of research will not counter an overall question, so maintain the large picture in mind. Where do you go next? The best studies unlock new avenues of study. What questions remain?
- Recommendations for detailed papers will offer supplementary suggestions.

Approach:

When you refer to information, differentiate data generated by your own studies from other available information. Present work done by specific persons (including you) in past tense.

Describe generally acknowledged facts and main beliefs in present tense.

The Administration Rules

Administration Rules to Be Strictly Followed before Submitting Your Research Paper to Global Journals Inc.

Please read the following rules and regulations carefully before submitting your research paper to Global Journals Inc. to avoid rejection.

Segment draft and final research paper: You have to strictly follow the template of a research paper, failing which your paper may get rejected. You are expected to write each part of the paper wholly on your own. The peer reviewers need to identify your own perspective of the concepts in your own terms. Please do not extract straight from any other source, and do not rephrase someone else's analysis. Do not allow anyone else to proofread your manuscript.

Written material: You may discuss this with your guides and key sources. Do not copy anyone else's paper, even if this is only imitation, otherwise it will be rejected on the grounds of plagiarism, which is illegal. Various methods to avoid plagiarism are strictly applied by us to every paper, and, if found guilty, you may be blacklisted, which could affect your career adversely. To guard yourself and others from possible illegal use, please do not permit anyone to use or even read your paper and file.

Criterion for Grading a Research Paper (Compilation) by Global Journals

Please note that following table is only a Grading of "Paper Compilation" and not on "Performed/Stated Research" whose grading solely depends on Individual Assigned Peer Reviewer and Editorial Board Member. These can be available only on request and after decision of Paper. This report will be the property of Global Journals.

Topics	Grades		
	A-B	**C-D**	**E-F**
Abstract	Clear and concise with appropriate content, Correct format. 200 words or below	Unclear summary and no specific data, Incorrect form Above 200 words	No specific data with ambiguous information Above 250 words
Introduction	Containing all background details with clear goal and appropriate details, flow specification, no grammar and spelling mistake, well organized sentence and paragraph, reference cited	Unclear and confusing data, appropriate format, grammar and spelling errors with unorganized matter	Out of place depth and content, hazy format
Methods and Procedures	Clear and to the point with well arranged paragraph, precision and accuracy of facts and figures, well organized subheads	Difficult to comprehend with embarrassed text, too much explanation but completed	Incorrect and unorganized structure with hazy meaning
Result	Well organized, Clear and specific, Correct units with precision, correct data, well structuring of paragraph, no grammar and spelling mistake	Complete and embarrassed text, difficult to comprehend	Irregular format with wrong facts and figures
Discussion	Well organized, meaningful specification, sound conclusion, logical and concise explanation, highly structured paragraph reference cited	Wordy, unclear conclusion, spurious	Conclusion is not cited, unorganized, difficult to comprehend
References	Complete and correct format, well organized	Beside the point, Incomplete	Wrong format and structuring

INDEX

save our planet

Global Journal of Researches in Engineering

Visit us on the Web at www.GlobalJournals.org | www.EngineeringResearch.org
or email us at helpdesk@globaljournals.org

ISSN 9755861